Hydrogenations and hydro-acylations using homogeneous platinum metal catalysts

Heeres, Hans

Hydrogenations and hydro-acylations using homogeneous platinum metal catalysts

Hans Heeres

Cover design: Idea by Hans Heeres, redesigned by Maarit Mustonen

RIJKSUNIVERSITEIT GRONINGEN

Hydrogenations and hydro-acylations using homogeneous platinum metal catalysts

Proefschrift

ter verkrijging van het doctoraat in de
Wiskunde en Natuurwetenschappen
aan de Rijksuniversiteit Groningen
op gezag van de
Rector Magnificus, dr. F. Zwarts,
in het openbaar te verdedigen op
vrijdag 22 januari 2010
om 13.15 uur

door

Hans Heeres
geboren op 30 juli 1977
te Veendam

Promotor:	Prof. dr. ir. H.J. Heeres
Beoordelingscommissie:	Prof. dr. A.A. Broekhuis
	Prof. dr. ir. A.J. Minnaard
	Prof. dr. J. G. de Vries

ISBN: 978-90-367-4160-6
ISBN: 978-90-367-4159-0 (elektronische versie)

Table of contents

Summary

Precious metals are rare metals having a high chemical inertness and a high melting point. The best known precious metals are gold, silver and platinum. Other precious metals are the platinum metals ruthenium, rhodium, palladium, osmium and iridium. Platinum metals have the ability to catalyse many reactions and are widely used in the chemical industry. Heterogeneous platinum catalysts are for example applied in the hydrotreatment of hydrocarbons and the production of vitamin K_4. Examples of the application of homogeneous platinum metals are the production of methyl acetate and polyketones. For homogeneous catalysis, a broad range of ligands are available to increase the activity or selectivity of the catalyst for a certain reaction. Asymmetric catalysis is a powerful methodology for the preparation of enantio-pure organic molecules for the fine chemical- and pharmaceutical industry. In asymmetric catalysis, especially in asymmetric hydrogenation- and carbonylation reactions, platinum metals such as Rh, Ir and Ru are frequently used.

Chapter 1 provides an introduction into platinum metal catalysis. A general overview of the use of homogeneous and heterogeneous platinum metal catalysts in the industry is given. Subsequently the most important developments over the years for the platinum metals catalysed homogeneous hydrogenation- and carbonylation reactions are reviewed, with an emphasis on asymmetric catalysis.

Chapter 2 is dedicated to catalytic hydrocarbonylation reactions. This transformation involves the reactions of syngas with 1-alkenes to form oxygenated product like aldehydes/alcohols, oligomers/polymers and monoketones (Scheme 1).

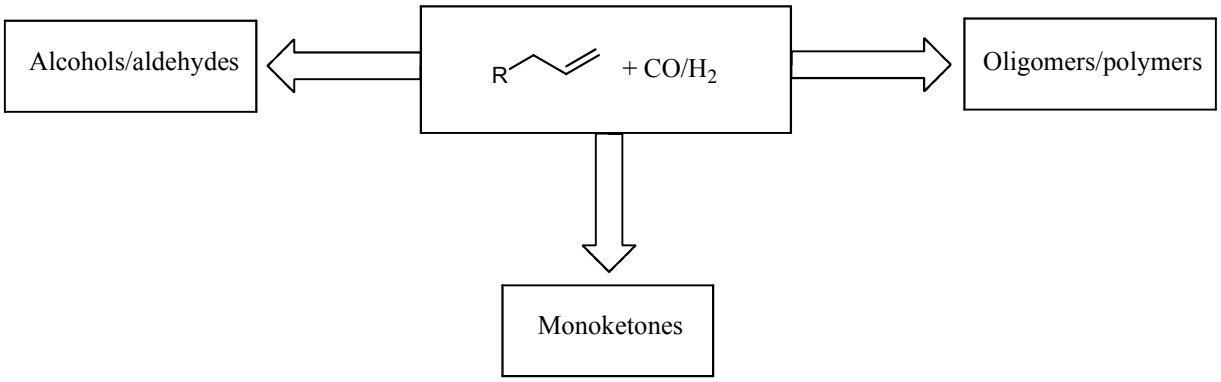

Scheme 1 Overview of the olefin/syngas product tree.

The selective production of monoketones is known as a hydro-acylation reaction. Drent and Budzelaar were the first to provide the proof of principle for the selective formation of ketones by hydrocarbonylation of higher olefins with a homogeneous palladium diphosphine catalyst of the type L_2PdX_2. Here L_2 represents a bidentate alkylphosphine, and X stands for a weakly or non-coordinating anion.

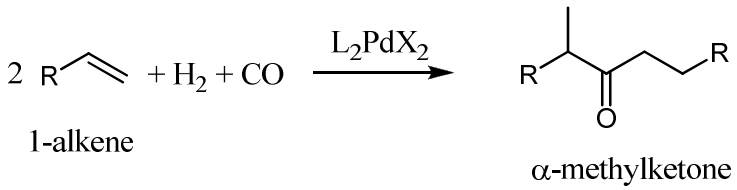

Scheme 2 Hydro-acylation of 1-alkenes to α-substituted ketones.

In Chapter 2 the influence of process conditions on the activity and selectivity of the hydro-acylation of 1-alkenes with syngas to head-to-tail monoketones (α-methylketones) using homogeneous palladium catalysts of the type L_2PdX_2 (Scheme 2) is described. A bidentate alkylphosphine, 1,3-bis(di-sec-butylphosphino)propane, in combination with a weakly coordinating anion in the form of a triflate was used. A typical molar ratio of the catalyst components was Pd: L_2: X = 1:2.4:8. The reaction temperature was varied between 30-125 °C. Remarkably, the catalyst was even active at 30 °C. The chemoselectivity of the reaction was, among others, a function of the temperature. The highest selectivity for monoketones was obtained with 1-pentene in dichloromethane at 60 °C, namely 98% for the head-to-tail

monoketones (P = 60 bar). Other products were diketones and olefin dimers. The olefin conversion was negatively affected by olefin isomerisation, a process that appeared very facile at temperatures above 60 °C.

In Chapter 3 an experimental study on the synthesis of enantio-enriched 4-methyl-5-decanone (head-to-tail monoketone) by a Pd-catalyzed asymmetric hydro-acylation of 1-pentene with H_2/CO mixtures is reported. A homogeneous palladium catalyst of the type $(L_2)Pd(OTf)_2$ was used where L_2 represents a chiral diphosphine ligand. A total of 16 diphosphine ligands belonging to four different chiral ligand classes (Josiphos, DuPhos, Walphos and ferroTANE) were studied. The reactions were carried out in dichloromethane at reaction temperatures between 60-125 °C and at initial H_2 and CO pressures of 30 bar each. The enantio-, chemo- and regioselectivity of the reaction are a clear function of the diphosphine ligand and the temperature. The highest ee for the desired 4-methyl-5-decanone was 39% for a Josiphos (Figure 1) type ligand (60 °C), though the product selectivity was low (6 mol%). Lower ee values (< 20%) were obtained for the Duphos ligands, albeit at a higher product selectivity (> 42 mol%).

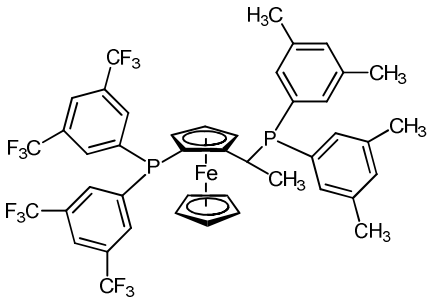

(R,S)-SL-J008-1

Figure 1 Josiphos (R,S)-SL-J008-1 ligand.

In Chapter 4, the effect of process conditions (temperature, partial pressures of CO and H_2) on the product selectivity and ee of the palladium catalysed asymmetric hydro-acylation of 1-pentene in dichloromethane with the chiral Josiphos ligand (SL-J008-1) was investigated. The highest ee value (73%) was obtained at the lowest temperature in the range (30 °C). The 4-methyl-5-decanone selectivity was between 12 and 20 mol% at these conditions. Statistical

modeling was applied to quantify the influence of the process conditions on the product selectivity and ee.

In the fifth chapter of this dissertation the overall kinetics of the enantioselective hydrogenation of methyl 2-acetamido acrylate to 2-acetylamino-propionic acid methyl ester with hydrogen using a chiral Rhodium/MonoPhos™-complex [Rh-((S)-Monophos)$_2$(COD)]BF_4 in IPA (iso-propanol) was investigated in a batch reactor (Scheme 3). All experiments were performed isothermally at a reaction temperature of 10 ºC, with variable initial hydrogen pressures (6-10 bara), catalyst precursor concentration (0.1-0.4 mmol/l) and substrate concentration (17-77 mmol/l). The product ee was > 97.6 % for all experiments with a S/C ratio < 400). The experimental data of 12 experiments was modeled successfully using a kinetic expression derived from the Halpern hydrogenation mechanism for bidentate phosphine ligands combined with catalyst activation and deactivation terms.

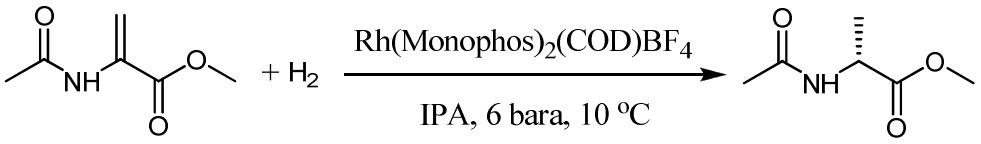

Scheme 3 Hydrogenation of methyl 2-acetamido acrylate using a rhodium/Monophos complex.

In the sixth chapter, the platinum metal ruthenium was used as a catalyst for a one pot synthesis of γ-valerolactone (GVL) from C6-sugars (Scheme 4). GVL is considered a very interesting green, bio-based platform chemical with high application potential. D-glucose, D-fructose, sucrose and cellulose were applied as the substrates and an acid catalyst in combination with a hydrogenation catalyst (Ru/C) and either molecular hydrogen or formic acid as the hydrogen donor were used. For formic acid, the highest yield of GVL (52 mol%) was obtained at 180 °C, 16 h reaction time and D-fructose as the C6-sugar source in combination with TFA and Ru/C in water. The major by-products were insoluble solids, known as humins, formed during the acid catalysed conversion of D-fructose to the intermediate levulinic acid (LA). When using molecular hydrogen as the hydrogen source, the highest yield of GVL (62 mol%) was obtained using D-fructose in combination with TFA and Ru/C in water (180 °C, 94 bar H_2, 8 h). Complete

conversion of D-fructose was observed at these conditions. The major by-products were formic acid and insoluble solid materials (humins). The use of a pre-formed homogeneous water soluble ruthenium catalysts from $RuCl_3$ and tris(3-sulfonatophenyl)phosphane (TPPTS) in combination with TFA gave quantitative C6-sugar conversions but a lower GVL yield (23 mol%) compared to the heterogeneous Ru catalyst.

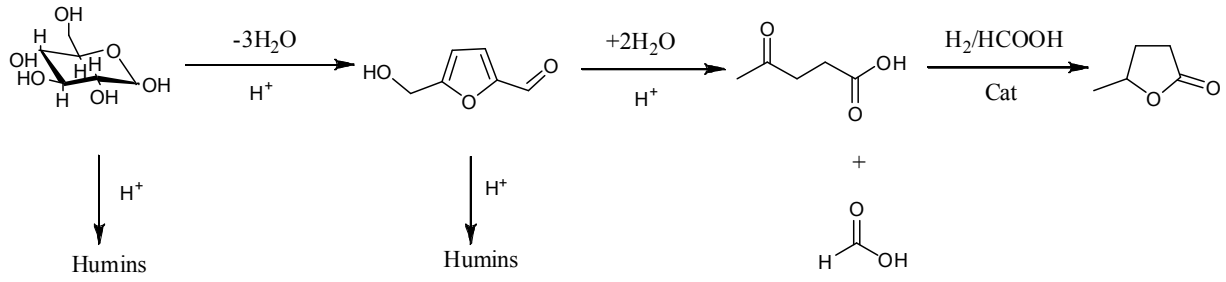

Scheme 4 The acid catalysed hydrolysis of D-glucose to LA and subsequently hydrogenation of LA to GVL.

Samenvatting

Edelmetalen zijn zeldzame metalen met een hoge chemische inertheid en een hoog smeltpunt. De bekendste edelmetalen zijn goud, zilver en platina. Andere minder bekende edelmetalen zijn de platinametalen ruthenium, rhodium, palladium, osmium and iridium.

Platinametalen hebben de eigenschap om vele soorten reacties te kunnen katalyseren en worden daarom veel gebruikt als katalysator in de chemische industrie. Heterogene platina katalysatoren worden bijvoorbeeld toegepast voor de behandeling van koolwaterstoffen met waterstof en in de productie van vitamine K_4. Homogene platinametalen worden gebruikt voor de productie van methylacetaat en polyketonen. De activiteit en selectiviteit van een homogene katalysator kan gestuurd worden door ligand variatie. Bij toepassing van chirale liganden is het mogelijk om een reactie enantioselectief te maken, we spreken dan van asymmetrische katalyse. Dit is een krachtige methode gebleken voor de bereiding van enantio zuivere organische moleculen voor de fijnchemische en farmaceutische industrie. In de asymmetrische katalyse en met name in asymmetrische hydrogenerings- en carbonylerings reacties worden platinametalen zoals Rh, Ir en Ru veelvuldig gebruikt.

Hoofdstuk 1 geeft een inleiding over het gebruik van platinametalen in de katalyse. Als eerste wordt een algemeen overzicht gegeven van de toepassing van deze metalen als homogene en heterogene katalysatoren in de chemische industrie. Vervolgens worden de belangrijkste onderzoek ontwikkelingen in de afgelopen decennia geschetst met betrekking tot de toepassing van platinametalen als katalysatoren in hydrogenerings- en carbonylerings reacties. De nadruk ligt hierbij op de asymmetrische katalyse.

Hydrocarbonylerings reacties zijn reacties waarbij (eindstandige) olefines met synthesegas omgezet worden tot een divers scala aan producten zoals aldehyden/alcoholen, CO/olefine oligomeren/polymeren en monoketonen (Schema 1).

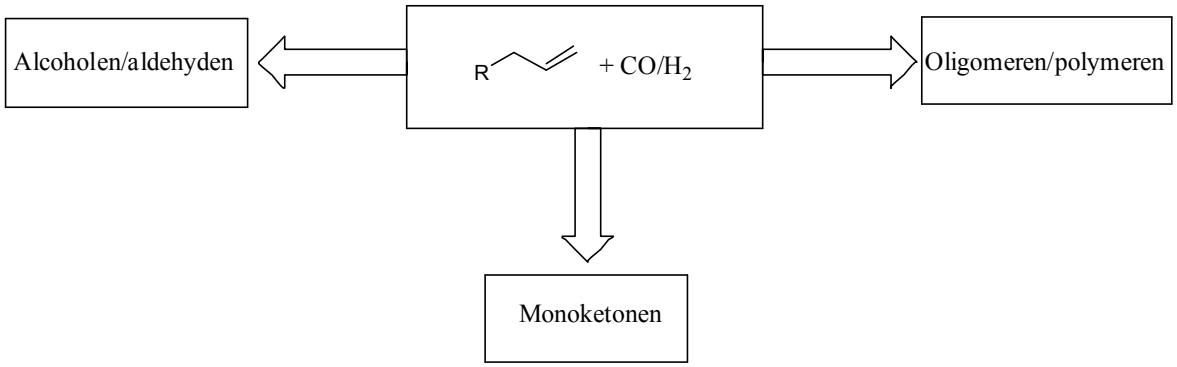

Schema 1 Overzicht van de olefine/synthesegas productboom.

De omzetting van olefines en synthesegas tot monoketonen wordt ook wel een hydro-acylerings reactie genoemd. Drent en Budzelaar waren de eersten die de selectieve vorming van ketonen door middel van een hydrocarbonylering van hogere olefines met een homogene palladium difosfine katalysator van het type L_2PdX_2 aantoonden. Als ligand L_2 wordt een bidentate alkylfosfine gebruikt en X is een zwak coördinerend of niet-coördinerende anion.

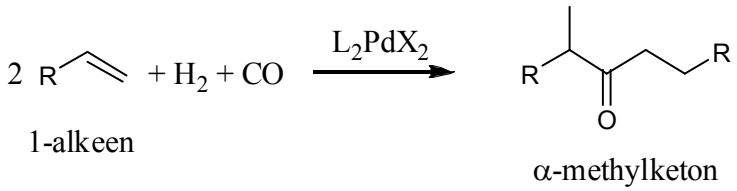

Schema 2 Hydro-acylering van 1-alkenen naar α-gesubstitueerde ketonen.

In hoofdstuk 2 wordt de invloed van procescondities op de activiteit en de selectiviteit van de hydro-acylering van 1-alkenen met synthesegas naar head-to-tail monoketonen (α-methylketonen) onderzocht met behulp van een homogene palladium katalysator van het type L_2PdX_2 (Schema 2). Het geselecteerde bidentate alkylfosfine was 1,3-bis(di-sec-butylfosfino)propaan. De molaire verhoudingen van katalysator componenten was Pd: L_2: X = 1:2.4:8. De reactietemperatuur werd gevarieerd tussen 30 en 125 °C. De chemoselectiviteit van de reactie is sterk afhankelijk van de temperatuur. De hoogste selectiviteit voor de vorming van monoketonen werd verkregen met 1-penteen in dichloormethaan bij 60 °C, namelijk 98% voor

head-to-tail monoketonen (P = 60 bar). Andere producten waren diketonen en olefine dimeren. Daarnaast bleek dat de olefine omzetting negatief werd beïnvloed door olefine isomerisatie.

In hoofdstuk 3 wordt een studie beschreven naar de enantioselectieve synthese van 4-methyl-5-decanone (head-to-tail monoketone) door gebruik te maken van een Pd-gekatalyseerde (asymmetrische) hydro-acylering van 1-penteen met H_2/CO mengsels. Hiervoor werd een homogene palladium katalysator van het type $(L_2)Pd(OTf)_2$ gebruikt. In totaal werden 16 difosfine liganden behorend tot vier verschillende chirale ligand groepen (Josiphos, DuPhos, Walphos en ferroTANE) getest. De reacties werden uitgevoerd in dichloormethaan bij reactietemperaturen variërend tussen 60-125 °C en een initiële H_2 en CO druk van 30 bar elk. De enantio-, chemo- en regioselectiviteit van de reactie zijn afhankelijk van het gebruikte difosfine ligand en de temperatuur. De hoogste ee voor het gewenste 4-methyl-5-decanone was 39% en werd verkregen met een Josiphos (Figuur 1) type ligand (60 °C), hoewel de product selectiviteit laag was (6 mol%). Lagere ee waarden (< 20%) werden verkregen met de Duphos liganden, maar met een hogere product selectiviteit (> 42 mol%).

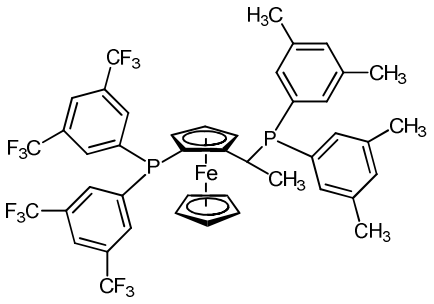

(R,S)-SL-J008-1

Figuur 1 Josiphos (R,S)-SL-J008-1 ligand.

In hoofdstuk 4 is de invloed van de procescondities (temperatuur, partiële CO en H_2 druk) op de product selectiviteit en de ee van de palladium gekatalyseerde asymmetrische hydro-acylering van 1-penteen in dichloormethaan met het chirale Josiphos ligand (SL-J008-1) onderzocht. De hoogste ee waarden (73%) werden verkregen bij de laagst gebruikte reactietemperatuur (30 °C). Een 4-methyl-5-decanone selectiviteit van tussen de 12 en 20 mol% werd verkregen bij deze

condities. De invloed van de procescondities op de productselectiviteit en ee is gekwantificeerd met statistisch modellen.

In het vijfde hoofdstuk van dit proefschrift wordt een experimentele studie naar de kinetiek van de enantioselectieve hydrogenering van methyl 2-aceetamido acrylaat met waterstof tot 2-acetylamino-propionzuur methyl ester met behulp van een chirale Rhodium/MonoPhos™-complex [Rh-((S)-Monophos)$_2$(COD)]BF_4 in IPA (iso-propanol) beschreven (Schema 3). Alle experimenten werden isotherm uitgevoerd in een batchreactor bij een temperatuur van 10 ºC, met variabele initiële waterstof drukken (6-10 bara), katalysator uitgangsstof concentraties (0.1-0.4 mmol/l) en substraat concentraties (17-77 mmol/l). De product ee was > 97.6% voor alle experimenten met een S/C verhouding < 400.

De experimentele data van 12 experimenten werd met succes gemodelleerd met behulp van een kinetische uitdrukking afgeleid van het Halpern hydrogenerings mechanisme voor bidentate fosfine liganden gecombineerd met een term voor katalysator activering en deactivering.

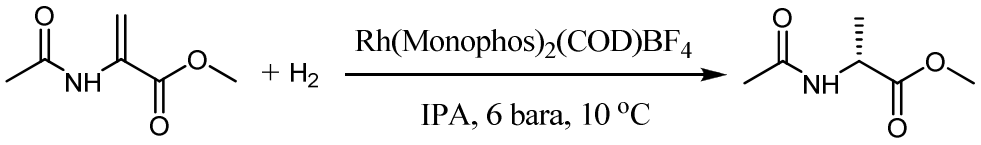

Schema 3 Hydrogenering van methyl 2-aceetamido acrylaat gebruikmakend van een rhodium/Monophos complex.

In het zesde hoofdstuk wordt onderzoek beschreven naar een ‘one pot’ synthese van γ-valerolactone (GVL) uit C6-suikers (Schema 4) met behulp van homogene en heterogene Ru katalysatoren. GVL wordt beschouwd als een zeer interessante groene, bio-gebaseerde grondstof met veel mogelijke toepassingen. In dit onderzoek beschrijven we een one pot katalytische synthese van GVL uit C6-suiker bronnen (D-glucose, D-fructose, sucrose en cellulose) met behulp van een zure katalysator in combinatie met een hydrogenerings katalysator (Ru/C) en moleculaire waterstof of mierenzuur als de waterstofdonor. Bij het gebruik van mierenzuur werd de hoogste opbrengst aan GVL (52 mol%) verkregen bij 180 °C, 16 uur reactietijd en met D-

fructose als de C6-suiker bron in combinatie met TFA en Ru/C in water. De belangrijkste bijproducten waren onoplosbare vaste stoffen, ook wel humins genoemd, gevormd tijdens de zuur gekatalyseerde omzetting van D-fructose naar het intermediaire levulinezuur (LA). Bij gebruik van moleculaire waterstof als waterstofbron werd het hoogste rendement aan GVL (62 mol%) behaald met D-fructose in combinatie met TFA en Ru/C in water (180 °C, 94 bar H_2, 8 uur). Een volledige D-fructose conversie werd verkregen bij deze condities. De belangrijkste bijproducten waren mierenzuur en onoplosbare vaste stoffen (humins). Het gebruik van een voorgevormde homogene water oplosbare ruthenium katalysator uit $RuCl_3$ en tris(3-sulfonatofenyl)phosphane (TPPTS) in combinatie met TFA gaf kwantitatieve C6-suiker conversies, maar met een lagere opbrengst aan GVL (23 mol%) dan vergeleken met de heterogene Ru katalysator.

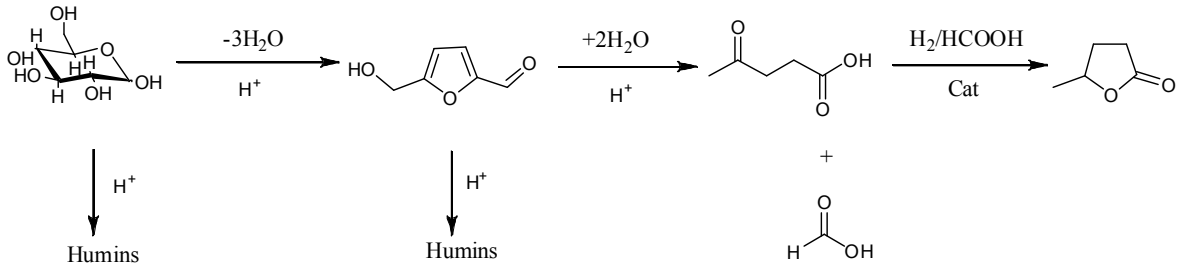

Schema 4 De zuur gekatalyseerde hydrolyse van D-glucose naar LA en vervolgens de hydrogenering van LA naar GVL.

Chapter 1. Introduction

1.1 Precious- and platinum metals

Precious metals like silver and gold are valuable metals that are relatively scarce and chemically rather inert. Gold and silver are not the only precious metals and another important group is formed by the platinum group metals, six elements clustered together in the periodic table consisting of platinum, ruthenium, rhodium, palladium, osmium and iridium.[1,2] Precious metals are mainly mined in Russia and South Africa, together these two countries contribute to more than half of the world's precious metals production.[1,2] Nowadays precious and platinum metals are still used for jewellery and as an alternative investment for global currencies and fixed assets in the financial sector (especially Au).[1,3] Platinum metals in the industrial sector are mainly used as catalysts. Examples are found in the chemical industry and in the automotive industry, where the metals are the major components in catalysts for exhaust gas cleaning. Other application areas are the glass industry (moulds) and the electronic and electrical industry.[2,4] As suggested by the name precious and platinum metals are expensive metals. This is illustrated in Table 1.1, where the trade prices (as per 15-05-2009) are given.

Table 1.1 Trade prices of precious metals.[5]

	Pt	Au	Ag	Rh	Ru	Pd	Os	Ir
Price ($/oz)	1123.00	926.30	14.02	1250.00	85.00	227.00	380.00	425.00

1.1.1 Platinum metals in catalysis

Precious metals were, despite their supposed inertness, already used in the early days of catalysis. In the beginning of the 19th century a series of discoveries were made involving the use of precious metals. Examples are the catalytic oxidation of coal gas and air by a Pt wire (Sir H. Davy, 1817), the Pt- catalysed oxidation of ethanol to produce acetic acid and water (J. W. Döbereiner, 1822) and the ignition of hydrogen and air by a platinum sponge (J. W. Döbereiner, 1823).[6-8] In general platinum metals in catalysis are versatile and broadly applicable, active at

milder conditions compared to other metals and show higher selectivities.[2] Nowadays, platinum metals are used to catalyse a broad range of reactions. Examples are hydrogenations, oxidations, dehydrogenations, hydrogenolysis, hydrosilylations, carbon-carbon and carbon-heteroatom coupling, carbonylations and hydroxylations.[2]

1.1.2 Platinum metals in industrial heterogeneous catalysis

The most important processes in industry involving heterogeneous platinum group metal catalysts in one of the processing steps are given chronologically in Table 1.2.

Table 1.2 The use of platinum group metals in heterogeneous catalysis throughout time.[8-11]

year	process	Catalyst (main component)
1870	SO_2 oxidation	Pt
1910	NH_3 oxidation to nitric acid	Pt/Rh nets
1940	Catalytic reforming of hydrocarbons (gasoline)	Pt/Al_2O_3
1940	Benzene hydrogenation to cyclohexene	Pt
1960	Xylene hydro-isomerisation	Pt
1960	Improved hydrocarbons reforming	Pt-Ir on Al_2O_3, Pt-Re on Al_2O_3
1960	Ethylene oxidation to vinyl acetate	Pd/Cu
1970	Auto exhaust gas catalysts	Pt, Rh, Pd on oxide
1970	Hydro-isomerisation	Pt/zeolite
1980	Vinyl acetate from ethene and acetic acid	Pd
1980	Hydrotreatment of hydrocarbons	Pt/zeolite
1980	Vitamin K_4 production (hydro-acetylation)	Pd membrane
1990	Complete combustion of natural gas	Precious metals and/or mixed oxides

The first real use of a heterogeneous platinum metal in an industrial process was the application of platinum for the oxidation of SO_2 to SO_3 in the production of sulphuric acid. In Germany at the start of the 20th century the need for nitrogen compounds for agriculture and later for weapon production stimulated the development of ammonia production processes and the oxidation of ammonia to produce nitric acid. For the latter purpose, the platinum metals platinum and rhodium were used extensively. Just before and during de second world war in Germany almost all hydrocarbons were produced from coal. Coal was treated in coke ovens to produce

ethylene form acetylene and aromatics, coal was hydrogenated into liquids used in chemical industry and gasified into synthesis gas. Platinum was used in reforming and hydrogenation reactions. In the sixties hydrocarbon reforming processes were greatly improved by using bimetallic catalyst of platinum with iridium or rhenium. Also the use of the platinum metal palladium in the oxidation of ethylene to vinyl acetate was introduced in industrial catalysis at this time. The use of platinum metals for car exhaust catalysts in the seventies gave a large boost to the use of platinum, rhodium and palladium for catalytic purposes. At that time, also improved hydro-isomerisation platinum based catalysts were introduced. In the eighties palladium catalysts were shown potential for the production of vinyl acetate from ethene and acetic acid and the production of vitamin K_4 (hydro-acetylation of 2-methyl 1,4-naphthoquinone). In the nineties precious and platinum metals were introduced as catalysts for the complete combustion of natural gas.[8-11]

1.1.3 Platinum metals in industrial homogenous catalysis

Homogeneous platinum metal catalysts for industrial scale processes were introduced much later than heterogeneous platinum metal catalysts. Already in 1870, the first heterogeneous platinum metal catalysts were applied industrially. The first industrial process with a homogeneous platinum metal catalyst was introduced more than 80 years later. It involves the Wacker oxidation of ethylene to acetaldehyde using a palladium catalyst.[8,12] In the seventies a real boost in the application of homogenous catalysts was observed, resulting in three new industrial processes namely the palladium catalysed ethylene oxidation to acetaldehyde, the rhodium catalysed methanol carbonylation to acetic acid and a rhodium catalysed asymmetric hydrogenation to L-DOPA.[8,9] The most important processes in the bulk chemical industry involving homogeneous platinum metal catalysts are given chronologically in Table 1.3.

Table 1.3 Platinum metals for homogeneous catalysis in bulk chemical processes.[8,9]

year	process	Catalyst (main component)
1950	Ethylene oxidation to acetaldehyde	Pd
1970	Acetic acid from MeOH (carbonylation)	Rh
1970	Improved hydroformylation	Rh
1970	L-DOPA process (fine chemicals)	Rh
1980	Methyl acetate (carbonylation)	Rh
1990	Polyketone (CO and ethene)	Pd

1.2 Homogeneous hydrogenation reactions with platinum metals

The first hydrogenation reaction involving a homogeneous catalyst is likely the reduction of quinone to hydroquinone by a homogeneous copper system (cuprous acetate-quinoline) in 1938 by Calvin.[13] The real breakthrough in hydrogenation reactions catalysed by homogeneous catalysts was the discovery of the Wilkinson catalyst ($RhCl(PPh_3)_3$) in the 1960's for the reduction of olefins with hydrogen.[12,14]

1.2.1 Homogenous asymmetric hydrogenation reactions

Asymmetric catalysis is a powerful methodology for the synthesis of chiral components. An important transformation is the asymmetric hydrogenation of prochiral substrates using chiral homogeneous metal catalysts. Asymmetric hydrogenations are mostly performed with the platinum metals Rh, Ir and Ru.[15] After the discovery of the Wilkinson catalyst for the hydrogenation of olefins, chemist also started working on catalysts for asymmetric hydrogenations, with an emphasis on chiral Rh/phosphine catalysts.[14,16,17] A well known chiral phosphine ligand is CAMP **1,** developed by Knowles in the 1970's.[18] This ligand was applied in the synthesis of L-DOPA **2**, an anti Parkinson drug. The synthesis involves the hydrogenation of a prochiral cinnamic acid derivative (**3**) and yielded the hydrogenated product with an ee of 88% (Scheme 1.1). This process is the first example of the use of asymmetric hydrogenation on an industrial scale.[16,17]

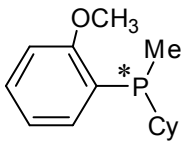

1

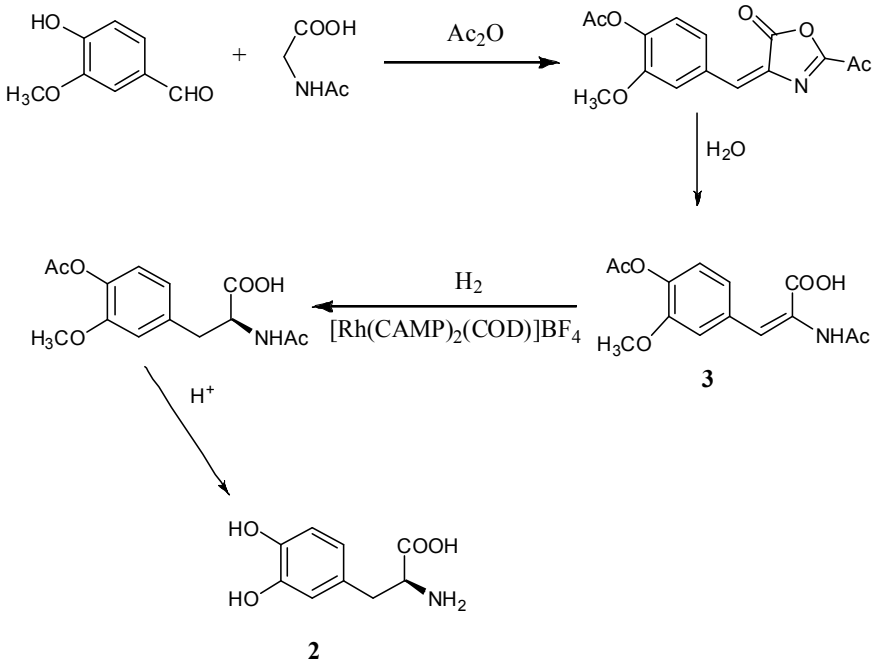

3

2

Scheme 1.1 L-DOPA process with the rhodium CAMP catalyst.

Further improvements involved the use of the DIOP ligand **4** by Kagan (1971) and DIPAMP **5** (1974), leading to product ee 's of up to 95%.[16,17,19,20]

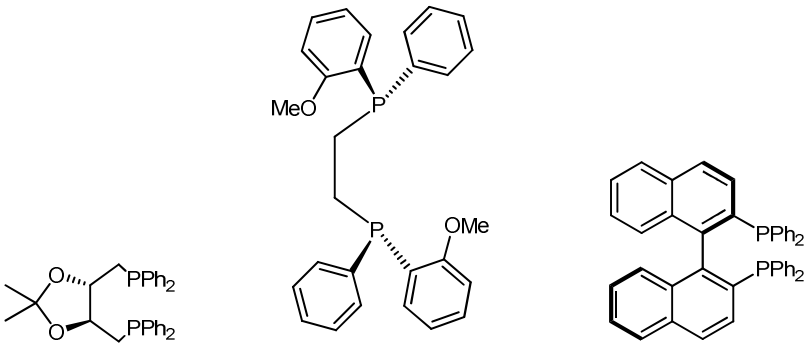

4 **5** **6**

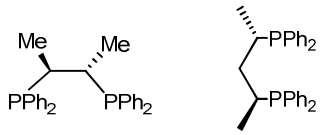

7 **8**

A major breakthrough in the field came by the introduction of the chiral BINAP ligand **6** in 1980 by Noyori[17] Rh-BINAP catalysts also showed to be excellent catalysts for the asymmetric isomerisation of allylic amines. This invention was successfully applied in one of the steps of the (-)-menthol process.[17] Other versatile diphosphine ligands introduced at that time are the CHIRAPHOS (**7)** and SkewPhos (**8)** ligands, developed by Bosnisch (1980).[18,21,22] Subsequent studies showed that Ru-BINAP catalysts are also very versatile for, among others, the asymmetric hydrogenation of various functionalized olefins (activated ketones, α,β-unsaturated acids, allylic alcohols an enamides).[17,19,20,23] A recent example of an industrial process involving a Ru-BINAP catalyst is the production of intermediate **10** from a α-substituted-β-ketoester **9** (Scheme 1.2). This conversion is a key step on the synthesis of a carbapenem. This carbapenem is currently produced using this synthetic methodology at a scale of 100 tons per annum (Takasago process).[15,24]

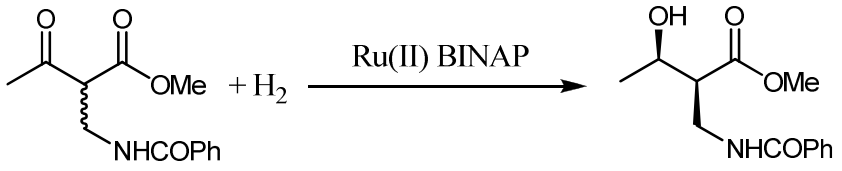

9 **10**

Scheme 1.2 Asymmetric hydrogenation by a ruthenium BINAP catalyst in a carbapenem process.

In the early 90's, Burk at Dupont developed the chiral phospholane ligands Duphos (**11)** and BPE (**12)**. The ligands were especially used for Rh-catalyzed hydrogenations, examples are the synthesis of α- or β-amino acids and the hydrogenation of arylenamides, itaconic acid derivatives, enol acetates.[24] An example of the use of Rh-Duphos catalysts in industrial asymmetric

hydrogenation is given in Scheme 1.3. It involves the hydrogenation of dimethyl itaconate (**14)** to produce (*s*)-dimethyl methylsuccinate (**15)**, which is a building block for the synthesis of several kinds of drugs (Dowpharma process).[19,24,25]

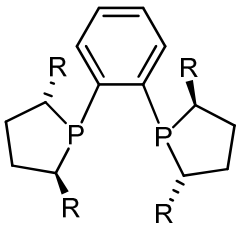

11

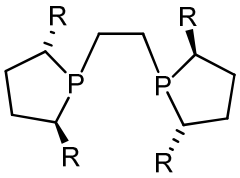

12

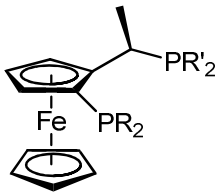

13

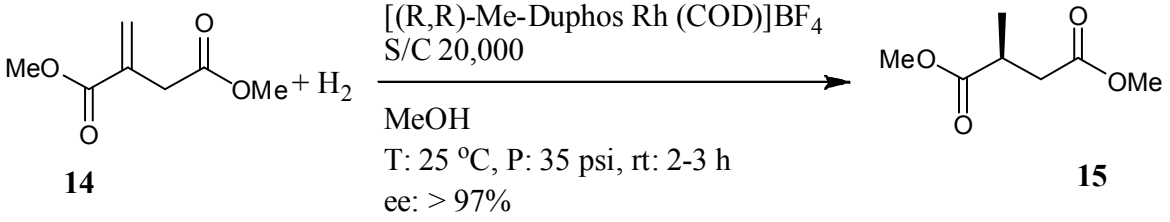

14 **15**

Scheme 1.3 Very active and selective asymmetric hydrogenation of dimethyl itaconate, with a rhodium Duphos catalyst.

In 1993 Togni reported the synthesis of various Josiphos ligands (**13**), which were shown to be very efficient for asymmetric hydrogenations (C=N and C=C bonds, itaconic acid derivatives and enamides).[12,23,26-28] The Josiphos ligands are particularly useful for library synthesis as the two chelating donors can be easily modified to provide ligands with a broad range in steric and electronic properties. An example of an industrial asymmetric hydrogenation reaction involving a iridium- Josiphos system (Xyliphos, **16**) is the asymmetric hydrogenation of MEA imine (**17)** to an intermediate (**18)** in the (*s*)-metolachlor (**19**) process (GibaGeigy/Syngenta process). At a reaction temperature of 50 ºC and a H_2 pressure of 80 bar, a TOF of 400,000 1/h and a product ee of 80% was obtained (Scheme 1.4).[24,26]

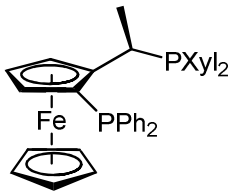

16

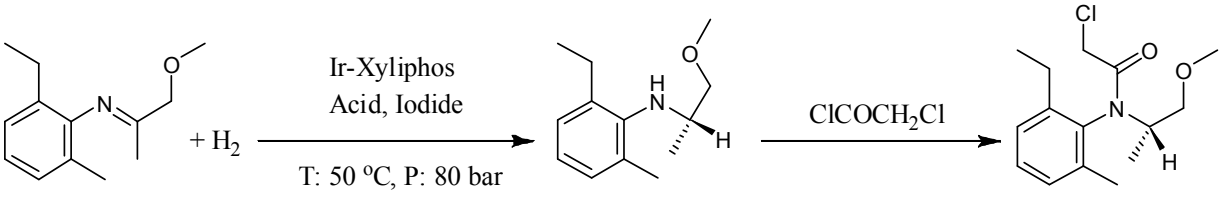

17 **18** **19**

Scheme 1.4 Very active hydrogenation of MEA imine with an iridium Xyliphos catalyst.

Examples of more recently developed chiral diphosphine ligands are BICP (**20)** developed by Zhang in 1997, MiniPHOS (**21)** reported by Imamoto in 1999 and SDP (**22)** developed by Zhou in 2003.[18,29-31]

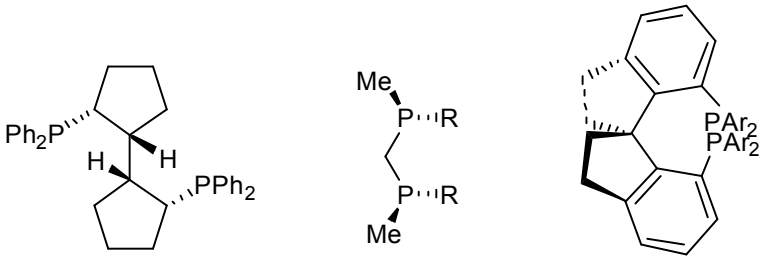

20 **21** **22**

Research activities aiming at the discovery and use of monodentate phosphine ligands in asymmetric catalysis were very limited after the discovery of chiral diphosphine ligands.[32] This was mainly due to the general belief that high stereo-discrimination in asymmetric catalysis was only possible by using diphosphine ligands. Almost 30 years after the discovery of CAMP,

pioneering studies by the groups of Feringa, de Vries and Minnaard (monodentate phosporamidite **23**)[33-36], Pringle (monodentate phosphonites **24**)[37], Reetz (monodentate phosphites **25**)[38,39] and Zhou (monodentate spiro phosphoramidites **26**)[40] showed that comparable or even better performance for the rhodium catalysed asymmetric hydrogenation of e.g. α-dehydroamino acids and itaconic acid derivatives could be obtained with these types of ligands.

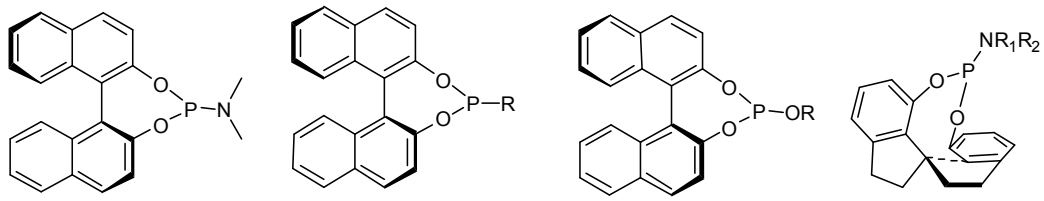

23 **24** **25** **26**

In general the synthesis of monodentate ligands is less complex compared to the synthesis of bidentate ligands and tuning the monodentate ligands is also relatively easy.[32, 41] An example of an industrial application of monodentate phosphorus ligands is the recently implemented asymmetric hydrogenation of the substituted acyclic acid **27** to **28** (Scheme 1.5), by using the phosphoramidate ligand **29** (mixed rhodium-**29**-PPh_3 catalyst), on a production scale by DSM.[42-44]

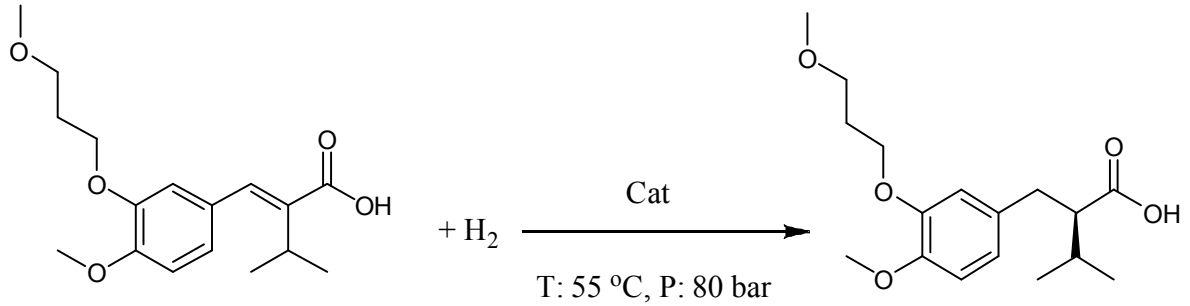

27 **28**

Scheme 1.5 Asymmetric hydrogenation of the substituted acyclic acid **27,** by a rhodium-**29**-PPh_3 catalyst, in the DSM process.

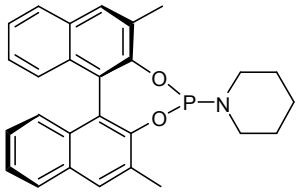

29

1.3 Homogeneous carbonylation reactions with platinum metals

Carbonylation reactions involve reactions of carbon monoxide with substrates, whereas hydrocarbonylation reactions are typically carried out with a mixture of CO and hydrogen instead of CO only. The first homogenous catalyst for carbonylation/hydrocarbonylation reactions was a cobalt catalyst (Roelen 1938), used for the production of aldehydes (commercialized in 1948).[8,12] The first homogeneous platinum metal for a carbonylation reaction on industrial scale was a rhodium (iodide promoted) complex. It was applied for the synthesis of acetic acid from methanol (Scheme 1.6). This process has been commercialised by Monsanto (1968).[8,12] Recently, the use of iridium for this reaction was successfully demonstrated on commercial scale by BP.[45] Some other examples of carbonylation reaction are methoxycarbonylation, olefin-CO copolymerisation and hydrocarbonylation reactions, the latter will be discussed in more detail in following sections.

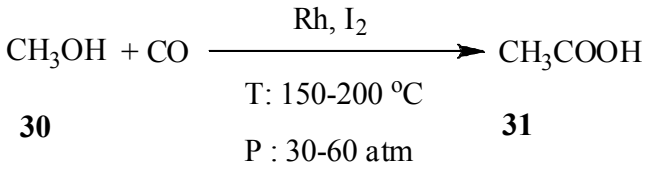

30 **31**

Scheme 1.6 Monsanto acetic acid process.

1.3.1 Hydroformylation/hydrocarbonylation reactions

Catalytic hydroformylation and hydrocarbonylation reactions, also known as the oxo-synthesis, were by accident discovered by Roelen in the late thirties of the previous century.[8,46] It was demonstrated that the reaction of ethene with CO and H_2 catalysed by cobalt resulted in the

production of mainly 1-propanal, some alcohols and minor amounts of ketones.[47] Scheme 1.7 illustrates the hydroformylation of a 1-alkene (**32**). Two aldehydes may be formed, a linear **(33)** and a branched **(34)** product. For most applications, the linear aldehyde is the preferred product and the formation of branched products should be suppressed as much as possible. Initially the catalyst was a heterogeneous supported cobalt catalyst, later it became clear that the active species is actually a soluble homogeneous $HCo(CO)_4$ species.

The first cobalt-catalysed hydroformylations were performed at high syngas pressures (200-300 bar) to maintain catalyst stability. In the sixties, tertiary alkyl-phosphine ligands were introduced. These were shown to have a positive effect on catalyst stability and allowed the development of a lower pressure, higher temperature process (Shell process). The reaction is slower than the original process but it is more selective to the desired linear product.[8,12,45,48] In the seventies the platinum metal rhodium was introduced as a hydroformylation catalyst. It showed to be more active and selective (towards linear product) than the cobalt-based catalyst under milder conditions.[8] Since these discoveries, Rh-based catalysts have been further improved and tuned to give better selectivities and activities.

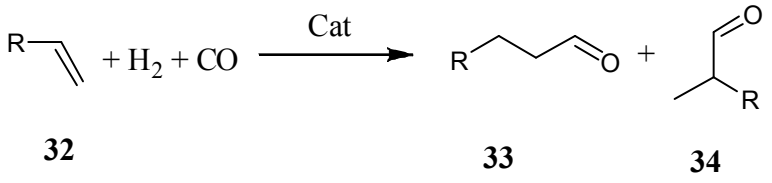

32 **33** **34**

Scheme 1.7 General representation of the hydroformylation of a 1-alkene

A major disadvantage of the use of rhodium catalysts is isomerisation of the α-olefin to internal olefins. Therefore the hydroformylation of higher alkenes is nowadays mainly still performed with cobalt catalysts.[8]

1.3.2 Chemoselectivity in the oxo-synthesis

As already demonstrated in the 30's by Roelen, the hydrocarbonylation of 1-alkenes allows the synthesis of aldehydes, alcohols and ketones. However, Roelen never succeeded in achieving reasonable chemoselectivity.[48] Drent and Budzelaar were the first to show the selective formation

of ketones by hydrocarbonylation of higher olefins with a homogeneous palladium diphosphine catalyst (Scheme 1.8).[48]

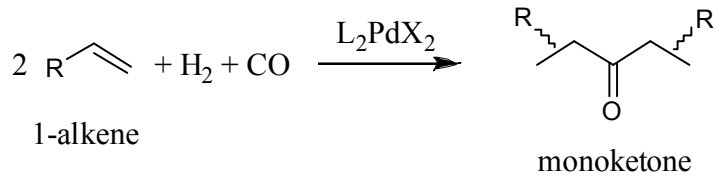

Scheme 1.8 Hydrocarbonylation of higher olefins to ketones with a homogeneous palladium diphosphine catalyst.

This catalyst was originally developed by Drent for the production of alternating copolymers from olefins and CO (Scheme 1.9).[48-50]

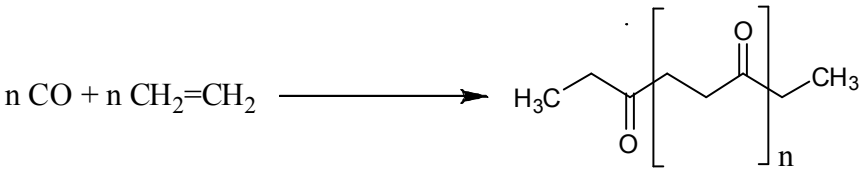

Scheme 1.9 Alternating copolymerisation of ethene and CO.

1.3.2.1 Palladium catalysed hydro-acylation and hydroformylation

In 2000 Drent and Budzelaar showed that it was possible to produce monoketones **37**, aldehydes/alcohols **38** and oligoketones **39** from higher alkenes using homogeneous Pd catalysts of the type L_2PdX_2 (L_2 represents a diphosphine ligand and X stands for a weakly or non-coordinating counter ion (Scheme 1.10). The chemo-selectivity may be steered to the desired product by the choice of the diphosphine ligand, process conditions and solvent.[48, 51, 52] Ligands with a relatively low basicity in combination with a strong acid favoured the selectivity towards oligoketones. An increase in ligand basicity shifts the selectivity towards monoketones. Suitable ligands for this purpose are alkyl substituted diphosphines, like 1,3-bis(di-sec-butylphosphino)propane (**35**). More basic ligand in combination with a relative weak acid favour aldehyde and alcohol formation.[48, 52, 53]

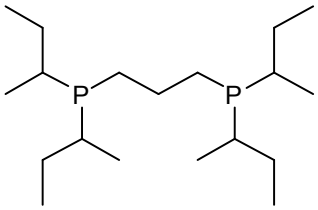

35

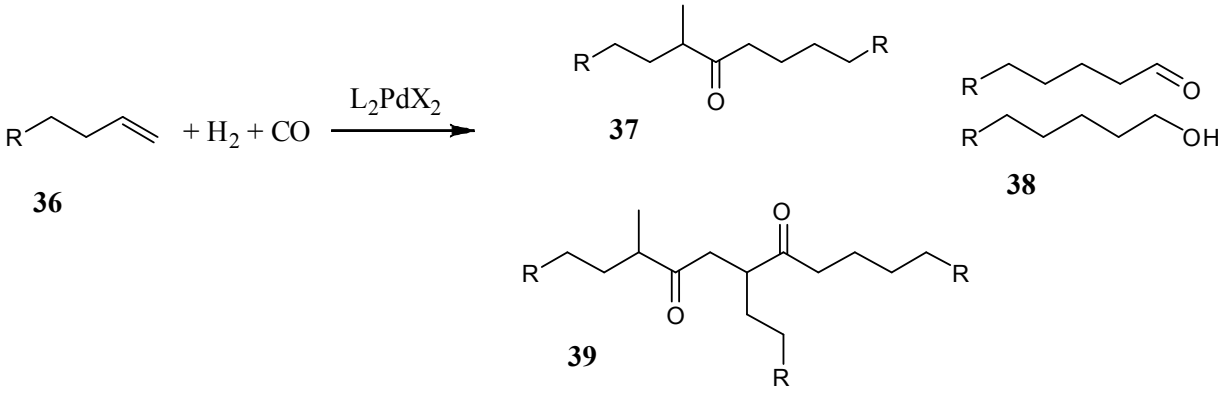

36 **37** **38** **39**

Scheme 1.10 Hydro-acylation, hydroformylation and co-oligomerisation of olefins (only one regio-isomer shown of each product class).

Recently Drent *et al* also demonstrated the hydroformylation of internal alkenes by a homogeneous palladium catalyst ((BCOPE)Pd(OTf)$_2$ **40**). Here the catalyst was capable of isomerising the double bond to the terminal position resulting in the production of high quantities of linear alcohols.[54]

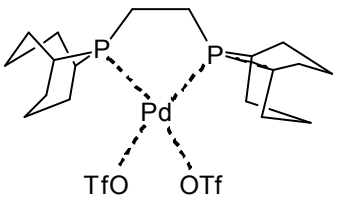

40

1.3.3 Asymmetric homogeneous hydroformylation

In the early days, the asymmetric hydroformylation of alkenes to chiral products (Scheme 1.11) was mainly performed with cobalt, rhodium and platinum catalysts.[55] Initially the branched aldehydes were only obtained with low ee's.

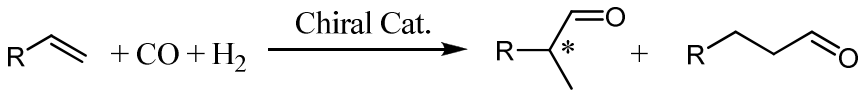

Scheme 1.11 Asymmetric hydroformylation of alkenes.

The application of modified Pt/Sn catalyst with diphosphine ligands (e.g. (R,R)-DIOP **4**), as developed by Consiglio *et al* for the asymmetric hydroformylation of styrene (and derivatives), led to branched aldehydes with considerably higher ee's.[55,56] Nowadays rhodium is mostly used for the asymmetric hydroformylation of alkenes. This was promoted by the development of (*R*,*S*)-BINAPHOS (**41)** by Takaya (1993)[57,58] and biphosphite ligands (*R,R*)-Chiraphite (**42)** developed by Babin and Whiteker (1992)[59,60] With BINAPHOS, > 95% ee was obtained for the asymmetric hydroformylation of substituted styrene, whereas ee values up to 90% were obtained for the hydroformylation of styrene using Chiraphite.[61]

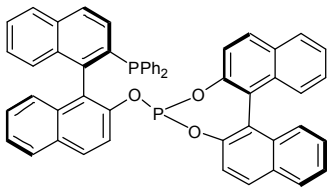

41

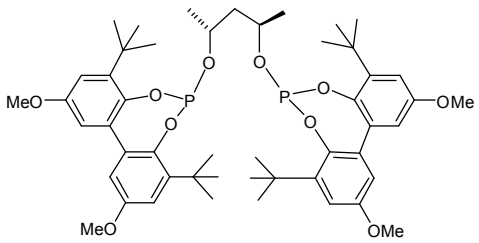

42

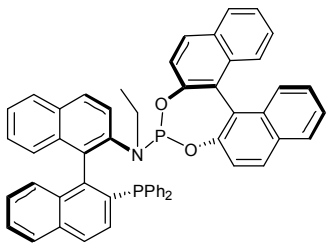

43

More recently Zhang *et al* developed (*R*,*S*)-Yanphos (**43)** a hybrid phosphine-phosphoramidite ligand.[62] It showed high reactivity and enantioselectivity for the rhodium catalyzed hydroformylation of styrene derivatives and vinyl acetate. Scheme 1.12 illustrates the rhodium catalyzed asymmetric hydroformylation of styrene **44** using ligands **41** and **43**.[62]

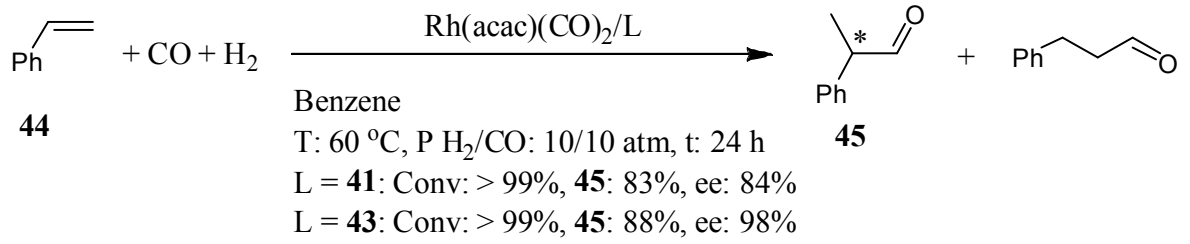

Scheme 1.12 Rhodium catalyzed asymmetric hydroformylation of styrene with BINAPHOS and Yanphos.

Other recently developed and effective ligands for the asymmetric hydroformylation are (*S*,*S*)-Kelliphite (**46)** and (*S*,*S*)-ESPHOS (**47,** for vinylacetate and allyl cyanide)[63-65], the bisphosphite ligand **48** (for styrene)[66], (*S*,*S*,*S*)-bisdiazaphos **49** (allyl cyanide, styrene, vinyl acetate)[65,67] and (*R*,*R*)-Binaphine **50** and (*R*,*R*)-Ph-BPE **51** (for styrene).[68,69]

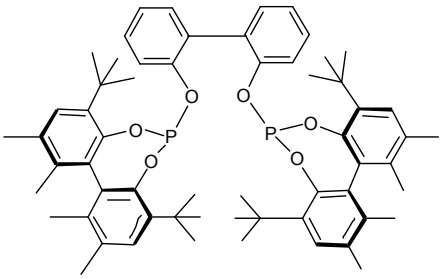

46

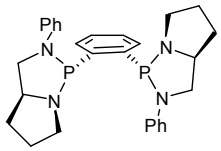

47

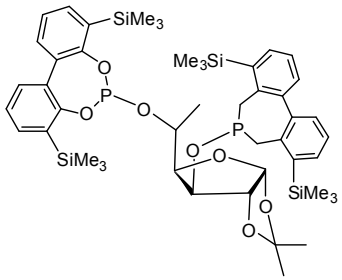

48

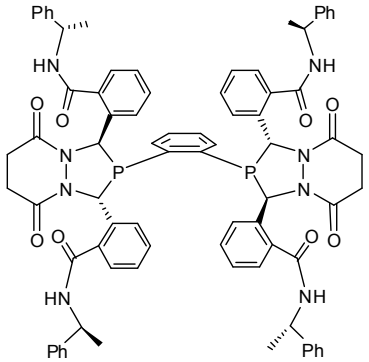

49

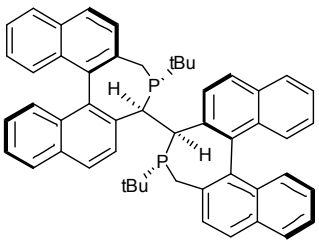

50

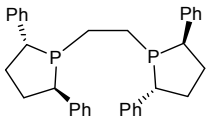

51

1.3.4 Asymmetric homogeneous hydro-acylation reactions

Asymmetric hydro-acylations of 1-alkenes and syngas may provide an interesting route for chiral α-methyl substituted ketones (Scheme 1.13).

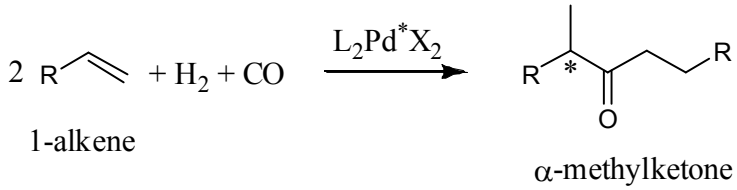

Scheme 1.13 Asymmetric hydro-acylations of 1-alkenes.

Such chiral ketones may be interesting building blocks for further chemistry to obtain novel products. To the best of our knowledge the asymmetric synthesis of α-methyl substituted ketones has only been accomplished by reducing α-methyleneketones by means of baker's yeast (Emulzint®) (Scheme 1.14).[70-72] Good results were obtained in for example the reduction of α-methyleneketone with R_1= Me and R_2= *n*-hexyl in water at 30 ºC. Here a conversion of 70% was obtained after 2 h with a product ee of > 99%.[72]

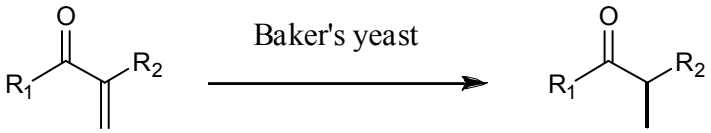

Scheme 1.14 Reduction of methyleneketones by baker's yeast.

To the best of our knowledge, the asymmetric hydro-acylation of olefins with synthesis gas by using homogeneous platinum metal catalysts has not been performed to date.

1.4 Aims and outline of this thesis

This thesis deals with the use of platinum metal group catalysts in homogeneous catalysis. The emphasis is on the use of homogeneous palladium complexes for the asymmetric synthesis of chiral ketones from syngas and olefins. This is an unexplored research area with the potential to synthesise (chiral) ketones for the bulk and fine- chemical industry. The objective was the identification of suitable catalysts and process conditions to achieve a high chemo-, regio- and enantioselectivity for the reaction. In addition, the use of chiral Rh complexes for the asymmetric synthesis of a propionic acid derivative and the use of Ru complexes for the synthesis of γ-valerolactone from simple carbohydrates like D-glucose and D-fructose was explored.

Chapter 1 gives an overview of the use of platinum group metals in catalysis with an emphasis on homogeneous catalysis**.**

In **Chapter 2** the results for the achiral hydro-acylation of 1-alkenes with syngas to mono-ketones using a homogeneous palladium catalyst of the type L_2PdX_2 are reported. In this study L was an alkyl-substituted diphospine (1,3-bis(di-sec-butylphosphino)propane) and X a non-coordinating anion (obtained from trifluoromethanesulfonic acid). The aim was to study the effect of process conditions on the chemo- and regioselectivity and to determine the optimum reaction conditions for the synthesis of monoketones. This contribution serves as a preliminary investigation for the development of an asymmetric version of the hydro-acylation reaction.

Chapter 3 describes an exploratory screening study on the asymmetric hydro-acylation reaction to chiral ketones using Pd-complexes of the type L_2PdX_2. The major objective was the identification of suitable chiral diphosphine ligands for the transformation. A broad variety of chiral diphosphine ligands was tested (Josiphos, Duphos, FerroTANE and Walphos ligands) and the best was selected for further studies.

Chapter 4 describes experimental studies on the asymmetric hydro-acylation reaction using a homogeneous Pd catalyst with a chiral Josiphos ligand. The effect of process conditions like reaction temperature, partial hydrogen and carbon monoxide pressure on the product ee and yield

was investigated in detail. The results were quantified using statistical modelling techniques, allowing selection of the optimum reaction conditions.

Chapter 5 deals with the enantioselective hydrogenation of methyl 2-acetamido acrylate to (R)-2-Acetylamino-propionic acid methyl ester with hydrogen using a Rhodium/MonoPhos™-complex in iso-propanol. The primary aim was the development of a kinetic model applicable for a broad range of reaction conditions. The information may be used for batch up scaling purposes and also to gain insights on mechanism of the catalytic reaction.

Chapter 6 describes experimental studies on the one pot synthesis of γ-valerolactone from simple carbohydrates (D-glucose, D-fructose, cellulose). γ-Valerolactone is considered an interesting bio-based chemical with high application potential in the biofuel and chemical industry. The initial objective was the identification of efficient homogeneous catalyst for the hydrogenation reaction using either hydrogen or formic acid. However, the homogeneous Ru-catalyst that was tested was not very efficient and the focus shifted to heterogeneous Ru catalysts. The study was exploratory in nature and aimed to identify the most suitable catalysts for this conversion and optimisation of process conditions.

1.5 References

1 http://en.wikipedia.org/wiki/Precious_metal

2 P. B. Kettler, *Org. Process Res. Dev.*, 2003, **7**, 342-354.

3 http://www.e-preciousmetals.com/Precious_Metals_Prices

4 A. Bischoff, *LBMA precious Metals Conference*, 2002, 33.

5 http://www.taxfreegold.co.uk/preciousmetalpricesusdollars.html

6 M. J. Krische, *Tetrahedron*, 2005, **61**, 6169-6170.

7 M. W. Roberts, *Catal. Lett.*, 2000, **67**, 1-4.

8 R. A. van Santen, P. W. N. M. van Leeuwen, J. A. Moulijn, and B. A. Averill, *Catalysis: An Integrated Approach*, second, 1999.

9 Hagen, J., *Industrial catalysis A practical approach*, WILEY-VCH, New York, First, 1999.

10 G. J. Hutchings and M. Haruta, *Appl. Catal. , A*, 2005, **291**, 2-5.

11 J. M. Thomas, and W. J. Thomas, *Principles and practice of heterogeneous catalysis*, John Wiley and Son Ltd, first, 1998.

12 P. W. N. M. van Leeuwen, *Homogeneous Catalysis: Understanding the Art*, Kluwer Academic Publishers, Dordrecht, first, 2004.

13 G. Dolcetti and N. W. Hoffman, *Inorg. Chim. Acta*, 1974, **9**, 269-303.

14 J. A. Osborn, F. H. Jardine, J. F. Young, and G. Wilkinson, *J. Chem. Soc.*, 1966, 1711-&.

15 H. Shimizu, I. Nagasaki, K. Matsumura, N. Sayo, and T. Saito, *Acc. Chem. Res.*, 2007, **40**, 1385-1393.

16 W. S. Knowles, *Adv. Synth. Catal.*, 2003, **345**, 3-13.

17 W. S. Knowles and R. Noyori, *Acc. Chem. Res.*, 2007, **40**, 1238-1239.

18 H. Guo, K. Ding, and L. Dai, *Chin. Sci. Bull.*, 2004, **49**, 2003-2016.

19 N. B. Johnson, I. C. Lennon, P. H. Moran, and J. A. Ramsden, *Acc. Chem. Res.*, 2007, **40**, 1291-1299.

20 R. Noyori, *Adv. Synth. Catal.*, 2003, **345**, 15-32.

21 M. B. Fryzuk, and B. Bosnich, *Chem. Soc.*, 1977, **99**, 6262-6267.

22 P. A. MacNeil, N. K. Roberts, and B. Bosnich, *J. Am. Chem. Soc.*, 1981, **103**, 2273-2280.

23 W. C. Zhang, Y. X. Chi, and X. M. Zhang, *Acc. Chem. Res.*, 2007, **40**, 1278-1290.

24 H. U. Blaser, C. Malan, B. Pugin, F. Spindler, H. Steiner, and M. Studer, *Adv. Synth. Catal.*, 2003, **345**, 103-151.

25 M. J. Burk, F. Bienewald, M. Harris, and A. Zanotti-Gerosa, *Angew. Chem. Int. Ed.*, 1998, **37**, 1931-1933.

26 H. U. Blaser, W. Brieden, B. Pugin, F. Spindler, M. Studer, and A. Togni, *Top. Catal.*, 2002, **19**, 3-16.

27 M. J. Burk, *J. Am. Chem. Soc.*, 1991, **113**, 8518-8519.

28 M. J. Burk and J. E. Feaster, *J. Am. Chem. Soc.*, 1992, **114**, 6266-6267.

29 J.-H. Xie, L.-X. Wang, Y. Fu, S.-F. Zhu, B.-M. Fan, H.-F. Duan, and Q.-L. Zhou, *J. Am. Chem. Soc.*, 2003, **125**, 4404-4405.

30 Y. Yamanoi and T. Imamoto, *J. Org. Chem.*, 1999, **64**, 2988-2989.

31 G. Zhu, P. Cao, Q Jiang, and X. Zhang, *J. Am. Chem. Soc.*, 1997, **119**, 1799-1800.

32 G. Erre, S. Enthaler, K. Junge, E. Gladiali, and M. Beller, *Coord. Chem. Rev.*, 2008, **252**, 471-491.

33 B. L. Feringa, M. Pineschi, L. A. Arnold, R. Imbos, and A. H. M. de Vries, *Angew. Chem. Int. Ed.*, 1997, **36**, 2620-2623.

34 B. L. Feringa, *Acc. Chem. Res.*, 2000, **33**, 346-353.

35 R. Naasz, L. A. Arnold, M. Pineschi, E. Keller, and B. L. Feringa, *J. Am. Chem. Soc.*, 1999, **121**, 1104-1105.

36 (a) M. Van den Berg, A. J. Minnaard, E. P. Schudde, J. van Esch, A. H. M. de Vries, J. G. de Vries, and B. L. Feringa, *J. Am. Chem. Soc.*, 2000, **122**, 11539-11540. (b) A. J. Minnaard, B. L. Feringa, L. Lefort and J. G. de Vries, *Acc. Chem. Res*., 2007, **40**, 1267-1277.

37 C. Claver, E. Fernandez, A. Gillon, K. Heslop, D. J. Hyett, A. Martorell, A. G. Orpen, and P. G. Pringle, *Chem. Commun.*, 2000, 961-962.

38 M. T. Reetz and G. Mehler, *Angew. Chem. Int. Ed.*, 2000, **39**, 3889-+.

39 M. T. Reetz and T. Sell, *Tetrahedron Lett.*, 2000, **41**, 6333-6336.

40 Y. Fu, J. H. Xie, A. G. Hu, H. Zhou, L. X. Wang, and Q. L. Zhou, *Chem. Commun.*, 2002, 480-481.

41 T. Jerphagnon, J. L. Renaud, and C. Bruneau, *Tetrahedron-Asymmetry*, 2004, **15**, 2101-2111.

42 T. Sturm, W. Weissensteiner, and F. Spindler, *Adv. Synth. Catal.*, 2003, **345**, 160-164.

43 J. G. de Vries, and C. J. Elsevier, *The handbook of homogeneous hydrogenation*, Wiley-VCH, Weinheim, 2007.

44 R. Hoen, J. A. F. Boogers, H. Bernsmann, A. J. Minnaard, A. Meetsma, T. D. Tiemersma-Wegman, A. H. M. de Vries, J. G. de Vries, and B. L. Feringa, *Angew. Chem. Int. Ed.*, 2005, **44**, 4209-4212.

45 H. U. Blaser, A. Indolese, and A. Schnyder, *Current Science*, 2000, **78**, 1336-1344.

46 B. Cornils, *J. Mol. Catal. A: Chem.*, 1999, **143**, 1-10.

47 O. Roelen, *DE Patent*, 849548, 1938.

48 E. Drent and P. H. M. Budzelaar, *J. Organomet. Chem.*, 2000, **594**, 211-225.

49 E. Drent, *Eur Patent*, 121965, 1984.

50 A. Sen, *Catalytic Synthesis of Alkene-Carbon Monoxide Copolymers and Cooligomers*, A Sen, Kluwer Academic Publishers, Boston, 2003, 27.

51 G. P. C. M. Dekker, C. J. Elsevier, K. Vrieze, P. W. N. M. van Leeuwen, and C. F. Roobeek, *J. Organomet. Chem.*, 1992, **430**, 357-372.

52 E. Drent, W. P. Mul, and P. H. M. Budzelaar, *Comments Inorg. Chem.*, 2002, **23**, 127-147.

53 J. Scheele, P. Timmerman, and D. N. Reinhoudt, *Chem. Commun.*, 1998, 2613-2614.

54 D. Konya, K. Q. A. Lenero, and E. Drent, *Organometallics*, 2006, **25**, 3166-3174.

55 R. van Duren, L. L. J. M. Cornelissen, J. I. Van der Vlugt, J. P. L. Huijbers, A. M. Mills, A. L. Spek, C. Muller, and D. Vogt, *Helv. Chim. Acta*, 2006, **89**, 1547-1558.

56 P. Haelg, G. Consiglio, and P. Pino, *Helv. Chim. Acta*, 1981, **64**, 1865-1869.

57 D. Hoegaerts and P. A. Jacobs, *Tetrahedron-Asymmetry*, 1999, **10**, 3039-3043.

58 N. Sakai, S. Mano, K. Nozaki, and H. Takaya, *J. Am. Chem. Soc.*, 1993, **115**, 7033-7034.

59 J. E. Babin and G. T. Whiteker, *WO Patent*, 9303839, 1992.

60 Y. P. Zou, Y. J. Yan, and X. M. Zhang, *Tetrahedron Lett.*, 2007, **48**, 4781-4784.

61 M. Beller, B. Cornils, C. D. Frohning, and C. W. Kohlpaintner, *J. Mol. Catal. A: Chem.*, 1995, **104**, 17-85.

62 Y. J. Yan and X. M. Zhang, *J. Am. Chem. Soc.*, 2006, **128**, 7198-7202.

63 C. J. Cobley, K. Gardner, J. Klosin, C. Praquin, C. Hill, G. T. Whiteker, A. Zanotti-Gerosa, J. L. Petersen, and K. A. Abboud, *J. Org. Chem.*, 2004, **69**, 4031-4040.

64 C. J. Cobley, J. Klosin, C. Qin, and G. T. Whiteker, *Org. Lett.*, 2004, **6**, 3277-3280.

65 A. L. Watkins, B. G. Hashiguchi, and C. R. Landis, *Org. Lett.*, 2008, **10**, 4553-4556.

66 M. Dieguez, O. Pamies, A. Ruiz, and C. Claver, *New J. Chem.*, 2002, **26**, 827-833.

67 T. P. Clark, C. R. Landis, S. L. Freed, J. Klosin, and K. A. Abboud, *J. Am. Chem. Soc.*, 2005, **127**, 5040-5042.

68 A. T. Axtell, J. Klosin, and K. A. Abboud, *Organometallics*, 2006, **25**, 5003-5009.

69 G. Erre, S. Enthaler, K. Junge, S. Gladiali, and M. Beller, *J. Mol. Catal. A: Chem.*, 2008, **280**, 148-155.

70 G. J. A. Conceicao, P. J. S. Moran, and J. A. R. Rodrigues, *Arkivoc*, 2003, 500-506.

71 F Gini, *PhD thesis University of Groningen*, 2007.

72 E. P. Siqueira, J. A. R. Rodrigues, and P. J. S. Moran, *Tetrahedron-Asymmetry*, 2001, **12**, 847-852.

Chapter 2. Experimental Studies on the Conversion of Olefins and Syngas to Ketones using Homogeneous Palladium-Diphosphine Catalysts

2.1 Introduction

Conversions of 1-alkenes and syngas using homogeneous transition metals catalysts are of prime industrial importance (oxo-synthesis). A variety of products is possible like low molecular aldehydes and alcohols (hydroformylation), ketones (hydro-acylation) and low- and high molecular weight polymers (Scheme 2.1).[1,2]

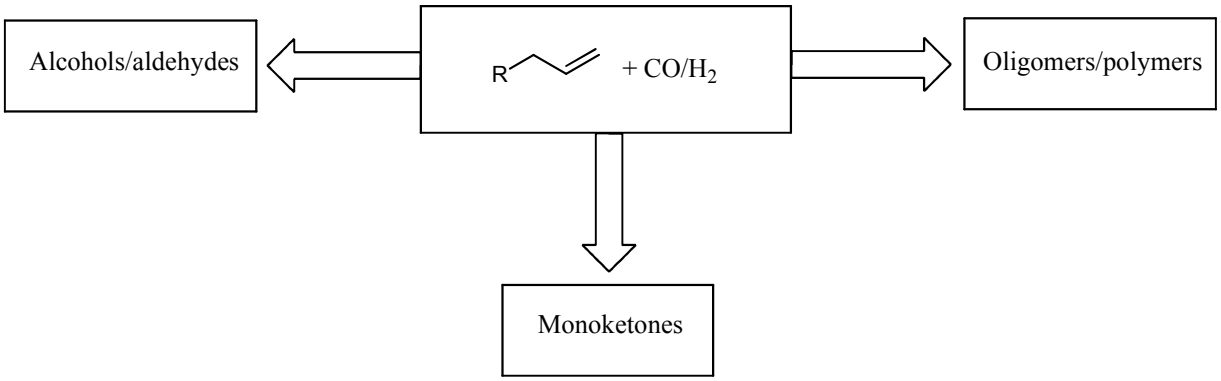

Scheme 2.1 Overview of the olefin/syngas product tree.

The use of cationic palladium(II) complexes with diphosphines ligands for the alternating copolymerization of CO and ethene was first reported by Drent *et al*.[3,4] Later the use of these catalysts was expanded to other CO/olefin copolymerisation reactions, for example CO/propene copolymerisation.[3] More recently Drent and Budzelaar demonstrated the application of L_2PdX_2 (L_2 represents an alkyldiphosphine ligand and X stands for a weakly or non-coordinating counter anion) catalysts for the selectively synthesis of monoketones from higher alkenes.[5,6] The reaction yields both saturated ketones and enones (Scheme 2.2).

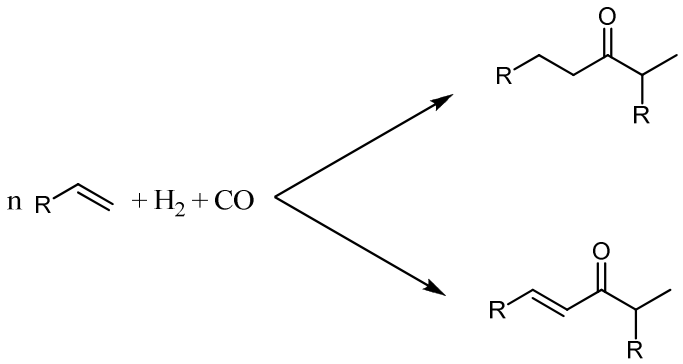

Scheme 2.2 Formation of saturated and unsaturated (enones) monoketones (for brevity, only one of the possible isomers is shown).

Three saturated monoketone regio-isomers may be formed in reaction, the head-to-tail, tail-to-tail and head-to-head regio-isomers (Figure 2.1).

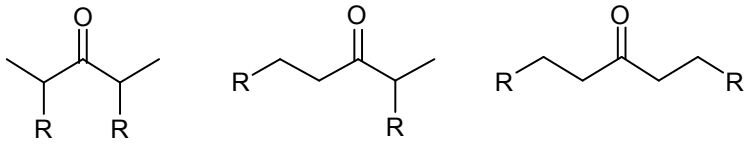

Figure 2.1 Saturated monoketone regio-isomers for 1-alkene hydro-acylation.

To obtain monoketones, catalysts with basic diphosphines like alkyldiphosphines in combination with a poorly or non-coordinating anion (e.g. triflate) are required. With a catalyst consisting of $Pd(OAc)_2$, 1,3-bis(di-n-butylphosphino)propane (DnBPP) and trifluoromethanesulphonic acid (HOTf) very promising results were obtained.[5,6] Using 1-octene, a saturated monoketone chemoselectivity of 98 mol% was obtained with a head-to-tail regioselectivity of 98 mol% (60 bar syngas, CO/H_2 ratio of 1, 125 °C, 5 h reaction time, diglyme).[5,6] The screening work by Drent *et al* focused mainly on ligand effects on chemoselectivity and the effect of process conditions on product selectivity as well as the potential of others solvents have not been determined in detail yet.

Saturated chiral monoketones with an α-methyl group (head-to-head and head-to-tail regio-isomers, see Figure 2.1) are very interesting building blocks in organic synthesis. The α-methyl carbonyl moiety is present in a variety of natural products and biologically active compounds.[7,8] We here report an exploratory study on the achiral hydro-acylation of 1-olefins (1-pentene and 1-octene) using a typical cationic Pd-diphosphine complex. The primary aim was to establish reaction conditions and solvents to obtain saturated monoketones with high chemo- and regioselectivity. On the basis of the screening work by Drent *et al*, the diphosphine ligand of choice was (1,3-bis(di-sec-butylphosphino)propane).

The results presented in this paper are input for further studies on asymmetric hydro-acylations using palladium complexes with chiral diphosphine ligands. Here, the aim is the (stereo-) selective synthesis of the head-to-tail regio-isomer (R= n-Pr (**1**) when using 1-pentene, and n-hexyl (**2**) when using 1-octene), which contains a chiral centre (Figure 2.2). The head-to-head regio-isomer contains two chiral centres but is of less interest as it is known to be formed in only very minor amounts.[5,6] These studies will be reported in forthcoming papers from our group.

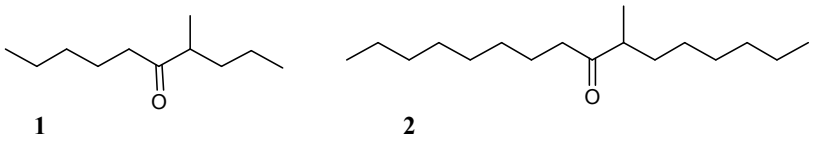

1 **2**

Figure 2.2 Desired head-to-tail monoketones **1** and **2**.

2.2 Experimental

2.2.1 Chemicals

The air-sensitive 1,3-bis(di-sec-butylphosphino)propane ligand (DsBPP, obtained as a gift from Prof. E. Drent, University of Leiden, The Netherlands) and the palladium acetate precursor (Sigma Aldrich > 98%) were stored in a glove box. Diglyme (Merck > 99%), dichloromethane (Lab-Scan 99.8%) and methanol (Lab-Scan 99.8%) were distilled from CaH_2 and stored in Schlenk flasks under nitrogen. The olefins (1-octene Merck > 97%, 1-pentene Sigma Aldrich 98%) were distilled from sodium and stored in Schlenk flasks under nitrogen.[9,10] Trifluoromethanesulfonic acid (HOTf) (Strem 99+%) was stored in a Schlenk flask under

nitrogen at 5 ºC. 1,9-Decadiene was obtained from Acros (97%). The synthesis gas used was a 50:50 pre-mixed CO/H_2 gas mixture (HiQ, high quality) and was purchased from Hoek Loos. The reference head-to-tail monoketone for both 1-octene and 1-pentene to be used for GC determinations were synthesised according to published procedures.[11]

2.2.2 Experimental setup

The catalytic reactions were carried out in a Parr autoclave (50 ml), which was operated in a batch mode with respect to the gas phase (Figure 2.3). The maximum operating pressure of the reactor is 200 bar, the maximum temperature 200 ºC. The reactor was electrically heated and the reactor content was stirred by a Parr overhead stirrer, equipped with a gas inducing impeller. Temperature and stirring speed were controlled by the Parr 4843 controller. The synthesis gas was fed from a premixed (50/50) storage bottle.

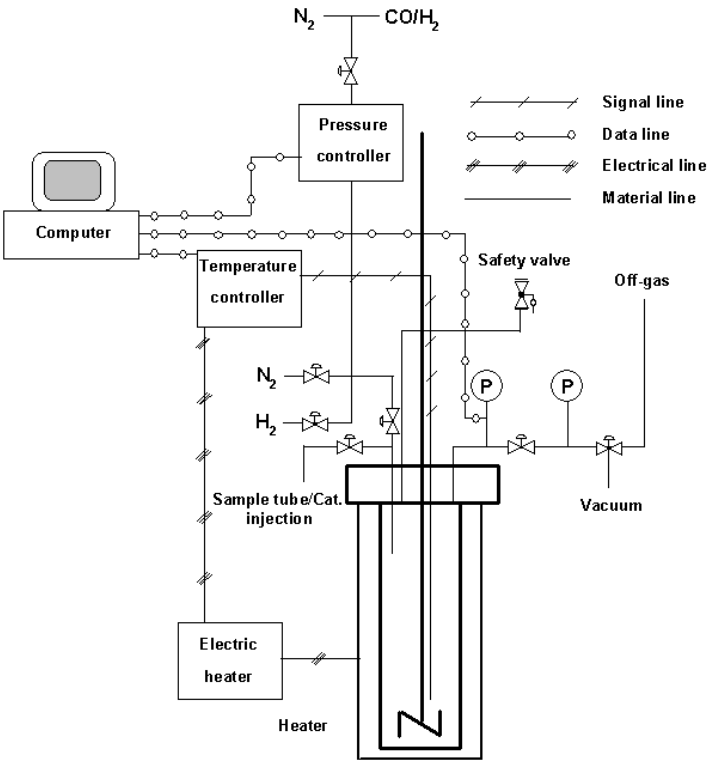

Figure 2.3 Schematic representation of the reactor setup.

2.2.3 General procedure

The catalyst was freshly prepared before each experiment under a protective nitrogen atmosphere using standard Schlenk techniques. $Pd(OAc)_2$ (11 mg, 0.05 mmol) was dissolved in the reaction solvent (either dichloromethane or methanol, 2 mL). After approximately 10 min the diphosphine ligand (0.12 mmol) dissolved in either dichloromethane or methanol (2 mL) was added. The solution was stirred for 10 min prior to the addition of HOTf (60 mg, 0.4 mmol) and stirred for another 10 minutes before use. The batch autoclave was charged with solvent (either dichloromethane or methanol, 10-18 ml), 1-pentene (4.0 ml, 36.5 mmol) or 1-octene (4.0 ml, 25 mmol) and the catalyst solution. The reactor was closed and flushed with nitrogen to remove air. The reactor was pressurised (60 bar) with synthesis gas (50/50 H_2/CO) and stirring was applied (1000 rpm). Subsequently the reactor was heated to the desired reaction temperature (30 or 125 ºC). After 5 h, the reactor was cooled to room temperature, depressurised, and flushed several times with N_2. The liquid product was filtered over silica gel to remove the catalyst.

2.2.4 Product analysis

The product composition in the liquid phase was analysed using a GC-FID HP-5890 series II, equipped with a 30 m HP-1 column and He as the carrier gas. The following temperature profile was applied: 10 minutes at 30 °C, from 30 °C to 325 °C at a rate of 10 °C/min, 15 min at 325 °C. Product compositions were obtained by comparing product peak areas by means of the 100% method.[12] The method was applied for peaks belonging to the most abundant product groups present in the samples: mono-oxygenates (ketones, aldehydes/alcohols and esters), olefin dimers and diketones. The response factors of all individual components are not known. To compensate for this, the concept of effective carbons was applied to determine the mol fraction of a product (Equation 2.1).[13]

$$X_j = \frac{F_j/(\sum C_{ef})_j}{\sum_1^n \frac{F_i}{(\sum C_{ef})_i}} \qquad (2.1)$$

Here X_j stands for the mol fraction of component j and F_j stands for the peak area of component j. F_j is divided by the sum of its effective carbons (C_{ef}) to obtain the 'effective area' of component j. The effective area of component j was divided by the sum of all effective areas of the relevant components in the chromatogram.[14] The 1-pentene conversion was determined by GC. The concentration of 1-pentene in the liquid phase after reaction was determined using calibration curves with known 1-pentene concentrations. The product solution was directly analysed after reaction to avoid excessive evaporation of 1-pentene. Product identification was performed by GC-MS and GC. GC-MS chromatograms were recorded on a GC (HP 6890) MS (HP-5973) equipped with a 30 m HP-5 MS column and He as the carrier gas (from 35 °C to 250 °C, rate 5 °C/min, final time 10 min.). GC spectra were recorded on a GC-FID HP-5890 series II, FID with a 30 m HP-1 column and He as the carrier gas (*vide supra*). Reference compounds, either obtained from chemical suppliers or prepared, were used to identify relevant components in the mixture.

2.3 Results

The catalyst precursor used in this study, (DsBPP)Pd$(OTf)_2$, was made in situ by mixing Pd$(OAc)_2$, DsBPP and trifluoromethanesulfonic acid (HOTf) in the reaction solvent.[5,6] The catalytic reactions were carried out with two representative 1-alkenes (1-pentene and 1-octene) in two different solvents (dichloromethane and methanol). The reactions were all performed at a reaction time of 5 h and a fixed syngas pressure of 60 bar with a CO/H_2 ratio of 1. Typically, 0.14 mol% of catalyst was used for 1- pentene and 0.20 mol% for 1-octene.

The target products are the saturated head-to-tail monoketones (**1** for 1-pentene and **2** for 1-octene). The following product selectivity was defined:

$$S_{product} = \text{(monoketone content in mixture) x (saturated h-to-t fraction in monoketones) (mol\%)} \quad (2.2)$$

Here, the monoketone content is the sum of all saturated and unsaturated ketones in the product mixture as determined by GC.

2.3.1 Catalytic hydro-acylation reactions in dichloromethane

A total of 8 experiments were performed in dichloromethane using 1-pentene and 1-octene as the substrate, see Table 2.1 for an overview.

Table 2.1 Overview of experiments using 1-octene and 1-pentene in dichloromethane[a]

			Product distribution[b]								
Entry	Olefin	T (°C)	MK (%)	Sat. h-to-t (%)	Enones h-to-t (%)	$S_{prosduct}$[c] (%)	Aldehydes/ Alcohols (%)	Diketones (%)	Olefin dimers (%)	Olefin trimers (%)	Olefin conv. (%)
1	C5	125	55	91	0	50	0	0	38	7	n.d.[e]
2	C5	90	96	73	18	70	0	3	0	0	n.d.
3	C5	60	81	4	94	3	0	19[d]	0	0	38
4	C5	30	0	0	0	0	0	Higher oligomers	0	0	n.d.
5	C8	125	55	78	0	43	13	0	29	3	n.d.
6	C8	90	59	83	0	49	12	0	25	4	n.d.
7	C8	60	80	44	18	35	5	0	3	12	42
8	C8	30	76	32	24	24	0	14	0	9	n.d.

a. Intake: 25 mmol of 1-octene 36.5 mmol of 1-pentene; 0.05 mmol of Pd; HOTf as the acid,; Pd:L2:X molar ratio = 1 : 2.4 : 8, 5 h reaction time, $P_{H2} = P_{CO} = 30$ bar. b. Products: MK.: total monoketones formed (sum of all isomers, saturated + enones); Sat. h-to-t: Fraction of saturated h-to-tail monoketone in the MK fraction; Enones h-to-t: Fraction of unsaturated (enone) head-to-tail isomer in the MK fraction; (tail-to-tail-isomers and h-to-h regio-isomers were not quantified. c. defined according to eq 2.2. d. Also higher oligomers observed. e. Not determined.

At typical hydro-acylation conditions (125 °C, 60 bar total pressure) and using 1-pentene, the main products were monoketones (saturated and unsaturated, 55 mol%) and olefin dimers (38 mol%) and trimers (7%, Table 2.1, entry 1), leading to a product selectivity for **1** of 50 mol%. At these conditions, aldehydes/alcohols and higher CO/olefin oligomers were not present in the product mixture. The 1-alkene dimers and trimers were positively identified by GC-MS (M^+: 140, 207 for 1-pentene). The formation of olefin oligomers was not anticipated at forehand and was also not reported in the hydro-acylation studies performed by Drent et al.[5,6] A further discussion on possible reaction pathways for these olefin oligomers is given in the discussion section.

When using 1-octene at 125 °C and 60 bar total pressure, the selectivity to the desired product **2** (43 mol%) is slightly lower than for 1-pentene and besides olefin dimers and trimers, some

aldehyde/alcohols were formed as well. For 1-pentene, aldehyde/alcohol formation was not observed; indicating that chemoselectivity of the reaction is also depending on the size of the olefin. In the research by Drent *et al.* a chemoselectivity shift as a function of the length of the alkyl chain of the 1-alkene was also observed. For instance, in the hydrocarbonylation of propene and 1-octene with a palladium catalyst containing the DnBPP (1,3-bis(di-n-butylphosphino)propane ligand and p-toluenesulfonic acid as the acid component, a mixture of aldehydes/alcohols (40 mol%) and monoketones (50 mol%) was observed compared to mainly aldehydes/alcohols and no ketones for 1-pentene (diglyme, 125 ºC). [5,6] Thus, at otherwise similar conditions aldehyde/ketone formation occurs to a larger extent for olefins with a longer alkyl chain.

The selectivity of the reaction for the desired compounds **1** and **2** is highly temperature depending, see Figure 2.4 for details.

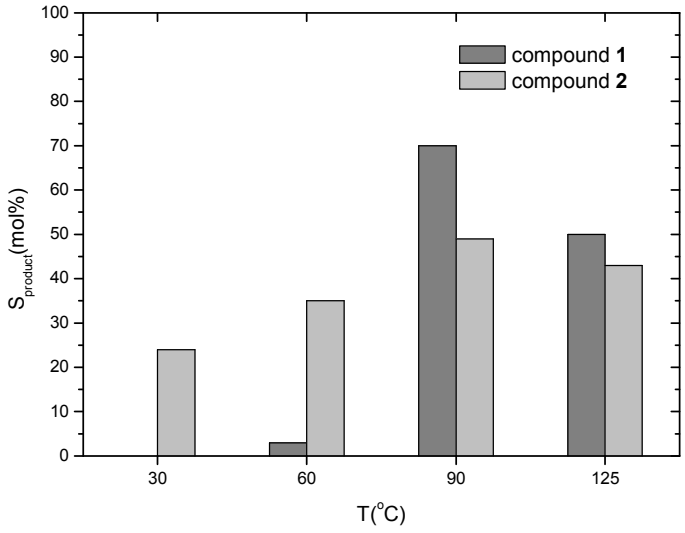

Figure 2.4 Chemoselectivity for **1** and **2** versus the temperature.

For 1-pentene, the monoketone selectivity shows a clear temperature optimum. The highest monoketone selectivity (96 mol%) was obtained at 90° C, with a selectivity of 70 mol% for **1**. At 125 °C, the chemoselectivity of the reaction is reduced considerably due to the formation of olefin dimers and trimers. At temperatures below 90 °C, oligoketone formation was observed to a

significant extent. At 30 °C, the sole product was a white solid. The solid was characterised by GPC and NMR and revealed that it is an alternating CO/olefin polymer with a M_n of 8000 g/mol.

The chemoselectivity for hydro-acylation is considerably lower for 1-octene than for 1-pentene. The highest selectivity for monoketones (80 mol%) was obtained at 60 °C, the highest selectivity for **2** at 90 °C (49 mol%). Olefin dimerisation and trimerisation occurred to a significant extent at higher temperatures and this is in line with the results for 1-pentene. At elevated temperatures considerable amounts of aldehydes/alcohols were formed as well, which was not observed with 1-pentene.

Catalyst activity was determined for experiments with 1-octene and 1-pentene at 60 °C after 5 h. The olefin conversion for 1-octene was 42% and that of 1-pentene 38% corresponding with an average turn-over frequency (TOF) for the 5 h batch time of 42 (1-octene) and 55 (1-pentene) mol/(mol Pd.h). Typical values reported in the literature for hydro-acylations using alkylphosphines at 125 °C are about 100 mol/(mol Pd.h) for higher olefins like 1-octene.[5,6] Data at lower temperature at not available in the literature and this makes a proper comparison impossible. However, it is very interesting to see that the hydro-acylation reactions also occur at considerable lower temperatures than those reported in the literature.

From the experiments performed with 1-octene, the olefin composition after the reaction was determined and the results are given in Figure 2.5. At temperatures above 90 °C only limited amounts of 1-octene were present in the reaction mixture after reaction. The main C8 olefins were 1-octene isomers, a clear indication that the catalyst is an active olefin isomerisation catalyst. At 30 °C and 60 °C, olefin isomerisation occurs with a much lower rate and 1-octene is by far the most abundant olefin isomer in the mixture. Thus, at higher temperatures the isomerisation of the α-olefin into less reactive internal olefins occurs, which could have a negative effect on catalyst activity.[15-19]

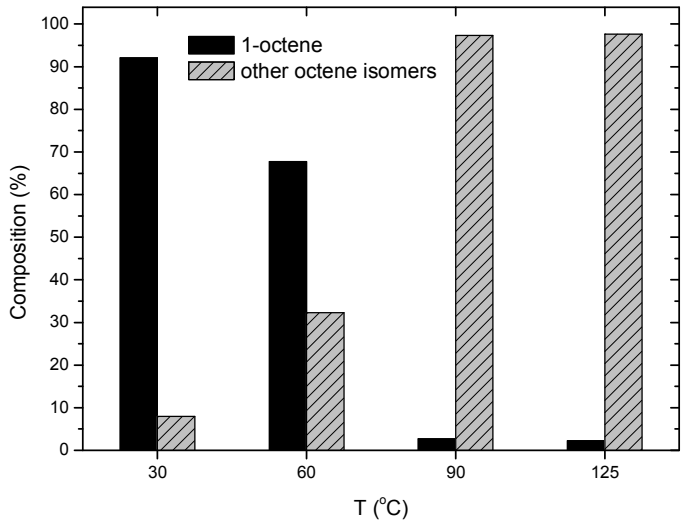

Figure 2.5 Composition of the remaining mono-olefins after reaction of syngas with 1-octene at different temperatures in dichloromethane.

2.3.2 Catalytic hydro-acylation reactions in methanol

A total of 8 experiments were performed in methanol with 1-octene and 1-pentene as the substrates. An overview of the results is given in Table 2.2.

Table 2.2 Overview of experiments using 1-pentene and 1-octene in methanol[a]

				Product distribution[b]							
Entry	Olefin	T (°C)	P (bar)	MK (%)	Sat. h-to-t (%)	Enones h-to-t (%)	$S_{prosduct}$[c] (%)	Aldehydes/ Alcohols (%)	Esters (%)	Diketones (%)	Olefin conv. (%)
1	C5	125	60	19	91	0	17	57	24	0	n.d.[d]
2	C5	90	60	20	81	4	16	56	23	1	n.d
3	C5	60	60	44	1	10	1	38	10	7	n.d
4	C5	30	60	29	0	5	0	41	5	25	n.d
5	C8	125	60	23	86	1	20	53	23	1	34
6	C8	90	60	21	79	1	17	54	23	2	37
7	C8	60	60	40	2	9	1	41	15	5	63
8	C8	30	60	27	1	7	0	36	22	15	45

a. Intake: 25 mmol of 1-octene 36.5 mmol of 1-pentene; 0.05 mmol of Pd; HOTf as the acid,; Pd:L2:X molar ratio = 1 : 2.4 : 8, 5 h reaction time, $P_{H2} = P_{CO}$ = 30 bar, unless stated otherwise. b. Products: MK.: total monoketones formed (sum of all isomers, saturated + enones); Sat. h-to-t: Fraction of saturated h-to-tail monoketone in the MK fraction; Enones h-to-t: Fraction of unsaturated (enone) head-to-tail isomer in the MK fraction; (tail-to-tail-isomers and h-to-h regio-isomers were not quantified). c. defined according to eq 2.2. d. not determined.

The selectivity for the desired compounds **1** and **2** in methanol is much lower than in dichloromethane. The highest value for 1-pentene was 17 mol% at 125 ºC, compared to 70 mol% for dichloromethane (90 ºC). Thus, dichloromethane is preferred above methanol to obtain saturated head-to-tail monoketones.

The dominant reaction pathway in methanol is hydroformylation, leading to the formation of large amounts of aldehydes/alcohols (Table 2.2). Olefin dimerisation and trimerisation, a noticeable pathway in dichloromethane was not observed. Instead, ester formation (5-24%) occurred to a significant extent (Scheme 2.3). Ester formation for CO/olefin conversions in methanol using cationic Pd complexes is well established.[20-22]

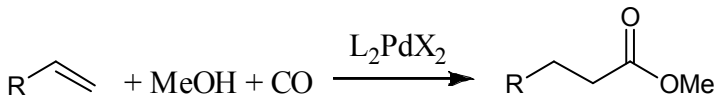

Scheme 2.3 Ester formation in methanol.

The chemoselectivity of the reaction is, like in dichloromethane, a strong function of temperature. Diketone formation is favoured at lower temperatures, in line with literature data on olefin-CO co-oligomerisation and polymerisation.[3,23] Hydroformylation activity seems to be enhanced at higher temperatures, whereas ester formation is nearly independent of the temperature for 1-octene.

Catalyst activity in methanol was determined for 1-octene. The results are provided in Figure 2.6. The activity is a clear function of the temperature. At typical hydro-acylation conditions used in the literature (60 bar, 125 ºC) the olefin conversion was 34 %.

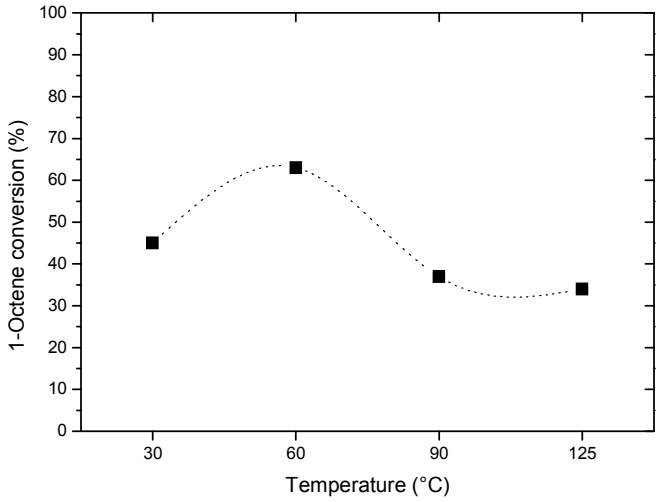

Figure 2.6 1-Octene conversion as a function of the temperature in methanol.

Remarkably, considerable higher olefin conversions were observed at 60 °C (63 mol/mol/h), which is somewhat higher than the TOF obtained in dichloromethane (42 mol/mol/h). A further lowering of the temperature to 30 °C again led to a reduction in catalyst activity. The observed trend is likely the result of two opposing effects on catalytic activity. Typically, higher temperatures lead to higher catalyst activities. Catalyst deactivation at higher temperatures may lead to a lowering of the reaction rates. Alternatively, reductions in catalyst activities at higher temperatures may be caused by olefin isomerisation to less reactive internal olefins.[15-19] This was confirmed by determining the olefin composition of the remaining 1-octene after the reaction

(Figure 2.7). At 30 °C, isomerisation is not taking place, whereas only small amounts of 1-octene are left at temperatures exceeding 90 °C.

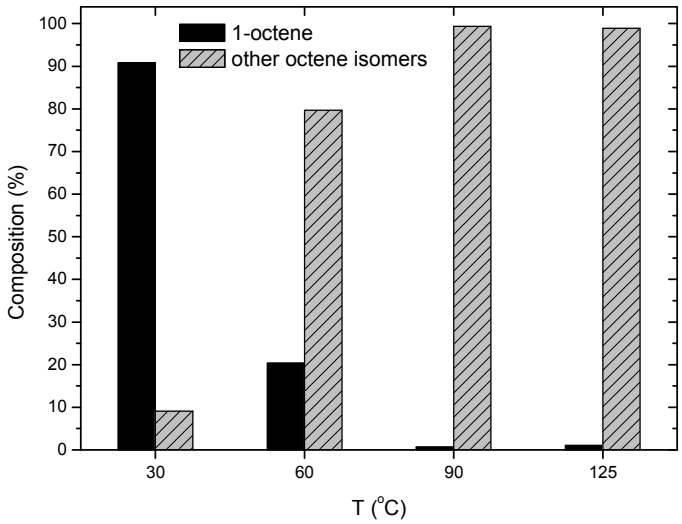

Figure 2.7 Composition of the remaining olefins after reaction of syngas with 1-octene at different temperatures.

2.4 Discussion

A mechanistic scheme for the conversion of syngas and olefins to ketones, aldehydes/alcohols and CO/olefin polymers with cationic palladium catalyst is provided in Scheme 2.4.[5,6]

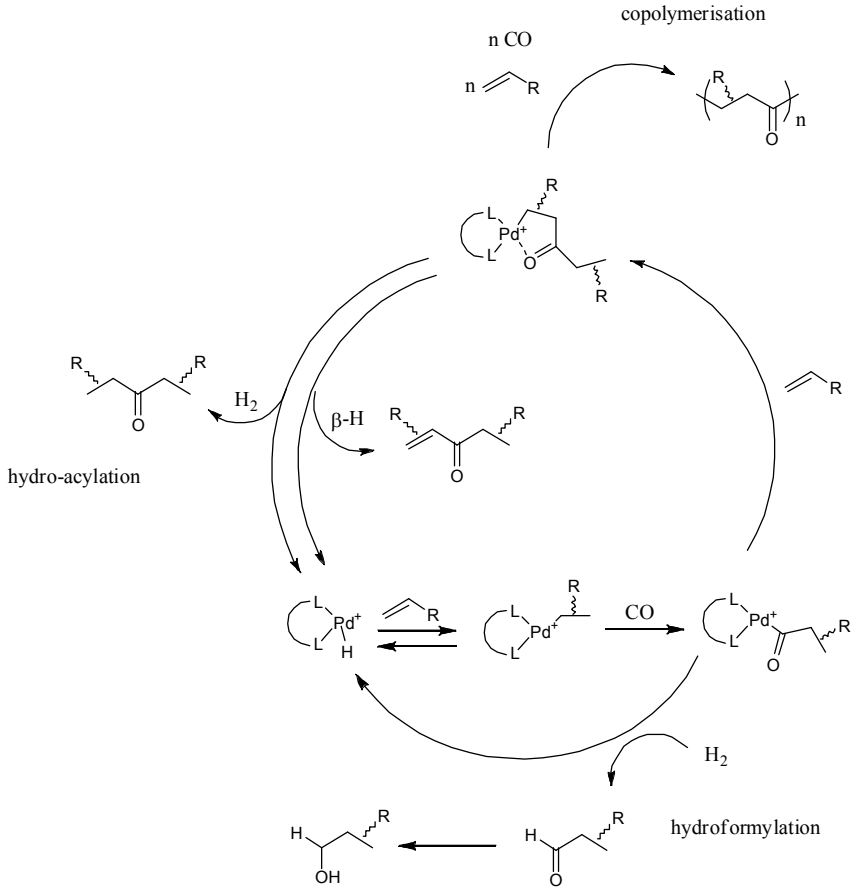

Scheme 2.4 Proposed catalytic cycle for the Pd(II) catalysed reactions of 1-alkenes and syngas.

In this mechanism $L_2Pd\text{-}H^+$ is a common intermediate. To obtain saturated monoketones by hydro-acylation, the olefin has to insert in the Pd-H bond to form a palladium alkyl species. Subsequent CO insertion followed by a second olefin insertion leads to a Pd-alkyl species with coordination of the pendant carbonyl group to the metal leading to a 5 membered chelate. The regioselectivity of the reaction is believed to be determined in the second olefin insertion step.[5,6] The 5-membered chelate may react with hydrogen to re-form the Pd-H and the desired saturated monoketone. Alternatively, β-hydrogen elimination may occur, leading to the formation of an enone. Enones are not the target molecules in our study and thus hydrogenolysis is preferred over β-hydrogen elimination.

The chemoselectivity of the reaction of syngas with 1-pentene in dichloromethane was a strong function of the reaction temperature. A qualitative trend on the basis of the data in Table 2.1 is given in Figure 2.8.

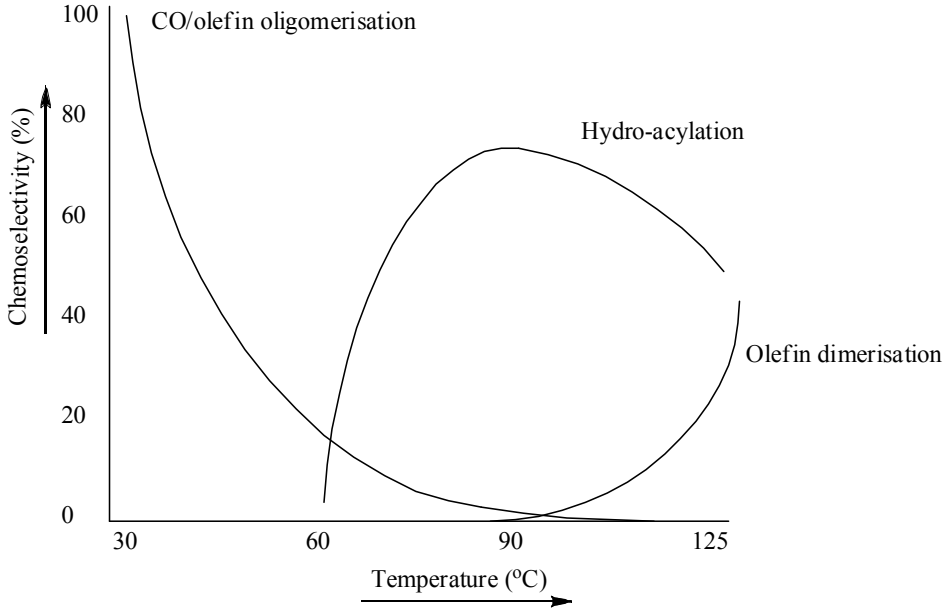

Figure 2.8 Qualitative trend for the chemoselectivity of the hydro-acylation of 1-pentene with CO/H_2 in dichloromethane.

The total amount of monoketones (saturated and unsaturated) shows a clear optimum with respect to temperature. At 90 ºC, the amount of monoketones (saturated and unsaturated) is highest and 96 mol%. The highest selectivity of the desired saturated head-to-tail monoketone **1** was also obtained at 90 ºC (70 mol%). The amount of unsaturated monoketones (enones) within the monoketone fraction is a clear function of the temperature and seems to increase at lower temperatures. The only exception at first sight is 30 ºC, where no enones are formed. However, at this temperature only CO/1-pentene oligomers are formed of which the end-groups (saturated or unsaturated) have not been determined. Thus, it seems that β-hydrogen elimination of the 5-membered chelate is promoted at lower temperatures which was also observed in the research by Drent *et al*.[5,6]

Furthermore, it is clear that diketone and higher CO/olefin oligomers are favoured at lower temperatures. This is in line with CO/olefin co-polymerisation experiments, where the molecular

weight increases at lower temperatures.[3,23] Thus both chain transfer by hydrogenolysis and β-hydrogen elimination are less facile at lower temperature and insertion of CO and subsequently an olefin is favoured.

At 125 ºC the formation of 1-pentene dimers and trimers was observed, lowering the chemoselectivity to a great extent. A number of explanations may be put forward for olefin oligomerisation. It is well possible that these are palladium catalysed by successive olefin insertions in a Pd-H followed by β-hydrogen elimination. However, olefin dimerisation in the presence of CO for cationic Pd-complexes of the type $L_2Pd^+ X^-$ has to the best of our knowledge not been reported to date. Some studies were performed in the absence of CO. For instance, Drent showed that cationic palladium carbonylation catalyst containing a mono- or diphosphine ligand are active for olefin dimerization.[24-26] The dimerisation activity of monodentate phosphine complexes was low, but the addition of a weakly coordinating anion (e.g. OTs) instead of a strongly coordinating anion like Cl^- increased the activity significantly (from 30 to 200 mol/mol Pd.h). With diphosphine complexes and weakly coordinating anions much higher ethene dimerisation activity was obtained (6000 mol/mol Pd.h).

An alternative explanation is a strong acid catalysed (here HOTF, which is used in an excess) oligomerisation of 1-olefin. Further studies are needed to confirm the exact mechanism for olefin oligomerisation. Those are beyond the scope of the current study aiming for identification of optimum process conditions for the synthesis of saturated head-to-tail monoketones **1** and **2**.

Notable differences in chemoselectivity in dichloromethane as a function of the temperature between 1-pentene and 1-octene were observed. The maximum amount of the head-to-tail saturated monoketone for 1-octene (**2**) was lower than for 1-pentene (49 versus 70 mol%). This suggests that research on smaller olefins like 1-butene might be advantageous with respect to chemoselectivity. Furthermore, the formation of small though significant amounts of alcohols and aldehydes were observed with 1-octene at higher temperatures. The exact reasons for the differences between 1-pentene and 1-octene are not yet clearly understood. It is well possible that small though relevant steric effects play a role, although others factors (e.g. polarity changes of mixture, extent of olefin isomerisation) cannot be ruled out a-priori.

The hydro-acylation experiments of 1-octene and 1-pentene in methanol showed to be less selective towards the formation of monoketones compared to the experiments performed in dichloromethane. In general the reactions performed in methanol gave more esters and

aldehydes/alcohols. The proposed mechanism for ester formation is given in Scheme 2.5 and involves insertion of an olefin in the Pd-H bond, followed by CO insertion and termination by the alcohol with the formation of an ester and regeneration of the Pd-H.[21,22] Ester formation when using cationic Pd complexes in methanol is well known. Drent reported efficient ethene methoxycarbonylation catalysts based on Pd catalysts with the dtbpp (1,3-bis(di-t-butylphosphino)propane) ligand.[20] Tooze *et al* showed that replacement of the dtbpp ligand with 1,2-bis(di-t-butylphoshpinomethyl)benzene resulted in even higher activities for the formation of methyl propionate.[22]

The observed solvent effects on chemoselectivity implies that the reactivity of the intermediate Pd-acyl in the catalytic cycle (Scheme 2.5) in methanol and dichloromethane differ considerably. These differences in chemoselectivity between dichloromethane and methanol are likely related to the electrophilicity of the palladium centre. Hydro-acylation and copolymerisation pathways are generally favoured for more electrophilic palladium complex.[5,6] Apparently, the electrophilicity of the Pd centre is lower in methanol than dichloromethane, presumably due to solvent-metal interactions.

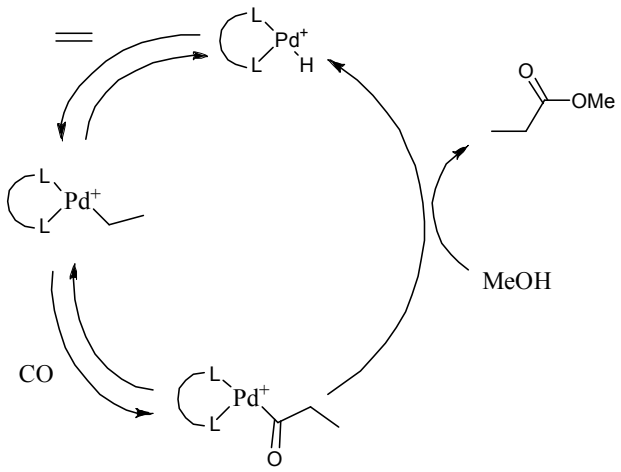

Scheme 2.5 Proposed mechanism for the methoxycarbonylation of ethylene.

2.5 Conclusions

The aim of this study was to investigate the influence of process conditions and particularly temperature on the hydro-acylation of 1-pentene and 1-octene using a cationic Pd catalysts with the basic 1,3-bis(di-sec-butylphosphino)propane ligand for the high yield synthesis of the saturated monoketones **1** (for 1-pentene) and **2** (for 1-octene). The highest selectivity's for **1** and **2** were obtained in dichloromethane at 90 °C and were 70 and 49 mol%, respectively. Major by-products were unsaturated monoketones (enones), diketones, aldehydes/alcohols and, in some cases, olefin oligomers. The chemoselectivity is a clear function of the temperature. Surprisingly, the catalysts are also active at 30 and 60 °C, which is much lower than the typical hydro-acylation temperatures reported in the literature for cationic homogeneous palladium complexes (125 °C). Olefin isomerisation to internal olefins occurred to a significant extent at temperatures above 60 °C, and this may have a negative effect on catalyst activity. The anion may also have an effect on the isomerisation, but this was not studied here.

The results presented in this paper are used as input for further studies on asymmetric hydro-acylations using palladium complexes with chiral diphosphine ligands to obtain enantiopure **1** and **2.** These studies will be reported in forthcoming papers from our group.

2.6 References

1 B. Cornils, and W. A. Herrmann, *Applied homogeneous catalysis with organometallic compounds a comprehensive handbook in three volumes*, Wiley-VCH, Weinheim, 2nd. ed, 2002.

2 R. A. van Santen, P. W. N. M. van Leeuwen, J. A. Moulijn, and B. A. Averill, Catalysis: An Integrated Approach.1999; 14-15.

3 C. Bianchini and A. Meli, *Coord. Chem. Rev.*, 2002, **225**, 35-66.

4 E. Drent, J. A. M. v an Broekhoven, and M. J. Doyle, *J. Organomet. Chem.*, 1991, **417**, 235-251.

5 E. Drent, W. P. Mul, and P. H. M. Budzelaar, *Comments Inorg. Chem.*, 2002, **23**, 127-147.

6 E. Drent and P. H. M. Budzelaar, *J. Organomet. Chem.*, 2000, **594**, 211-225.

7 W. A. Loughlin, *Bioresour. Technol.*, 2000, **74**, 49-62.

8 K. Mori and S. Harashima, *Tetrahedron Lett.*, 1991, **32**, 5995-5998.

9 D. D. Perrin, and W. L. F. Armarego, *Purification of laboratory chemicals*, Pergamon Press, Oxford, 3rd ed, 1988.

10 P. W. N. M. van Leeuwen, *Appl. Catal. ,A*, 2001, **212**, 61-81.

11 F Gini, *PhD thesis University of Groningen*, 2007.

12 W. G. M. Braam, *Chromatografie*, Educatieve Partners Nederland BV, Culemborg, The Netherlands, 5, 1994.

13 V Svojanovský, M Krejí, K Tesaík, and J Janák, *Chromatogr. Rev.*, 1966, **8**, 90-171.

14 A. D. Jorgensen, K. C. Picel, and V. C. Stamoudis, *Anal. Chem.*, 1990, **62**, 683-689.

15 G. C. Bond and M. Hellier, *J. Catal.*, 1965, **4**, 1-&.

16 D. B. Dahl, C. Davies, R. Hyden, M. L. Kirova, and W. G. Lloyd, *J. Mol. Catal. A:Chem.*, 1997, **123**, 91-101.

17 J. F. Harrod and A. J. Chalk, *J. Am. Chem. Soc.*, 1964, **86**, 1776-&.

18 A. Sen and T. W. Lai, *Inorg. Chem.*, 1984, **23**, 3257-3258.

19 H. G. Tang and D. C. Sherrington, *J. Mol. Catal.*, 1994, **94**, 7-17.

20 R. I. Pugh and E. Drent, *Adv. Synth. Catal.*, 2002, **344**, 837-840.

21 A. Sen, *Catalytic synthesis of alkene-carbon monoxide copolymers and cooligomers*, Kluwer Academic, Dordrecht, 2003.

22 R. P. Tooze, K. Whiston, A. P. Malyan, M. J. Taylor, and N. W. Wilson, *J. Chem. Soc. , Dalton Trans.*, 2000, 3441-3444.

23 R. A. M. Robertson and D. J. Cole-Hamilton, *Coord. Chem. Rev.*, 2002, **225**, 67-90.

24 E. Drent, *Eur Patent*, 01701311, 1986.

25 E. Drent, *Eur Patent*, 0280373, 1988.

26 E. Drent, *Pure Appl. Chem.*, 1990, **62**, 661-669.

Chapter 3. Enantioselective Hydro-acylations of 1-Alkenes to α-Methylketones using Palladium/Diphosphine Catalysts

3.1 Introduction

Asymmetric catalysis is an excellent methodology for the synthesis of chiral building blocks for the fine-chemical and pharmaceutical industry.[1,2] A wide variety of chemical transformations can nowadays be carried out in a catalytic asymmetric fashion. Well known examples are the synthesis of (–)-menthol using chiral BINAP-rhodium catalysts[2,3] and Naproxen, where a chiral phosphine is used in a hydrocyanation reaction (not commercialised).[4] However, synthetic routes to enantiopure α-alkyl-substituted ketones by catalytic asymmetric strategies are limited to date, despite the presence of especially the α-methyl carbonyl moiety in a variety of natural products and biologically active compounds.[5,6] To the best of our knowledge, the catalytic asymmetric synthesis of α-methyl ketones has only been accomplished by means of baker's yeast in the reduction of α-methyleneketones.[7-9]

A potentially very attractive catalytic methodology for the synthesis of α-methylketones is the palladium catalysed hydro-acylation of 1-alkenes with syngas (Scheme 3.1).

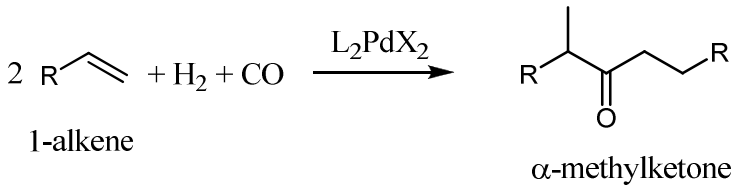

Scheme 3.1 Hydro-acylation of 1-alkenes to α-substituted ketones.

Besides the desired saturated ketones, however, a range of other products may be formed. Examples are enones (unsaturated ketones), oligo- and polyketones by co-polymerisation reactions and aldehydes/ alcohols by hydroformylation reactions (Scheme 3.2).

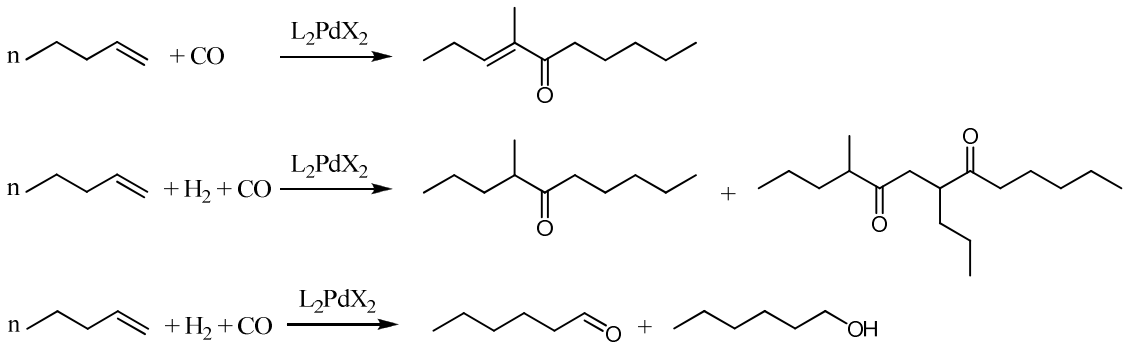

Scheme 3.2 Possible by-products for olefin hydro-acylations (for brevity, only one of the possible isomers is shown)

In addition, the hydro-acylation of olefins like 1-pentene can result in the formation of three saturated monoketone regio-isomers (Figure 3.1).

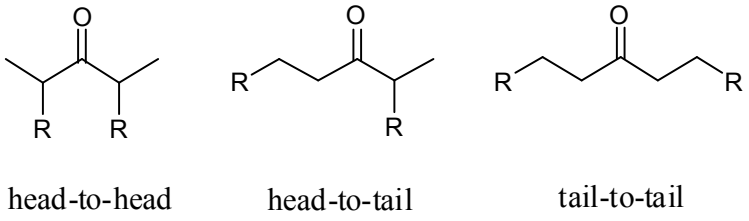

Figure 3.1 Saturated monoketone regio-isomers for 1-alkene hydro-acylation.

Drent and Budzelaar have demonstrated that the use of palladium catalysts of the type $(L_2)PdX_2$, where L_2 represents a bidentate alkylphosphine and X stands for a weakly or non-coordinating anion[10,11], allows the selective production of monoketones. Very promising results were obtained using alkyl-diphosphines like 1,3-bis(di-n-butylphosphino)propane (DnBPP) in combination with $Pd(OAc)_2$ and trifluoromethanesulphonic acid (HOTf). For 1-octene, a monoketone chemoselectivity of 98 mol% was obtained with a head-to-tail regio-selectivity of 98 mol%.[10,11] The counter-ion plays a major role and when trifluoroacetic acid (TFA) instead of HOTf was used as the anion, the selective formation of aldehydes was observed.

An asymmetric version of the palladium catalysed hydro-acylation of 1-alkenes to monoketones has to the best of our knowledge not been reported to date. However, the use of chiral palladium catalysts $(L_2)PdX_2$ for the closely related asymmetric copolymerisation and oligomerisation of 1-alkenes with CO is known (Scheme 3.3).[12-14]

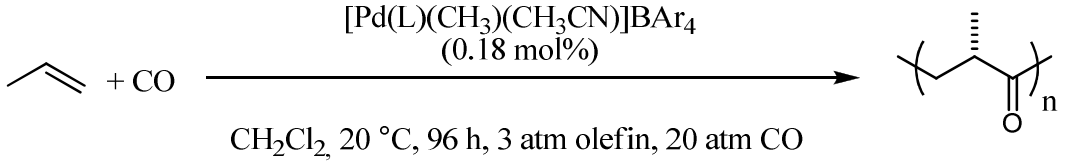

Scheme 3.3 Copolymerisation of CO/propene with a palladium-BINAPHOS catalyst system.

Consiglio reported the asymmetric alternating copolymerisation of propene and CO using the chiral Bichep ligand (Figure 3.2) with about 72% enantioselectivity.[15-17] Further improvements were made by Sen who obtained enantioselectivity's exceeding 90% when using Me-Duphos as ligand (Figure 3.2) .[16,17]

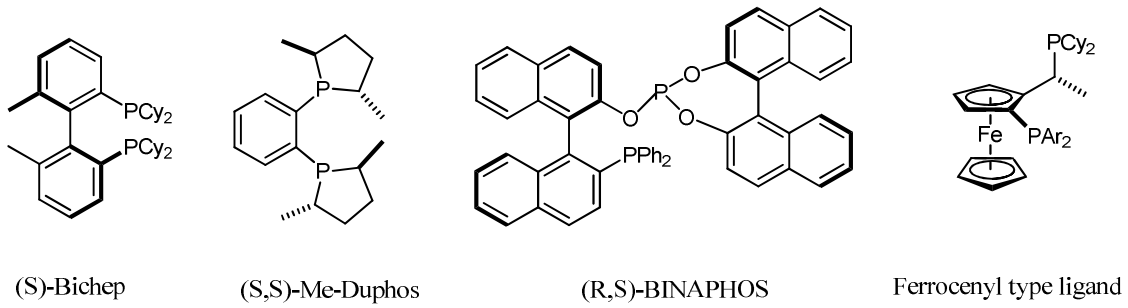

Figure 3.2 Chiral ligands for 1-alkene-CO co-polymerisation.

Other examples involve the use of BINAPHOS (Scheme 5)[12-14,16] and ferrocenyl-type ligands (e.g. Josiphos ligands, Figure 3.2).[16,18] For 1-propene-CO copolymerisations, high regioregularities (>99% head-to-tail) and high stereoregularity (> 96% isotacticity) were obtained. For high productivity and regioselectivity, the combination of a basic PCy_2 and a more electron withdrawing PAr_2 moiety appeared necessary. With the proof of concept for asymmetric induction available for the synthesis of medium-high molecular weight components, further activities shifted to the synthesis of chiral 1-alkene-CO dimers. For instance, Consiglio reported

the diastereo- and enantioselective synthesis of low molecular weight copolymers from propene and carbon monoxide in the presence of methanol to produce dimethyl-4-oxopentanoates.[18,19] The use of modified Bichep ((R)-MeO-Bichep) and Josiphos ligands gave the highest regioselectivity for head-to-tail enchainment, although the diastereoselectivity (66%) and enantioselectivity (72%) were lower for the Josiphos ligand when compared to the selectivity's obtained for copolymer synthesis.[19, 20]

The aim of the current study is the development of an asymmetric version of the hydro-acylation of 1-pentene to give 4-methyl-5-decanone with high chemo-, regio- and enantioselectivity (Scheme 3.1). For this purpose, chiral Pd complexes of the type L_2PdOTf_2 were applied. Four different classes of chiral diphosphines ligands were tested (Josiphos, Duphos, Walphos and ferroTane) at a range of process conditions. The first two ligand classes were selected on the basis of successful asymmetric conversions of CO/1-alkenes to chiral oligomers and polymers (*vide supra*).

3.2 Experimental

3.2.1 Chemicals

All chiral diphosphine ligands were obtained from Strem Chemicals. The ligands and the palladium acetate precursor (Sigma Aldrich >98%) were stored in a glove box. Dichloromethane (Lab-Scan 99.8%) and methanol (Lab-Scan 99.8%) were distilled from CaH_2 before use and stored under nitrogen. 1-Pentene (Sigma Aldrich 98%) was distilled from sodium and stored under nitrogen.[21,22] Trifluoromethanesulfonic acid (HOTf) (Strem 99+%) was stored under nitrogen at 5 ºC. The synthesis gas used was a 50:50 pre-mixed CO/H_2 gas mixture (HiQ, high quality) and was purchased from Hoek Loos. Racemic 4-methyl-5-decanone was synthesised using established procedures.[8,23] Enantio-enriched (80% ee) 4-methyl-5-decanone was synthesised in a four step procedure.[8,24] Enantio-enriched 4-methyl-nonanone (90% ee) was prepared using a three step procedure.[8,25] The tail-to-tail monoketone, 6-undecanone, was purchased from Sigma Aldrich (97%).

3.2.2 Experimental set-up

The catalytic reactions were carried out in a Parr autoclave (50 ml), which was operated in a batch mode with respect to the gas phase (Figure 3.3). The maximum operating pressure of the reactor is 200 bar, the maximum temperature 200 ºC. The reactor is electrically heated and the reactor content is stirred by a Parr overhead stirrer, equipped with a gas inducing impeller. Temperature and stirring speed are controlled by the Parr 4843 controller. The synthesis gas was fed from a premixed (50/50) storage bottle.

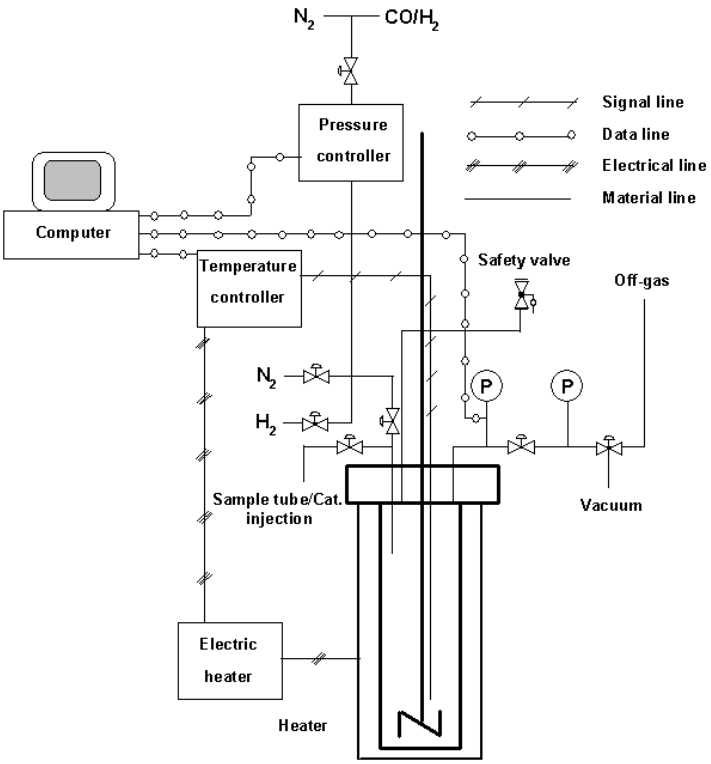

Figure 3.3 Schematic representation of the reactor setup.

3.2.3 General procedure

The catalyst was freshly prepared before each experiment under a protective nitrogen atmosphere using standard Schlenk techniques. $Pd(OAc)_2$ (9 mg, 0.04 mmol) was dissolved in the reaction solvent (either dichloromethane or methanol, 2 mL). After approximately 10 min the

diphosphine ligand (0.04 mmol) dissolved in either dichloromethane or methanol (2 mL) was added. The solution was stirred for 10 min prior to the addition of HOTf (30 mg, 0.2 mmol) and stirred for another 10 minutes before use. The batch autoclave was charged with solvent (either dichloromethane or methanol, 10 ml), 1-pentene (4.0 ml, 36.5 mmol) and the catalyst solution. The reactor was closed and flushed with nitrogen to remove air. The reactor was pressurised (60 bar) with synthesis gas (50/50 H_2/CO) and stirring was applied (1000 rpm). Subsequently the reactor was heated to the desired reaction temperature (60 or 125 ºC). After 5 h, the reactor was cooled to room temperature, depressurised, and flushed several times with N_2. The liquid product was filtered over silica gel to remove the catalyst.

3.2.4 Product analyses

The product composition in the liquid phase was analysed using a GC-FID HP-5890 series II, equipped with a 30 m HP-1 column and He as the carrier gas. The following temperature profile was applied: 10 minutes at 30 °C, from 30 °C to 325 °C at a rate of 10 °C/min, 15 min at 325 °C. Product compositions were obtained by comparing product peak areas by means of the 100% method.[26] The method was applied for peaks belonging to the most abundant product groups present in the samples: mono-oxygenates (ketones, aldehydes/alcohols and esters), olefin dimers and diketones. The response factors of all individual components are not known. To compensate for this, the concept of effective carbons was applied to determine the mol fraction of a product as is given in equation 3.1.[27]

$$X_j = \frac{F_j/(\sum C_{ef})_j}{\sum_1^n \frac{F_i}{(\sum C_{ef})_i}} \qquad (3.1)$$

Here X_j stands for the mol fraction of component j and F_j stands for the peak area of component j. F_j is divided by the sum of its effective carbons (C_{ef}) to obtain the 'effective area' of component j. The effective area of component j is divided by the sum of all effective areas of the relevant components in the chromatogram.[28]

The 1-pentene conversion was determined by GC. The concentration of 1-pentene in the liquid phase after reaction was determined using calibration curves with known 1-pentene

concentrations. The product solution was directly analyzed after reaction to avoid excessive evaporation of 1-pentene.

Product identification was performed by GC-MS and GC. GC-MS chromatograms were recorded on a GC (HP 6890) MS (HP-5973) equipped with a 30 m HP-5 MS column and He as the carrier gas (from 35 °C to 250 °C, rate 5 °C/min, final time 10 min.). GC spectra were recorded on a GC-FID HP-5890 series II, FID with a 30 m HP-1 column and He as the carrier gas (*vide supra*). Reference compounds, either obtained from chemical suppliers or prepared, were used to identify relevant components in the mixture.

The enantiomeric excess (ee) of 4-methyl-5-decanone was determined using a GC equipped with a 30 m chiral β-PM column with He as the carrier gas. The following temperature profile was applied: Initial temperature at 55 °C, hold time 100 min, then from 55 °C to 180 °C, rate 10 °C/min, final time 15 min. The retention times of the enantiomers were at 107.9 and 108.3 minutes at these conditions. A solvent change was required before the reaction products could be injected. For this purpose, the reaction solvent was removed under reduced pressure (100 mbar, 30 °C) to give yellow oil. The oil was re-dissolved in diethyl ether and analysed. The chromatograms were compared with the GC-MS and GC-FID analyses for peak identification and to identify possible overlap of individual enantiomers with by-products. Also the chromatograms were compared with those obtained with the reference materials (see section 3.2.1).

3.3 Results

The catalyst precursors $(L_2)Pd(OTf)_2$ were made in situ by mixing $Pd(OAc)_2$, the corresponding diphosphine and trifluoromethanesulfonic acid (HOTf) in either dichloromethane or methanol, see Scheme 3.4.[10,11]

$$L_2 + Pd(OAc)_2 + 2HOTf \longrightarrow (L_2)Pd(OTf)_2 + 2HOAc$$

Scheme 3.4 In situ formation of the catalyst precursor.

For all experiments a Pd to L_2 to HOTf molar ratio of 1.0 to 1.0 to 5.0 was applied. Experiments with different chiral diphosphine ligands belonging to four ligand families (Josiphos, Duphos, Walphos and ferroTANE) were performed.

3.3.1 Initial screening experiments using the a typical Josiphos ligand

Initially, a typical (R,S)-Josiphos ligand (L**1,** Figure 3.4) was screened in dichloromethane at 125 ºC and 60 bar pressure with a 1-pentene to catalyst ratio of 913 mol/mol. The results are given in Table 3.1 (entry 1).

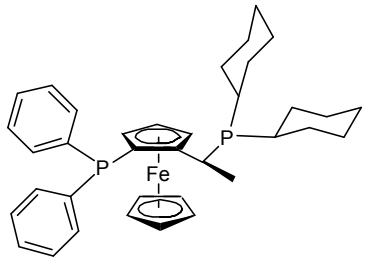

L**1**. (R,S)-Josiphos

Figure 3.4 Josiphos ligand L**1**

Table 3.1 Hydro-acylation of 1-pentene with Pd/(R,S)-Josiphos catalysts L**1**[a]

			Products[b] (mol%)									
Entry	T (°C)	Solvent	Sat. MK (%)	Sat. MK. h-to-t[c] (%)	S_{MD}[d]	ee[e] (%)	Sat. MK t-to-t[c] (%)	Enones (%)	Aldehydes/ Alcohols (%)	Esters (%)	Diketones (%)	Olefin dimers (%)
1	125	DCM	81	97	78	0	3	2	1	0	3	7
2	60	DCM	42	94	39	4	6	36	0	0	19	0
3	125	MeOH	17	94	16	4	6	1	42	40	1	0

a. Intake: 36.5 mmol of 1-pentene; 0.04 mmol of Pd; 0.04 mmol L_2; 0.2 mmol HOTf as the acid, 5 h reaction time, P_{H2} = P_{CO} = 30 bar. b. Products: Sat. MK: saturated monoketones (all regio-isomers); Enones: unsaturated monoketones (all regio-isomers); Total product composition = 100%. c. Fraction of saturated h-to-t monoketone or saturated head-to-head monoketone in the saturated MK fraction (h-to-h regio isomers were below the GC detection limit). d. Definition given in eq. 2. e. ee of the saturated head-to-tail monoketone, 4-methyl-5-decanone.

The enantiomeric excess (ee) of the desired 4-methyl-5-decanone, the head-to-tail monoketone, was negligible under these conditions. The selectivity towards 4-methyl-5-decanone (S_{MD}) was 78 mol%. Here the selectivity is defined as in equation 3.2.

S_{MD} = (saturated mono-ketones) x (h-to-t fraction in saturated mono-ketones) (mol%) (3.2)

Besides the desired saturated monoketones, small amounts of enones, diketones and olefin dimers (GC-MS, M^+= 140) were formed as well. The formation of diketones and enones is in line with literature data for achiral hydroacylations using $L_2Pd(OTf)_2$ catalysts with alkyldiphosphines.[10,11]

The olefin dimer fraction consisted of a mixture of isomeric C10 mono-unsaturated olefins of which the position of the double bond and the level of branching could not be established. The palladium catalysed dimerisation of olefins using diphosphine-palladium complexes of the type $(P_2)PdX_2$ is well known in the literature. Examples are the dimerisation of ethylene using Ph_2P-$(CH_2)_3$-PPh_2 in combination with $Pd(OAc)_2$ and p-toluenesulphonic acid (95 °C, 40 bar ethylene pressure) to give C4 dimers in more than 98% yield[29-31], the use of similar cationic Pd compounds with BF_4^- anions for the dimerisation of ethylene, propylene and styrene[32] and asymmetric styrene dimerisation using mixed palladium-indium species containing phosphite ligands.[33] However, olefin dimerisation under syngas conditions is remarkable. A further discussion and mechanistic implications will be given in the final section of this paper.

The selectivity for the desired 4-methyl-5-decanone is not only a function of the chemoselectivity but also a good regioselectivity towards the head-to-tail isomer is required. The regioselectivity in dichloromethane is excellent and the desired head- to-tail isomer was formed predominantly (97%), the remainder being mainly the tail-to-tail regio-isomer.

Various 1-pentene isomers were also found in the reaction mixture, a clear indication that the catalyst is also active in olefin isomerisation. This is not surprising as cationic Pd complexes of the type $(P_2)Pd^+ X^-$ are well established olefin isomerisation catalysts.[34-38]

To improve enantioselectivity, a hydro-acylation reaction was carried out at 60 ºC instead of 125 ºC. At these conditions, indeed a small though measurable ee was observed (4%, see Table 3.1, entry 2). However, the selectivity towards 4-methyl-5-decanone was reduced from 78 to 39 mol% due to the formation of considerable amounts of enones (36 mol%) and diketones (19

mol%). The formation of higher levels of diketones indicates that subsequent CO and olefin insertions occur more easily at lower temperatures leading to higher molecular weight products. This is a well established feature for CO/olefin co-oligomerisations and copolymerisations.[16, 39]

The formation of higher amounts of enones at 60 °C implies a change in termination mechanism when lowering the temperature. Both the saturated monoketones and enones are formed from a common intermediate (*vide infra)*. Termination by β-hydrogen elimination leads to enones, reaction with hydrogen to saturated monoketones. The shift towards enone formation suggests that termination by β-hydrogen elimination instead of the reaction with hydrogen becomes more pronounced at lower temperatures. A similar trend was reported by Drent and Budzelaar for related achiral Pd/diphosphine systems.[10, 11] Thus, lowering the temperature seems favourable for the enantioselectivity but has a negative effect on the chemoselectivity to saturated monoketones.

The 1-pentene conversion after 5 h at 60 °C was 84%. This corresponds with an average turn-over frequency (TOF) of 150 mol/(mol Pd.h). Typical values reported in the literature for achiral hydroacylations using alkylphosphines at 115 °C are about 1000 mol/(mol Pd.h) for 1-propene and about 100 mol/(mol Pd.h) for higher olefins like 1-octene.[10,11] Thus, particularly when considering the relatively low temperature for the experiment with the Josiphos ligand, the TOF for the Josiphos ligand is at the high end of the range given in the literature.

When the reaction was carried out in methanol (Table 3.1, entry 3), the selectivity to 4-methyl-5-decanone was only 16 mol%. Surprisingly, the major products here were alcohols/aldehydes (42 mol%) and esters (40 mol%). The alcohols/aldehydes are formed by hydroformylation (Scheme 3.2), the esters by methoxycarbonylation (Scheme 3.5), which are well established reaction pathways for syngas-1-alkene conversions in methanol using $(L_2)PdX_2$ catalysts, although no specific examples are known for the catalyst used here (with ferrocenyl type of ligands and HOTf).[10,11,40,41] Thus, methanol is not inert and is incorporated partly in the product.

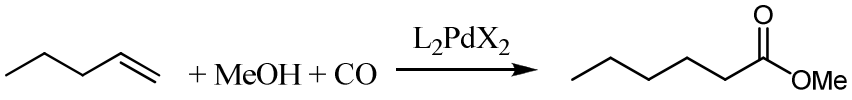

Scheme 3.5 Methoxycarbonylation of 1-pentene.

From these preliminary experiments it is concluded that Josiphos ligands are potentially attractive for hydro-acylation reactions, though the enantioselectivity for L**1** is poor at the conditions employed. The chemoselectivity of Josiphos L**1** in dichloromethane (high ketone selectivity, some diketones) shows resemblances with the results for typical cationic palladium-containing alkyldiphosphines like DnBPP and 1,3-bis(di-s-butylphosphino)propane (DsBPP) with HOTf as anion source.[10,11] However, the chemoselectivity in methanol differs considerably. With typical alkyldiphosphines like DsBPP and strong acids as the anion source, ketones are by far the main product and esters are not produced in considerable amounts when the reactions are performed in methanol. Only using the sterically very congested alkyldiphosphines like 1,3-bis(di-t-butylphosphino)propane, methyl esters are the main product.[41] Thus, the Josiphos ligand L**1** cannot be classified simply as an alkyldiphosphine and shows dual properties, in line with the presence of both an alkyl and arylphosphine group in the structure (Figure 3.4).

Based on the experiments with Josiphos L**1**, it was concluded that the subsequent screening experiments with a broader range of chiral ligands could be best performed in dichloromethane instead of methanol. A temperature of 60 °C or below was anticipated to have a positive effect on the enantioselectivity, although this might be at the expense of the chemoselectivity as well as the rate of the reaction.

3.3.2 Screening experiments with the Josiphos ligand family

The Josiphos ligands for the screening experiments are given in Figure 3.5. The experiments were performed at a reaction temperature of 60 °C in dichloromethane with 1-pentene as the olefin and using 30 bar H_2 and 30 bar CO pressure.

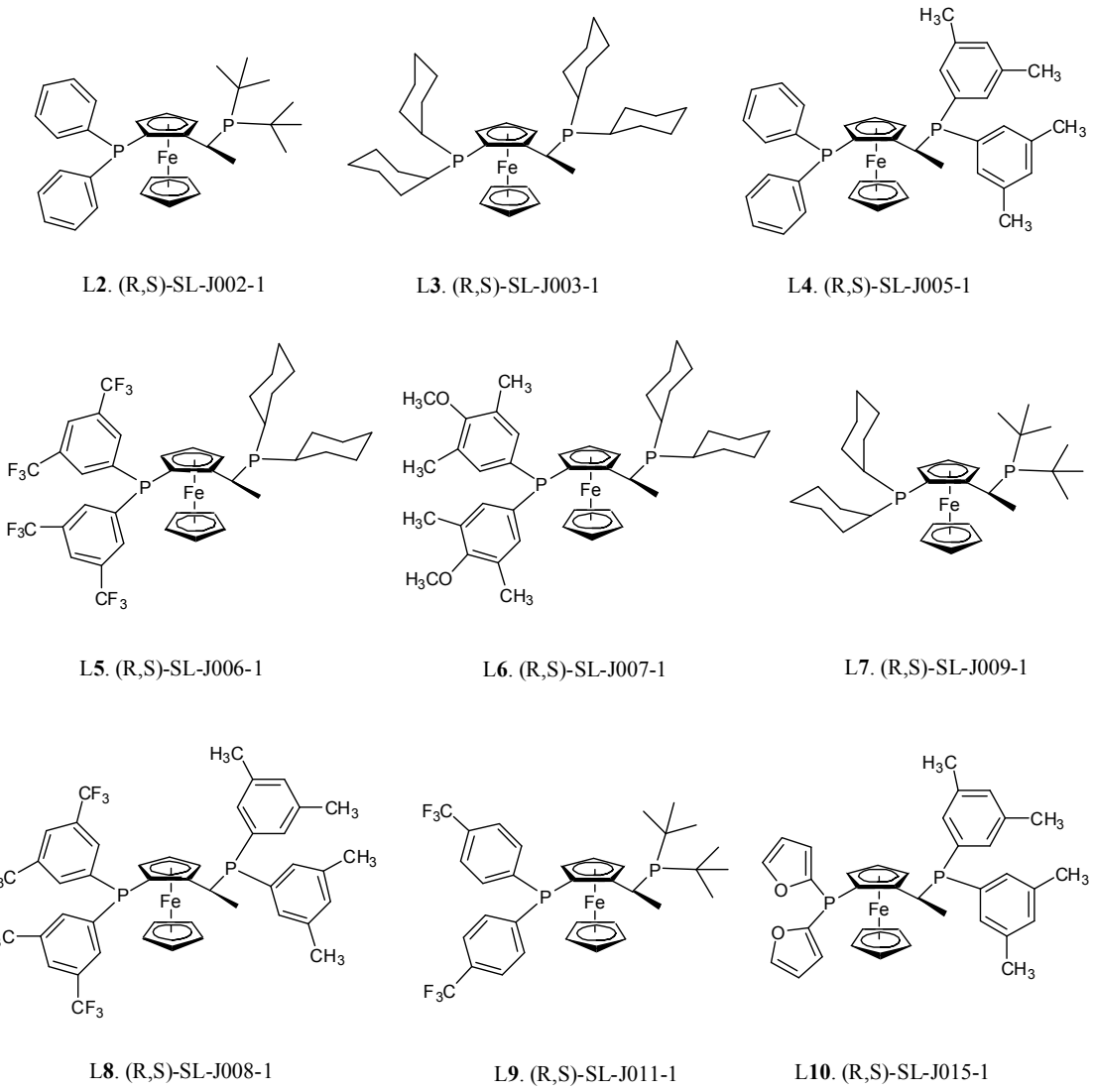

Figure 3.5 Josiphos type ligands L**2-10**

An overview of the results for the hydro-acylation reactions using the chiral Josiphos ligands is given in Table 3.2.

Table 3.2 Overview of results for catalytic hydro-acylations using the chiral Josiphos ligand family[a].

		Products[b] (mol%)								
Entry	Ligand	Sat. MK (%)	Sat. MK. h-to-t[c] (%)	S_{MD}[d]	ee[e]	Sat. MK t-to-t[c] (%)	Enones (%)	Aldehydes/ Alcohols (%)	Diketones (%)	Olefin conv. (%)
1	L**1**	42	94	39	4	6	36	0	19	84
2	L**2**	48	100	48	2	0	37	4	7	46
3	L**3**	16	100	16	25[f]	0	71	1	11	85
4	L**4**	55	60	33	1	40	20	0	22	48
5	L**5**	4	87	4	0	13	77	0	15	47
6	L**6**	41	97	39	4	3	32	0	23	39
7	L**7**[g]	14	100	14	1	0	59	4	7	62
8	L**8**	44	13	6	39	87	23	0	32	59
9	L**9**	32	99	32	1	1	60	2	4	59
10	L**10**	36	31	11	5	69	24	0	36	78

a. Intake: 36.5 mmol of 1-pentene; 0.04 mmol of Pd; 0.04 mmol L_2; 0.2 mmol HOTf as the acid, 5 h reaction time, $P_{H2} = P_{CO} = 30$ bar, dichloromethane, T = 60 °C. b. Products: Sat. MK: saturated monoketones (all regio-isomers); Enones: unsaturated monoketones (all regio-isomers); Total product composition = 100%. c. Fraction of saturated h-to-t monoketone or saturated head-to-head monoketone in the saturated MK fraction (h-to-h regio isomers were below the GC detection limit). d. Definition given in eq. 2. e. ee of the saturated head-to-tail monoketone, 4-methyl-5-decanone. f. Actual value likely lower due to some peak overlap in GC measurements. g. 15 mol% of 1-pentene dimers formed.

The enantioselectivity of the reaction is a clear function of the ligand. The highest ee for 4-methyl-5-decanone was 39% for ligand L**8**. For ligand L**3**, an ee of 25% was observed. However, the latter value is overestimated due to peak overlap of one of the enantiomers in the chiral GC chromatograms with small unidentified peaks. This was confirmed by comparing the chiral GC chromatograms with those obtained using a non-chiral GC column. The latter shows some, yet unidentified, additional peaks in the relevant region which hamper an accurate determination of the ee.

For all other ligands, the ee was below 5%. With this limited dataset, it is not possible to draw solid conclusions on the effects of the substituents of the Josiphos ligands (R and R') on the enantioselectivity. To confirm the ee values for the best Josiphos ligand in the series, an experiment with the (S,R) enantiomer of ligand L**8** was performed. This gave the opposite

enantiomer of 4-methyl-5-decanone with an ee of 42% and confirms that chiral induction indeed occurred with this ligand.

Although L**8** gave the highest ee of all Josiphos ligands, the selectivity to the desired 4-methyl-5-decanone (6 mol%) is at the low end of the range (4-48 mol%). This is visualised in Figure 3.6, where the selectivity is given as a function of the R and R' substituents on the Josiphos ligand. The aromatic R substituents are ordered according to their electronic properties[18,42,43], although some electronic effects cannot be excluded *a priori*. The R' groups are divided into alkyl and aryl substituents. Apparently, the selectivity is highest when using an unsubstituted Ph group at position R, whereas the R' group has a limited effect.

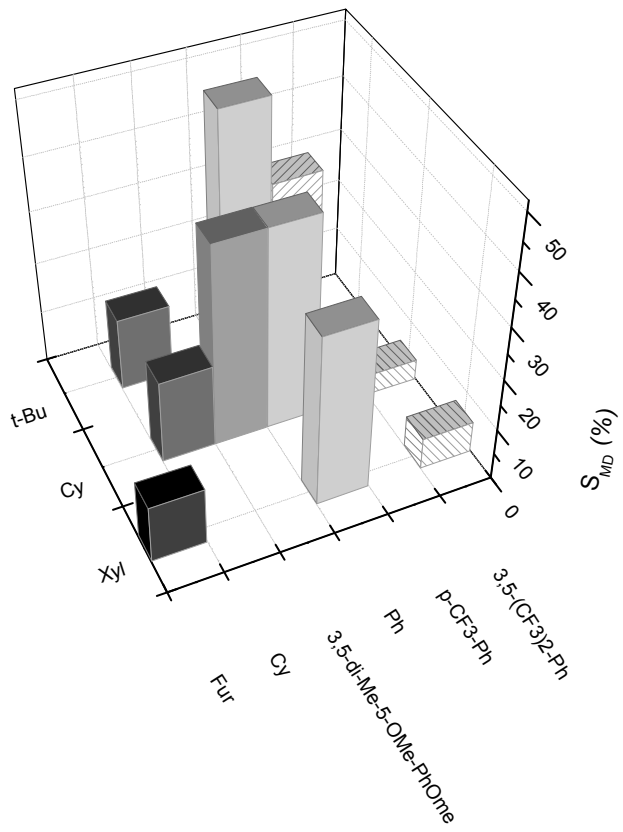

Figure 3.6 Selectivity to the 4-methyl-5-decanone (S_{MD}) as a function of the P-substituents of the Josiphos ligands L**1-10**.

The selectivity for 4-methyl-5-decanone is a function of both the chemo- and regioselectivity of the hydro-acylation reaction. These effects will be discussed separately. For all Josiphos ligands, the chemoselectivity as a function of the substituents on the phosphine ligands is given in Figure 3.7.

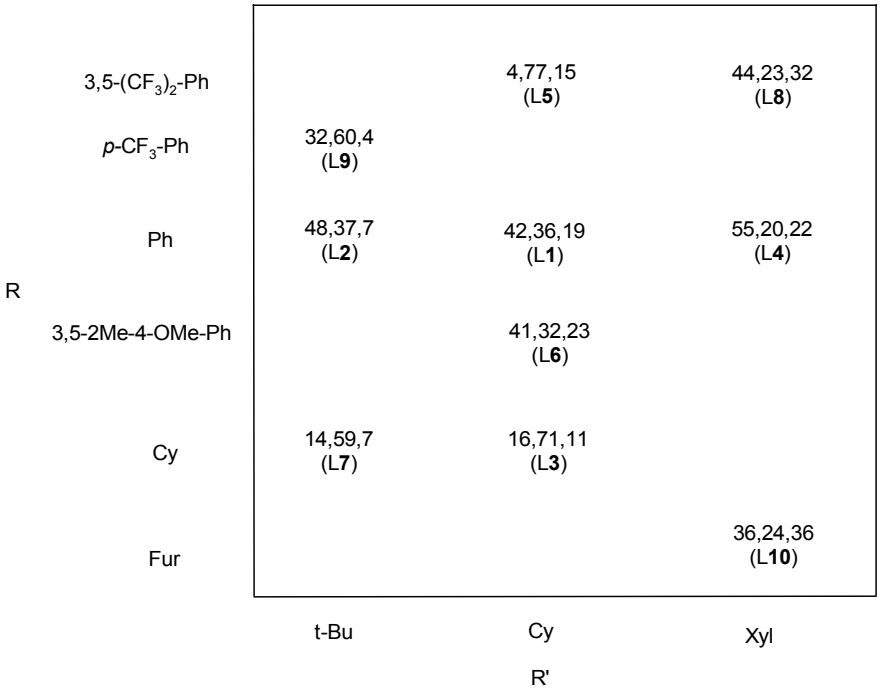

Figure 3.7 Chemoselectivity for the reaction of 1-pentene with synthesis gas using the Josiphos ligands L**1-10**. First number: saturated monoketone content (mol%); second: enone content, third: diketone content (mol%).

The chemoselectivity towards saturated monoketone formation varies between 55 and 4 mol%. Other products were enones and diketones and in one case olefin dimers were formed as well (L**7**, 15 mol%). Particularly the enones were formed in large amounts (up to 77 mol%) and for some of the ligands enones are actually the main product. Alcohols and aldehydes were present in amounts less than 5 mol%. The highest chemoselectivity with respect to saturated monoketone formation was obtained with ligand L**4** (entry 4, Table 3.1), namely 55 mol%. When considering Figure 3.7, the highest chemoselectivity to saturated monoketones was found for R

groups with intermediate electronic properties (Ph, 3,5-dimethyl-4-OMe-Ph) whereas the influence of the group R' seems limited.

For most of the ligands, the major regio-isomer in the saturated monoketone fraction is the desired head-to-tail regio-isomer (Figure 3.1). The only exceptions are ligand L**4**, L**8** and L**10** where the tail-to-tail isomers are predominantly formed. These three ligands contain an aromatic xylyl group at the R' position and a phenyl or furan group at position R and may be viewed as aromatic diphosphines. It is well established in the literature that the use of arylphosphines leads to lower amounts of the head-to-tail regio-isomers than alkylphosphines.[10,11]

Thus, it is concluded that chiral induction to obtain enantio-enriched 4-methyl-5-decanone is possible with Josiphos ligands. The best results were obtained with the (R,S)-L**8** ligand and an ee of 39% was observed. Unfortunately, the selectivity of 4-methyl-5-decanone was low (6 mol%) with this particular ligand at the process conditions applied to obtain the 39% ee. The main issue is a poor regioselectivity leading to the formation of considerable amounts of the tail-to-tail regio-isomer.

3.3.3 Screening results for the Duphos ligand family and a Walphos and ferroTANE ligand

A number of experiments were performed with three members of the Duphos ligand family (Figure 3.8) and a Walphos and FerroTANE ligand (Figure 3.9). The experiments were carried out with 1-pentene at 60 °C in dichloromethane using 30 bar H_2 and 30 bar CO pressure.

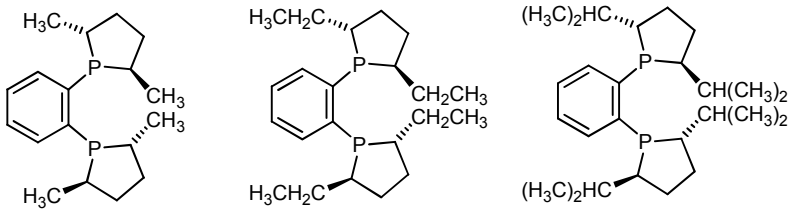

L**11**. (R,R)-Me-Duphos L**12**. (R,R)-Et-Duphos L**13**. (R,R)-i-Pr-Duphos

Figure 3.8 Duphos ligands.

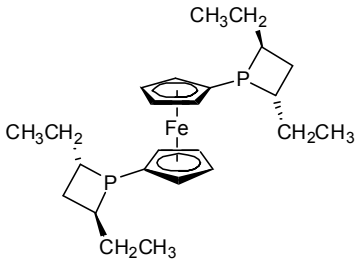

L**14**. (S,S)-Et-FerroTANE

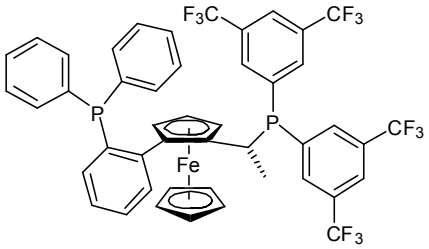

L**15**. (R,R)-Walphos SL-W001-1

Figure 3.9 FerroTANE and Walphos ligand.

The results for all experiments are given in Table 3.3

Table 3.3 Overview of results for catalytic hydro-acylations of 1-pentene using the chiral Duphos, FerroTANE and Walphos ligands [a].

		Products[b] (mol%)								
Entry	Ligand	Sat. MK (%)	Sat. MK h-to-t[c] (%)	S_{MD}[d]	ee[e] (%)	Sat. MK t-to-t[c] (%)	Enones (%)	Aldehydes/ Alcohols (%)	Diketones (%)	Olefin Conv. (%)
1	L**11**	69	95	66	16[f]	5	4	1	17	58
2	L**12**	59	96	57	20[f]	4	2	0	34	32
3	L**13**	42	100	42	6	0	16	0	37	72
4	L**14**	16	44	7	4	56	48	1	27	39
5	L**15**[g]	15	47	7	6	53	36	0	24	73

a. Intake: 36.5 mmol of 1-pentene; 0.04 mmol of Pd; 0.04 mmol L_2; HOTf as the acid, 5 h reaction time, $P_{H2} = P_{CO}$ = 30 bar, dichloromethane, 60°C. b. Products: Sat. MK: saturated monoketones (all regio-isomers); Enones: unsaturated monoketones (all regio-isomers); Total product composition = 100%. c. Fraction of saturated h-to-t monoketone or saturated head-to-head monoketone in the saturated MK fraction (h-to-h regio isomers were below the GC detection limit). d. Definition given in eq. 2. e. ee of the saturated head-to-tail monoketone, 4-methyl-5-decanone. f. Actual value likely lower due to some peak overlap in GC measurements. g. 15 mol% of 1-pentene dimers formed.

The selectivity to the desired saturated head-to-tail monoketone (4-methyl-5-decanone) for the Duphos ligands (42-66 mol%) is considerably higher than for the best Josiphos ligand (<48 mol%). However, the ee of the product is between 6 and 20%, which is considerably lower than

the highest value observed for the L**8** Josiphos ligand (39%) at similar conditions. The ee values are also likely slightly overestimated due to peak overlap in the chiral GC, as also observed for one of the Josiphos ligands (*vide supra*).

The chemoselectivity for saturated monoketone formation as a function of the substituents on the Duphos ligands is given in Figure 3.10. The values range between 42 and 69% and are considerably higher than for the Josiphos family (4-48 mol%). Major by-products are enones and diketones. Alcohols/aldehydes and olefin dimers were absent. The (R,R)-Me-Duphos (L**11**) ligand is the most selective for saturated monoketone formation. When increasing the bulk of the alkyl-substituent the preference for monoketone formation is reduced and diketones and enones are formed in considerable amounts.

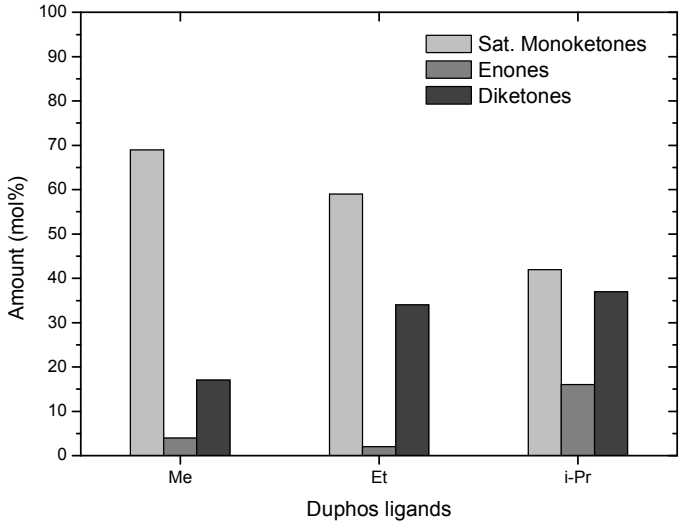

Figure 3.10 Chemoselectivity for the Duphos ligand family.

Of particular interest is the high regioselectivity towards the desired saturated head-to-tail isomer for the Duphos ligand family (> 95 mol%). This observation is in line with earlier work by Drent et al. on the palladium catalysed hydrocarbonylation of propene. Of all diphosphine $R_2P(CH_2)_nPR_2$ ligands tested, alkyldiphosphine ligands led to higher amounts of the desired head-to-tail regio-isomer than arylphosphines.[10,11]

The results for the Walphos and FerroTANE ligands (Figure 3.9) were not very promising. Low chiral inductions (ee < 6%) were observed (Table 3.3) and the selectivity to the desired saturated head-to-tail monoketone, 4-methyl-5-decanone, was also low (7 mol%). The poor selectivity is caused by a low chemoselectivity to saturated monoketones (large amounts of enones formed) and an intermediate regioselectivity (Table 3.3).

3.4 Discussion and mechanistic aspects

The hydrocarbonylation of olefins using $(L_2)PdX_2$ catalysts may lead to the formation of the desired monoketones (hydro-acylation) as well as to alcohols/aldehydes by hydroformylation and higher ketones by copolymerization reactions.[10,11] A proposed catalytic cycle including the formation of the various product classes is given in Scheme 3.6. The active species is commonly accepted to be a square-planar cationic Pd-hydride complex. Insertion of an olefin into the Pd-hydride bond followed by coordination and migratory insertion of a CO molecule results in the formation of a Pd-acyl species. The latter can either react with hydrogen (hydrogenolysis) to give an aldehyde/alcohol (hydroformylation) or with a second olefin leading to the formation of a Pd-alkyl species. Further successive insertions of CO and olefins will result in the production of polyketones (copolymerisation). Direct hydrogenolysis of the Pd-alkyl species will lead to the formation of saturated monoketones (hydro-acylation), whereas β-hydride elimination gives unsaturated monoketones (also hydro-acylation).

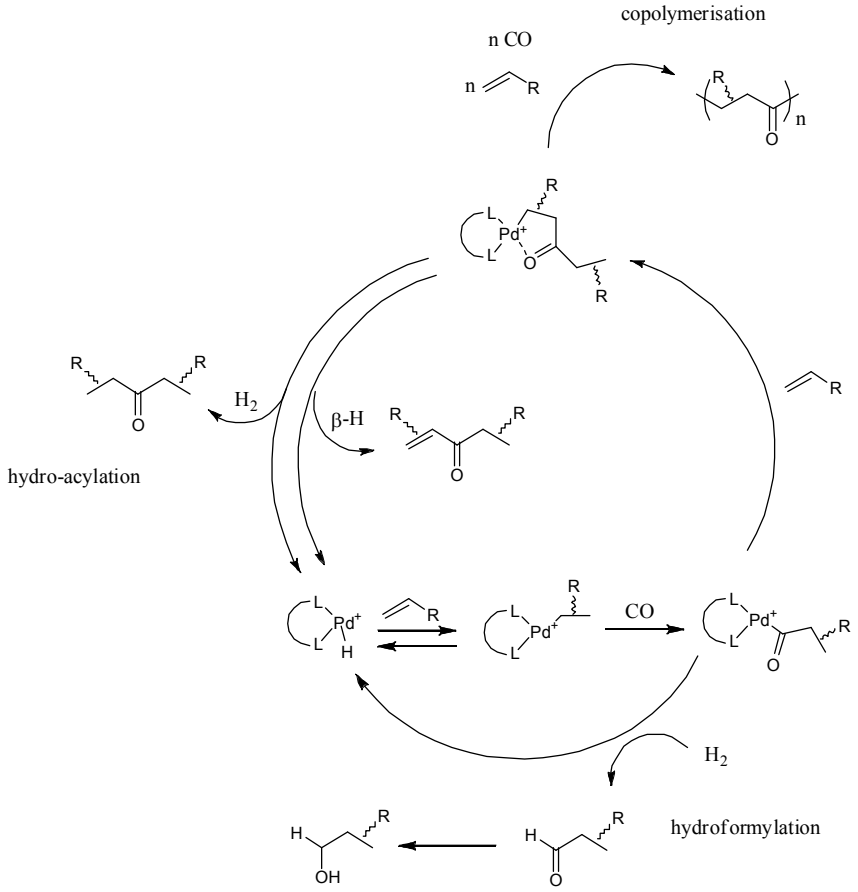

Scheme 3.6 Proposed catalytic cycle for the Pd(II) catalysed reactions of 1-alkenes and syngas.

3.4.1 Chemoselectivity

The chemoselectivity of the 1-alkene/syngas reactions catalysed by $(L)_2PdX_2$ complexes can be tuned by the choice of the diphosphine ligand, anion, reaction conditions and the solvent.[10,11] When using the Josiphos ligand family for the palladium catalyst hydro-acylation of 1-pentene in DCM at 60 °C using the triflate anion, the chemoselectivity towards the desired saturated monoketones is between 4 and 55 mol%. The highest chemoselectivity is observed with the ligands containing a Ph group at position R. Enones (23-71 mol%) and diketones (4- 36 mol%) are by far the most important by-products (Figure 3.7). Both the saturated monoketones and the enones are formed from the same intermediate, a Pd-alkyl species with a pendant ketone group

(Scheme 3.6). Enones are formed by β-hydrogen elimination, saturated ketones by hydrogenolysis. The formation of large amounts of enones is indicative for a strong electrophilic metal centre with a high affinity for β-hydrogen elimination. The relative reaction rates of both reactions determine the chemoselectivity of the reaction. Hydrogenolysis is assumed to proceed via heterolytic hydrogen splitting, where formally a H^+ is transferred to the anion and H^- to the Pd centre. It is well possible that heterolytic splitting of hydrogen is rather difficult in this system due to the use of the triflate anion (a poor H^+ acceptor) in combination with a relatively polar solvent, leading to a large Pd-anion distance.

Higher temperatures favour hydrogenolysis over β-hydrogen elimination, as is concluded from the observed temperature effects for L**1** (higher amounts of saturated ketones at higher temperature, see Table 3.1). Another possible measure to reduce enone formation is to perform the reactions at higher hydrogen pressure to speed up the rate of the hydrogenolysis reaction.

The amount of saturated monoketones observed for the Duphos ligands (42-69 mol%) is much higher than for the Josiphos ligands. Apparently, termination by reaction with hydrogen is strongly favoured over β-hydride elimination for the Duphos ligands. Major by-products are diketones (17-37 mol%) and to a lower extent enones (4-16 mol%, Figure 3.10). The chemo-selectivity is highest for the smaller Duphos substituent (Me) and particularly the diketone fraction increases when going from R = Me to R = ^{i}Pr. This is a clear indication for a higher preference for CO insertion in the Pd-alkyl species with the pendant carbonyl group than hydrogenation/β-hydrogen elimination when using bulkier substituents.

Hydro-acylations with two of the Josiphos ligands and the Walphos ligand resulted in the formation of significant amounts of C10 mono-unsaturated olefins arising from 1-pentene dimerisation. The maximum amount was found for the Walphos ligand L**15** (19 mol%, Table 3.3). Palladium diphosphine compounds are well known olefin dimerisation catalysts. However, dimerisations in the presence of CO have to the best of our knowledge not been reported to date. One possible explanation for olefin dimer formation is the (strong) acid catalysed (here HOTf) dimerisation of 1-pentene. However when valid, olefin dimerisation would be expected to occur for all reactions and this is certainly not the case. An alternative explanation is the involvement of cationic Pd catalysts, even though CO is present. In this case, olefin insertion has to compete with CO insertion in a Pd-alkyl bond. Support for the involvement of Pd complexes in the dimerisation reaction comes from a subsequent optimisation study using the Josiphos ligand L**8**.

Here, the content of olefin dimers in the reaction mixture was found to be a clear function of the CO pressure, with low pressures leading to a higher dimer contents. Thus, it is reasonable to assume that olefin dimerisation is a metal catalysed reaction and that the Josiphos ligand in this respect shows unique behaviour.

3.4.2 Regioselectivity

The regioselectivity of the saturated monoketone fraction depends on the mode of olefin insertion in a Pd-H bond (first insertion) and a Pd-acyl bond (second insertion, see Scheme 3.7). The desired head-to-tail isomer may be obtained by either two consecutive 1,2 insertions or two consecutive 2,1 insertions.

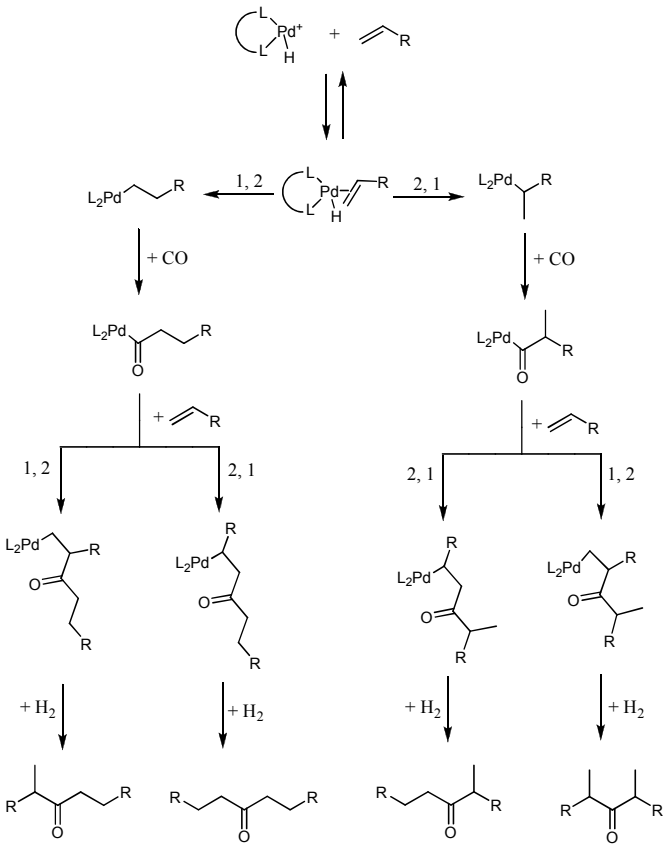

Scheme 3.7 Regioselectivity for saturated monoketone formation. **1,2**; 1,2-insertion, **2,1**: 2,1-insertion.

For the Josiphos ligand family, the regioselectivity towards the various saturated monoketone isomers (Figure 3.1) is a strong function of the R' group (Figure 3.7), with alkyl substituents (^{t}Bu, Cy) leading to the highest amounts of the desired head-to-tail isomer. The head-to-head regio-isomer was below the GC detection limit. This implies that 2,1 insertion of 1-pentene followed by 1,2 insertion does not occur to a significant extent. This is in line with literature data on related catalysts which indicate that 2,1 insertion of an-alkyl substituted olefin into a Pd-H bond does not take place easily.[10,44] It suggests that the left pathway in Scheme 3.7 is the most likely. Thus, the desired 4-methyl-5-decanone is most probably formed by two consecutive 1,2 insertions of 1-pentene.

For the Josiphos ligands with xylyl substituents at the R' position, the tail-to-tail isomers are predominantly formed. This suggests that the regioselectivity is a strong function of the basicity of the phosphine ligands, with less basic arylphosphines leading to a higher portion of the tail-to-tail isomer. This is in line with research by Drent et al. on the palladium(II) catalysed hydrocarbonylation of propene. Here the use of alkylphosphines led to higher amounts of the desired head-to-tail regio-isomer than with the arylphosphines.[10,11]

3.4.3 Enantioselectivity

The enantioselectivity's for the desired saturated head-to-tail isomer, 4-methyl-5-decanone, is in general low and only for four ligands out of the sixteen tested, ee values exceeding 10% were observed. A possible reason for these relatively low ee values is enolization of already formed 4-methyl-5-decanone in the course of the reaction.[45] We investigated this possibility by performing a hydro-acylation reaction in the presence of enantio-enriched 4-methyl-5-nonanone using a catalyst with **L**1 as the diphosphine ligand for the hydro-acylation of 1-pentene (dichloromethane, 50 °C, 24 h, 60 bar, 1 to 1 CO/H_2 ratio). After the reaction, the ee of the added enantio-enriched 4-methyl-5-nonanone was similar to the starting material. This experiment indicates that *in-situ* racemisation during the reaction, at least at 50°C, is not likely.

The enantioselectivity of the reaction is most likely determined by the second insertion of the olefin in the Pd-alkyl bond (Scheme 3.6) and not by the first one. The second olefin insertion should proceed in a 1,2 fashion (*vide supra*) to obtain the desired head-to-tail isomer (Scheme 3.7).

A possible explanation for the relatively low ee values is epimerisation of the stereogenic centre formed after the second olefin insertion. Epimerisation might occur by β-hydrogen elimination followed by re-insertion (Scheme 3.8). In this sequence the chirality at the α-position of the ketone is reduced or even lost.

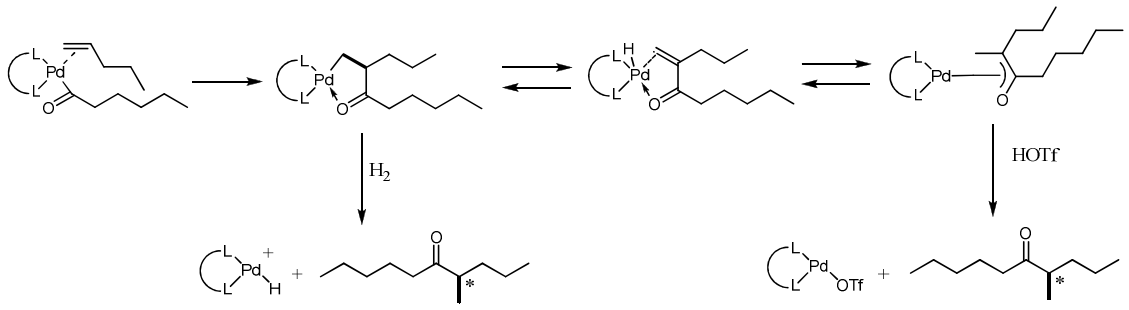

Scheme 3.8 Epimerisation of the stereogenic centre.

The Pd-H species with the coordinated enone may rearrange to form a Pd-enolate, as was shown by Klusener et al.[46] Two termination reactions may be envisaged: i. reaction of the chelate formed after the second olefin insertion step with hydrogen giving a Pd-H and 4-methyl-5-decanone and ii. reaction of the Pd-enolate with HOTf to form (racemic) 4-methyl-5-decanone and $L_2Pd(OTf)_2$. Thus, in case epimerisation plays a role and leads to a reduction of the product ee, the rate of epimerisation (initiated by β-hydrogen elimination) versus the rate of reaction of the Pd-alkyl bond with hydrogen will affect the product ee. When this hypothesis is valid and when assuming that the rate of hydrogenolysis is a function of the hydrogen pressure, higher product ee's are expected at higher hydrogen pressures. All experiments performed so far were performed at a constant hydrogen pressure, making it impossible to ground this hypothesis.

The highest ee value in the Josiphos family was obtained for ligand L**8**, an arylphosphine with xylyl and 3,5-$(CF_3)_2$-Ph substituents. The question arises why this particular ligand gives the highest enantioselectivity. The chemoselectivity to saturated monoketones is within the range of the Josiphos ligands. More remarkable is a poor regioselectivity, actually by far the worst of all Josiphos ligands, with the dominant formation of the tail-to-tail isomer (87 mol% of the saturated monoketone fraction). It implies that 2,1 insertion for the second olefin insertion step is highly favoured. This change in insertion mode compared to the other ligands may either be steric or

electronic in origin. The common insertion mode for alkyl substituted terminal olefins is a 1,2 mode. Thus, one could argue that this change in regioselectivity has a steric origin, suggesting the presence of a rather crowded metal centre. This crowdedness might lead to a high enantio-discrimination for the insertion step. However, further studies (to be reported) for the L**8** ligand at a wide range of process conditions reveal that modest ee values are also possible at good regioselectivities, indicating that this hypothesis is likely not valid. An alternative explanation for the performance of L**8** could be a high rate of hydrogenolysis compared to epimerisation (Scheme 3.8). Support for this statement comes from the observation that the amount of enones is the lowest for all Josiphos ligands. Thus, β-elimination seems less facile than hydrogenation. When considering that epimerisation involves β-hydrogen elimination, although without release of the product olefin from the metal coordination sphere, it could be speculated that the rate of epimerisation compared to hydrogenolysis is low for L**8**, leading to enhanced product ee's.

3.5 Conclusions

Sixteen chiral diphosphine ligands were screened for the chiral hydro-acylation of 1-pentene to 4-methyl-5-decanone (saturated head-to-tail monoketone) using Pd catalysts of the type $(L_2)Pd(OTf)_2$. The highest ee was found for the (R,S) Josiphos ligand L**8** (39% ee), albeit the product selectivity was low (6 mol%) due to a poor regioselectivity. Enantiomeric discrimination by this ligand was confirmed by reactions with the (S,R) Josiphos ligand L**8**, giving the other enantiomer of 4-methyl-5-decanone with a similar ee. The highest ee value for a Duphos ligand was 20%, although this value is slightly overestimated due to peak overlap in chiral GC analyses. The selectivity to 4-methyl-5-decanone is much better for the Duphos ligands (up to 66 mol%) than the Josiphos ligands. The research described in this paper indicates that chiral induction in catalytic hydro-acylation reactions is possible and that both arylphosphines (Josiphos L**8**) and alkylphosphines (Duphos) have potential for further research to increase the ee and the yield. These studies will be reported in forthcoming papers.

3.6 References

1 N. B. Johnson, I. C. Lennon, P. H. Moran, and J. A. Ramsden, *Acc. Chem. Res.*, 2007, **40**, 1291-1299.

2 R. Noyori, *Adv. Synth. Catal.*, 2003, **345**, 15-32.

3 W. S. Knowles and R. Noyori, *Acc. Chem. Res.*, 2007, **40**, 1238-1239.

4 H. Alper and N. Hamel, *J. Am. Chem. Soc.*, 1990, **112**, 2803-2804.

5 W. A. Loughlin, *Bioresour. Technol.*, 2000, **74**, 49-62.

6 K. Mori and S. Harashima, *Tetrahedron Lett.*, 1991, **32**, 5995-5998.

7 G. J. A. Conceicao, P. J. S. Moran, and J. A. R. Rodrigues, *Arkivoc*, 2003, 500-506.

8 F Gini, *PhD thesis University of Groningen*, 2007.

9 E. P. Siqueira, J. A. R. Rodrigues, and P. J. S. Moran, *Tetrahedron-Asymmetry*, 2001, **12**, 847-852.

10 E. Drent and P. H. M. Budzelaar, *J. Organomet. Chem.*, 2000, **594**, 211-225.

11 E. Drent, W. P. Mul, and P. H. M. Budzelaar, *Comments Inorg. Chem.*, 2002, **23**, 127-147.

12 K. Nozaki, N. Sato, and H. Takaya, *J. Am. Chem. Soc.*, 1995, **117**, 9911-9912.

13 K. Nozaki, *Pure Appl. Chem.*, 2004, **76**, 541-546.

14 K. Nozaki, *Polym. J.*, 2005, **37**, 871-876.

15 M. Barsacchi, A. Batistini, G. Consiglio, and U. W. Suster, *Macromolecules*, 1992, **25**, 3604-3606.

16 C. Bianchini and A. Meli, *Coord. Chem. Rev.*, 2002, **225**, 35-66.

17 S. Bronco, G. Consiglio, R. Hutter, A. Batistini, and U. W. Suster, *Macromolecules*, 1994, **27**, 4436-4440.

18 C. Gambs, S. Chaloupka, G. Consiglio, and A. Togni, *Angew. Chem. Int. Ed.*, 2000, **39**, 2486-2488.

19 M. Sperrle and G. Consiglio, *J. Am. Chem. Soc.*, 1995, **117**, 12130-12136.

20 S. Bronco, G. Consiglio, S. Dibenedetto, M. Fehr, F. Spindler, and A. Togni, *Helv. Chim. Acta*, 1995, **78**, 883-886.

21 D. D. Perrin, and W. L. F. Armarego, *Purification of laboratory chemicals*, Pergamon Press, Oxford, 3rd ed, 1988.

22 P. W. N. M. van Leeuwen, *Appl. Catal. ,A*, 2001, **212**, 61-81.

23 O. H. Oldenziel, D. van Leusen, and A. M. van Leusen, *J. Org. Chem.*, 1977, **42**, 3114-3118.

24 P. Wipf, Y. Kim, and P. C. Fritch, *J. Org. Chem.*, 1993, **58**, 7195-7203.

25 E. J. Corey and D. Enders, *Tetrahedron Lett.*, 1976, **17**, 3-6.

26 W. G. M. Braam, *Chromatografie*, Educatieve Partners Nederland BV, Culemborg, The Netherlands, 5, 1994.

27 V. Svojanovský, M. Krejí, K. Tesaík, and J. Janák, *Chromatogr. Rev.*, 1966, **8**, 90-171.

28 A. D. Jorgensen, K. C. Picel, and V. C. Stamoudis, *Anal. Chem.*, 1990, **62**, 683-689.

29 E. Drent, *Eur Patent*, 01701311, 1986.

30 E. Drent, *Eur Patent*, 0280373, 1988.

31 E. Drent, *Pure Appl. Chem.*, 1990, **62**, 661-669.

32 Z. Jiang and A. Sen, *Organometallics*, 1993, **12**, 1406-1415.

33 R. B. Bedford, M. Betham, M. E. Blake, A. Garce's, S. L. Millara, and S. Prashar, *Tetrahedron*, 2005, **61**, 9799-9807.

34 G. C. Bond and M. Hellier, *J. Catal.*, 1965, **4**, 1-&.

35 D. B. Dahl, C. Davies, R. Hyden, M. L. Kirova, and W. G. Lloyd, *J. Mol. Catal. A:Chem.*, 1997, **123**, 91-101.

36 J. F. Harrod and A. J. Chalk, *J. Am. Chem. Soc.*, 1964, **86**, 1776-&.

37 A. Sen and T. W. Lai, *Inorg. Chem.*, 1984, **23**, 3257-3258.

38 H. G. Tang and D. C. Sherrington, *J. Mol. Catal.*, 1994, **94**, 7-17.

39 R. A. M. Robertson and D. J. Cole-Hamilton, *Coord. Chem. Rev.*, 2002, **225**, 67-90.

40 W. Clegg, G. R. Eastham, M. R. J. Elsegood, R. P. Tooze, X. L. Wang, and K. Whiston, *Chem. Commun.*, 1999, 1877-1878.

41 R. I. Pugh and E. Drent, *Adv. Synth. Catal.*, 2002, **344**, 837-840.

42 K. P. Vollhardt, and N. E. Schore, *Organic chemistry structure and function*, W.H. Freeman, New York, 5th ed, 2007.

43 Q. Xu and L. B. Han, *Org. Lett.*, 2006, **8**, 2099-2101.

44 M. J. Burk and J. E. Feaster, *J. Am. Chem. Soc.*, 1992, **114**, 6266-6267.

45 R. T. Morrison, and R. N. Boyd, *Organic chemistry*, Prentice Hall, Englewood Cliffs, N.J, 6th ed, 1992.

46 M. A. Zuideveld, P. C. J. Kamer, P. W. N. M. van Leeuwen, P. A. A. Klusener, H. A. Stil, and C. F. Roobeek, *J. Am. Chem. Soc.*, 1998, **120**, 7977-7978.

Chapter 4. Enantioselective Syngas Conversions: Hydro-acylations of 1-Alkenes to α-Methylketones using a Palladium/Josiphos Catalyst

4.1 Introduction

The enantioselective production of linear α-substituted ketones is of particular interest as this structure element is present in many drugs and pheromones.[1,2] A known method for the asymmetric synthesis of α-methyl substituted ketones is the reduction of α-methylene ketones by the use of baker's yeast (Scheme 4.1).[3-5] Good results were obtained in, for example, the reduction of α-methyleneketone with R_1= Me and R_2= *n*-Hexyl at 30 ºC. A conversion of 70% was obtained after 2 h with a product ee of > 99%.[5]

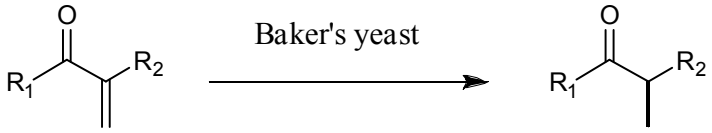

Scheme 4.1 Reduction of methyleneketones by baker's yeast.

An attractive alternative for the synthesis of α-methyl-substituted ketones could be the hydro-acylation of 1-alkenes with syngas (Scheme 4.2). Recently, Drent and Budzelaar reported a non-asymmetric version of this approach, using palladium diphosphine catalysts of the type L_2PdX_2 (in which X is a non-coordinating anion) for the selective production of monoketones (Scheme 4.2).[6,7]

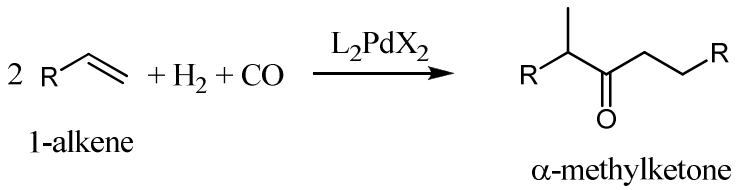

Scheme 4.2 Hydro-acylation of 1-alkenes to α-methylketones.

Very promising results were obtained using a catalyst prepared in situ from $Pd(OAc)_2$, an alkyl-diphosphine like DnBPP (1,3-bis(di-n-butylphosphino)propane), and trifluoromethanesulphonic acid (HOTf). For 1-octene, a chemoselectivity of 98 mol% was obtained when the reactions were performed in diglyme at 125 ºC with a $P_{CO} = P_{H2} = 30$ bar.[6,7]

We recently reported an asymmetric version of the hydro-acylation reaction given in Scheme 4.2. When using 1-pentene as the olefin, dichloromethane as the solvent and a temperature of 60 °C, the desired 4-methyl-5-decanone was obtained with an ee of 39% using a Josiphos type ligand (L**1**) (Figure 4.1).

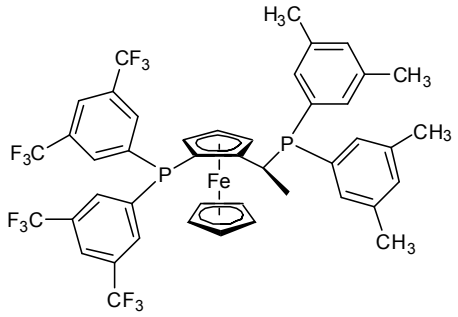

(R,S)-SL-J008-1

Figure 4.1 Josiphos (R,S)-SL-J008-1 ligand (L**1**).

At these conditions, the selectivity towards 4-methyl-5-decanone is only 6 mol%. Other products were enones, higher CO-olefin oligomers resulting from alternating CO-olefin copolymerisation and aldehydes/alcohols resulting from hydroformylation (Scheme 4.3).

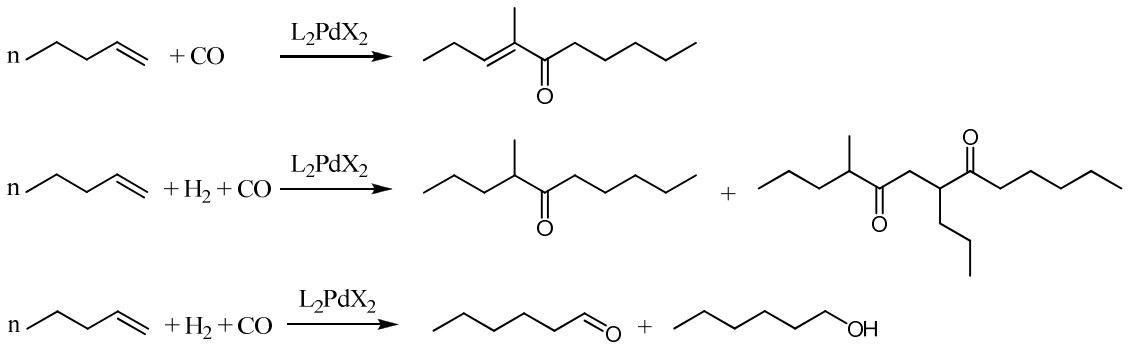

Scheme 4.3 Main and side products from the L_2PdX_2 catalyzed reactions of 1-pentene with syngas (only one isomer of the products is shown).

Furthermore, a number of regio-isomers of the saturated ketones are formed (Figure 4.2). The desired product is the head-to-tail regio-isomer (4-methyl-5-decanone, R = n-C_3H_7). However, with Josiphos ligand L**1** at 60 °C and 60 bar syngas pressure (1 to 1 ratio), the tail-to-tail regio-isomer is highly favoured (87% of the saturated monoketones).

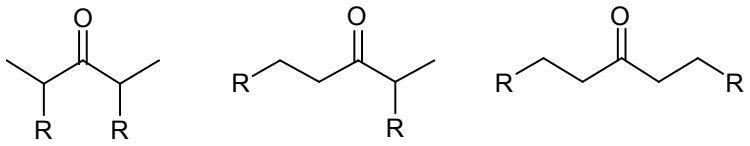

head-to-head head-to-tail tail-to-tail

Figure 4.2 Saturated monoketone regio-isomers for 1-alkene hydro-acylation.

Herein, we show the effect of the process conditions temperature and H_2/CO pressure on the hydro-acylation reaction of 1-pentene with ligand L**1,** with the objective to optimise the chemo-, regio- and enantioselectivity. Statistical modelling software (Design Expert) has been used to investigate and quantify the influence of these process conditions on reaction performance.

4.2 Experimental Section

4.2.1 Chemicals

Josiphos ligand L**1** ((R,S)-SL-J008-1, was purchased from Sigma Aldrich (≥ 97%). The ligand and palladium acetate (Sigma Aldrich >98%) were stored in a glove box. Dichloromethane (Lab-Scan 99.8%) was distilled from CaH_2 before use and stored under nitrogen. 1-Pentene (Sigma Aldrich 98%) was distilled from sodium and stored under nitrogen.[8,9] Trifluoromethanesulfonic acid (HOTf) (Strem 99+%) was stored under nitrogen at 5 ºC. The synthesis gas used was a 50:50 pre-mixed CO/H_2 gas mixture (HiQ (high quality), CO ≥ 99,997 vol%, H_2 ≥ 99.9999 vol%) and was purchased from Hoek Loos. Pure hydrogen gas was also obtained from Hoek Loos (HiQ, purity ≥ 99.9999 vol%). Racemic 4-methyl-5-decanone was synthesised using literature procedures.[4,10] Enantio-enriched (80% ee) 4-methyl-5-decanone was synthesised in a four step procedure.[4,11] Enantio-enriched 4-methyl-nonanone (90% ee) was prepared using a three step procedure.[4,12] The tail-to-tail monoketone, 6-undecanone, was purchased from Sigma Aldrich (97%).

4.2.2 Experimental set-up

The catalytic reactions were carried out in a Parr autoclave (50 ml), which was operated in a batch mode with respect to the gas phase (Figure 4.3). The maximum operating pressure of the reactor was 200 bar, the maximum temperature 200 ºC. The reactor was electrically heated and the reactor content stirred by a Parr overhead stirrer, equipped with a gas inducing impeller. Temperature and stirring speed were controlled by the Parr 4843 controller. The synthesis gas was fed from a premixed (50/50) gas cylinder and additional hydrogen was added manually from a separate gas cylinder.

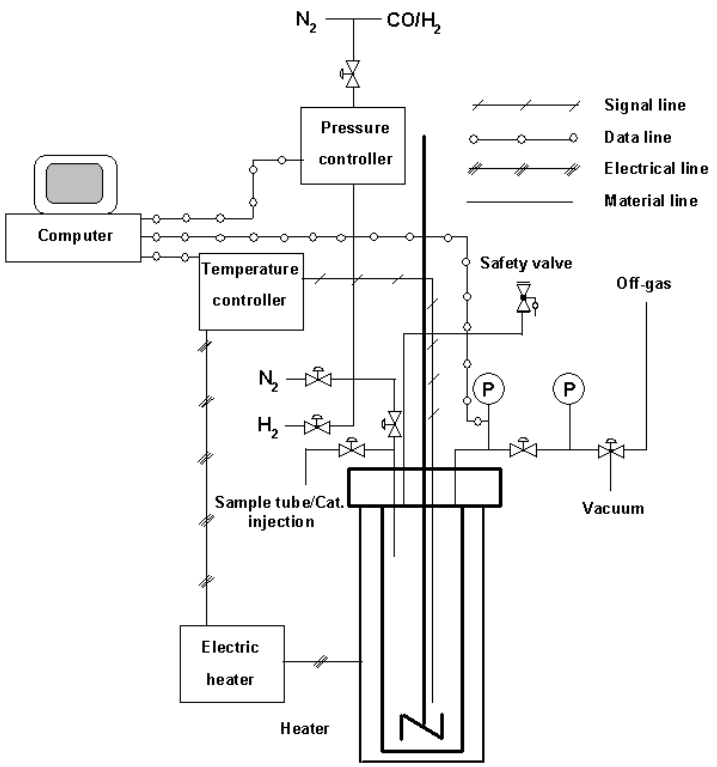

Figure 4.3 Schematic representation of the reactor setup.

4.2.3 General procedure

The catalyst was freshly prepared before each experiment under a nitrogen atmosphere using standard Schlenk techniques. $Pd(OAc)_2$ (9 mg, 0.04 mmol) was dissolved in dichloromethane (2 mL). After approximately 10 min the diphosphine ligand L**1** (0.04 mmol) dissolved in dichloromethane (2 mL) was added. The solution was stirred for 10 min prior to the addition of HOTf (30 mg, 0.2 mmol) and stirred for another 10 minutes before use. The batch autoclave was charged with solvent (dichloromethane, 10 ml), 1-pentene (4.0 ml, 36.5 mmol) and the catalyst solution. The reactor was closed and flushed with nitrogen to remove air. The reactor was pressurised (10-100 bar) with synthesis gas (50/50 H_2/CO), and when required, H_2 (10-140 bar) was added. Subsequently, the reactor was heated to the desired reaction temperature (30, 60 or 90 ºC). During reaction, the stirrer speed was maintained at 1000 rpm. After 5 h, the reactor was

cooled to room temperature, depressurised, and flushed several times with N_2. The liquid product was filtered over silica gel to remove the catalyst.

4.2.4 Product analyses

The product composition in the liquid phase was analysed using a GC-FID HP-5890 series II, equipped with a 30 m HP-1 column and He as the carrier gas. The following temperature profile was applied: 10 minutes at 30 °C, from 30 °C to 325 °C at a rate of 10 °C/min, 15 min at 325 °C. Product compositions were obtained by comparing product peak areas by means of the 100% method.[13] The method was applied for peaks belonging to the most abundant product groups present in the samples: mono-oxygenates (ketones, aldehydes/alcohols), olefin dimers and trimers and diketones. The response factors of all individual components are not known. To compensate for this, the concept of effective carbons was applied to determine the mol fraction of a product. (eq 4.1).[14]

$$X_j = \frac{F_j / (\sum C_{ef})_j}{\sum_{1}^{n} \frac{F_i}{(\sum C_{ef})_i}} \qquad (4.1)$$

Here X_j stands for the mol fraction of component j and F_j stands for the peak area of component j. F_j is divided by the sum of its effective carbons (C_{ef}) to obtain the 'effective area' of component j. The effective area of component j is divided by the sum of all effective areas of the relevant components in the chromatogram.[15]

The 1-pentene conversion was determined using the same GC equipment. The concentration of 1-pentene in the liquid phase after reaction was determined using calibration curves with known 1-pentene concentrations. The product solution was directly analyzed after reaction to avoid excessive evaporation of 1-pentene.

Product identification was performed by GC-MS and GC. GC-MS chromatograms were recorded on a GC (HP 6890) MS (HP-5973) equipped with a 30 m HP-5 MS column and He as the carrier gas (from 35 °C to 250 °C, rate 5 °C/min, final time 10 min.). GC chromatograms were recorded on a GC-FID HP-5890 series II, with FID on a 30 m HP-1 column and He as the

carrier gas (*vide supra*). Reference compounds, either obtained from chemical suppliers or prepared, were used to identify relevant components in the mixture.

The enantiomeric excess of the desired 4-methyl-5-decanone was determined using a GC equipped with a 30 m chiral β-PM column with He as the carrier gas. The following temperature profile was applied: 50 °C to 55 °C, rate 10 °C/min, hold time 100 min, then from 55 °C to 180 °C, rate 10 °C/min, final time 15 min. A solvent change was required before the reaction products could be injected. For this purpose, the dichloromethane was removed under reduced pressure (100 mbar, 30 °C) to give a yellow oil. The oil was re-dissolved in diethyl ether and analysed. The retention times of the enantiomers were 107.9 and 108.3 minutes. The chromatograms were compared with the GC-MS and GC-FID analyses for peak identification and to identify possible overlap of individual enantiomers with by-products of the reaction. Also the chromatograms were compared with those obtained with the reference materials (see section 4.2.1).

4.2.5 Statistical modeling using Design Expert

The experimental results for each response were analyzed using the Design Expert 7 software package. Responses are modeled using standard expressions (equation (4.2)):

$$y = b_0 + \sum_i b_i x_i + \sum b_{ii} x_i^{\,2} + \sum_j \sum_k b_{jk} x_i x_k \qquad (4.2)$$

Here, i = A to C, j = B to C and k = A to C with A, B, C representing the independent variables; *bi*, *bii* and *bjk* are the regression coefficients which are obtained by statistical analyses of the data. Significant factors were selected on the basis of their p value in the ANOVA analyses. Factors with a p value lower than 0.05 are regarded as significant and included in the response model. Backward elimination was applied to eliminate all statistically insignificant terms. After each elimination step, a new ANOVA table was generated to select the subsequent non-significant factor.

4.3 Results

4.3.1 Experimental window and approach

A total of 10 experiments was carried at different process conditions (temperature and partial CO and hydrogen pressure) using an *in situ* formed Pd-catalyst based on $Pd(OAc)_2$, Josiphos ligand L**1** and HOTf as the acid component in dichloromethane. The experimental ranges for the independent variables are given in Table 4.1. For all experiments, a fixed Pd intake was applied and the substrate to catalyst ratio was set at 910 (about 0.1 mol%)

Table 4.1 Experimental ranges for the hydro-acylation of 1-pentene

	Lowest value	Highest value
T (°C)	30	90
P_{CO} (bar)	2.5	30
P_{H2} (bar)	17.5	105

For each experiment the olefin conversion, product distribution and the ee of the desired 4-methyl-5-decanone (**1**) was determined and the results are given in Table 4.2. The selectivity for the desired 4-methyl-5-decanone (**3**) is defined as follows:

$$S_{MD}=(\text{saturated monoketones})x(\text{h-to-t fraction in saturated monoketones})(\text{mol\%}) \quad (4.3)$$

The responses (ee, conversion, S_{MD}, chemo- and regioselectivity) at different process conditions were analysed using statistical software to obtain a quantitative relation between the responses and the process variables. An overview of the results is given in Table 4.2.

Table 4.2 Effects of process conditions on conversion, chemo-, regio- and enantioselectivity for the hydro-acylation of 1-pentene[a].

				Product (mol%)[b]										
Entry	T (°C)	P CO (bar)	P H_2 (bar)	Sat.MK (%)	Sat.MK h-to-t[c] (%)	S_{MD}[d]	ee[e]	Sat.MK. t-to-t[c] (%)	Enones (%)	alc/ald (%)	DK (%)	Dim (%)	Trim (%)	Olefin conv (%)
1	90	30	30	61	56	35	0	44	29	1	8	0	0	64
2	90	5	105	83	72	60	0	28	7	0	7	0	0	84
3	60	30	30	44	13	6	39	87	24	0	32	0	0	59
4	60	5	50	43	50	22	29	50	22	0	21	10	0	81
5	60	15	105	55	50	27	41	50	23	1	19	0	0	50
6	60	15	145	44	41	18	32	59	18	0	15	20	2	77
7	60	30	120	20	55	11	33	45	37	0	21	19	2	90
8	30	5	50	20	55	11	67	45	7	0	11	43	17	22
9	30	2.5	50	18	62	11	65	38	2	0	6	62	10	59
10	30	2.5	17.5	12	84	10	73	16	2	0	2	80	4	24

a. Intake: 36.5 mmol of 1-pentene; 0.04 mmol of Pd; 0.04 mmol L_2; 0.2 mmol HOTf as the acid, 5 h reaction time, dichloromethane. b. Products: Sat. MK: saturated monoketones (all regio-isomers); Enones: unsaturated monoketones (all regio-isomers); Alc/ald: alcohols and aldehydes; DK: Diketones; Dim: Dimers; Trim: Trimers; Total product composition = 100%. c. Fraction of saturated h-to-t monoketone or saturated head-to-head monoketone in the saturated MK fraction (h-to-h regio isomers were below the GC detection limit). d. defined according to eq. 1. e. ee of the saturated h-to-t monoketone, 4-methyl-5-decanone.

4.3.2 Effect of process conditions on the ee of 4-methyl-5-decanone

The ee of the desired 4-methyl-5-decanone is a strong function of the temperature. Highest ee values were obtained at 30 °C (67-73%, see Table 4.2). At a reaction temperature of 90 °C (Table 4.2, entry 1 and 2) the ee was negligible. A verification experiment was performed with the other enantiomer (S,R) of Josiphos ligand L**1** at 30 °C. In this case, the opposite enantiomer of 4-methyl-5-decanone was obtained with an ee of 67%, which is within the experimental error. The GC chromatograms for both experiments are given in Figure 4.4.

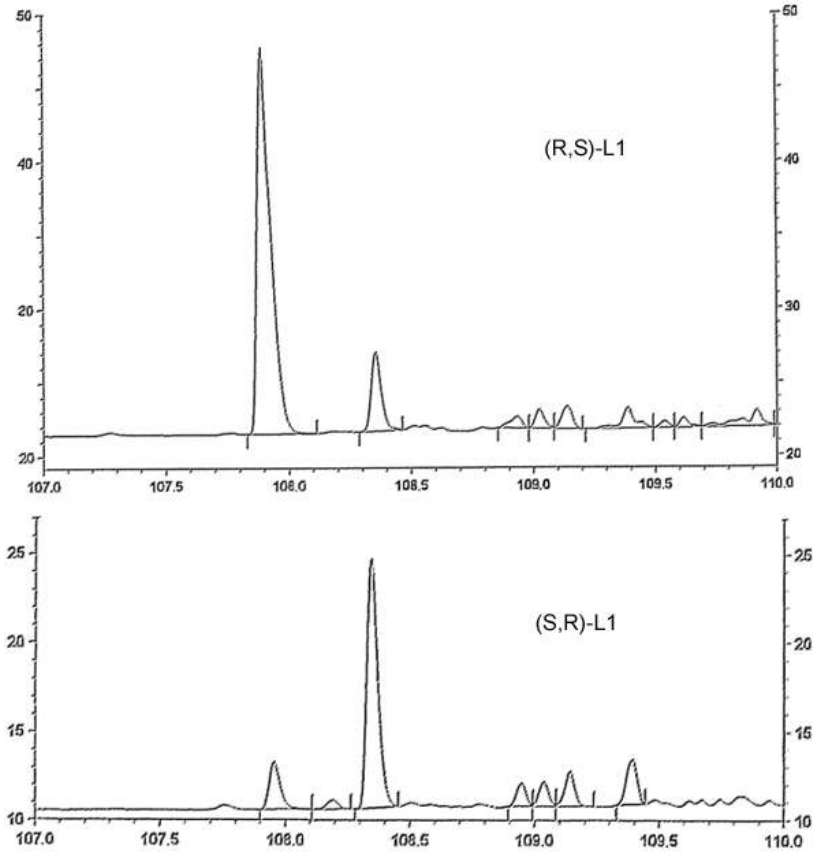

Figure 4.4 Chiral GC chromatograms of the experiment performed at 30 ºC, P CO = 2.5 bar and P H_2 = 17.5 bar with (R,S)-L**1** and (S,R)-L**1**.

The effect of the process conditions on the ee was quantified using statistical modelling. It was found that only the temperature and neither the hydrogen nor the CO partial pressure has a significant effect on the ee, leading to the following relation:

$$ee = 103 - 1.14 * T \qquad (4.4)$$

Clearly a low temperature has a positive effect on product ee. A parity plot for the predicted and experimental ee values using this equation is given in Figure 4.5, indicating that agreement between model and experimental data is good (adjusted R^2: 0.973).

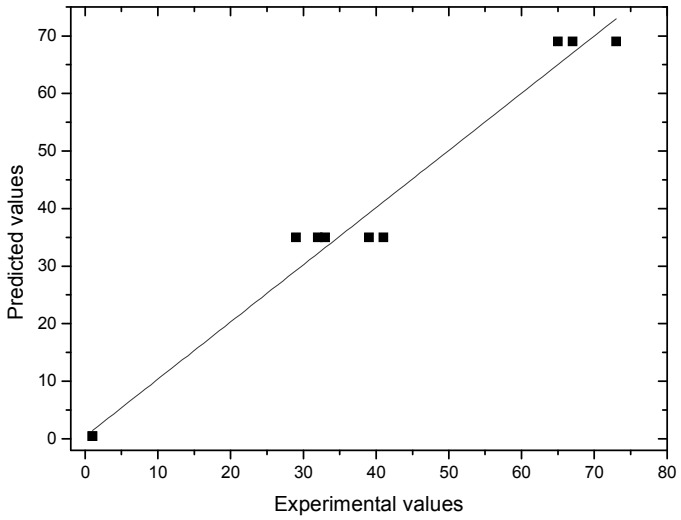

Figure 4.5 Experimental versus modeled ee values using equation (4.4).

4.3.3 Selectivity for 4-methyl-5-decanone (S_{MD}) as a function of process conditions

Statistical modeling of the data reveals that the S_{MD} is a function of both the reaction temperature and the partial CO pressure (eq. 4.5). The effect of hydrogen pressure is not significant.

$$S_{MD} = -13 + 0.81 * T - 0.90 * P_{CO} \qquad (4.5)$$

Thus, low partial CO pressures and higher reaction temperatures have a positive effect on S_{MD}. This is also illustrated in Figure 4.6, where the S_{MD} is provided as a function of the CO pressure and the reaction temperature. The highest selectivity (59 mol%) was obtained at a temperature of 90 °C and a P_{CO} of 5 bar.

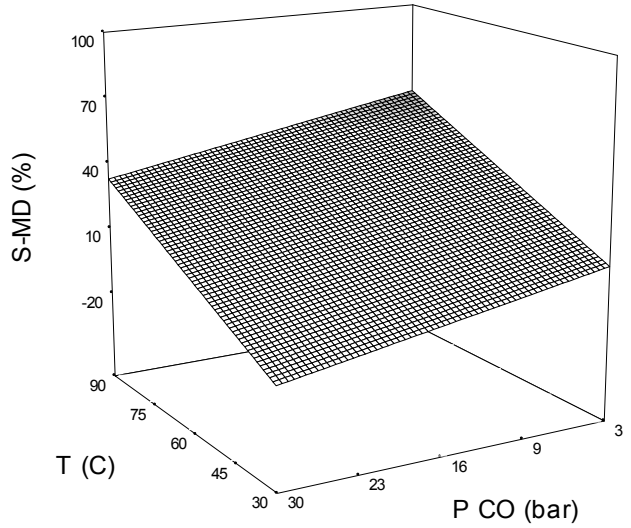

Figure 4.6 Selectivity towards 4-methyl-5-decanone (S_{MD}) versus reaction temperature and partial CO pressure (H_2 fixed at 80 bar).

Agreement between the model data and experimental data is adequate (adjusted R^2: 0.910), as is also illustrated by the parity plot given in Figure 4.7.

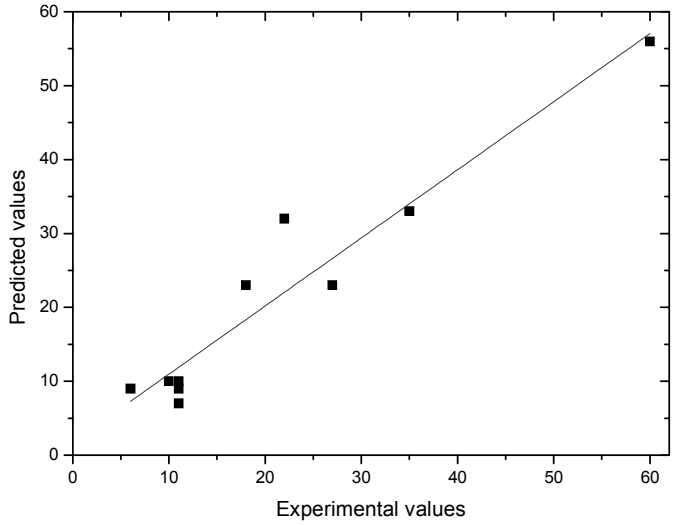

Figure 4.7 Predicted selectivity for 4-methyl-5-decanone versus the experimental values.

Evidently, it is desired to identify those process conditions that lead to 4-methyl-5-decanone with a high product selectivity and enantioselectivity. Unfortunately, these conditions appear to be conflicting. The highest ee is obtained at low temperature whereas the highest selectivity to 4-methyl-5-decanone is observed at the highest temperature in the range.

4.3.4 Chemoselectivity versus process conditions

The S_{MD} is a function of both the chemo- and regioselectivity of the hydro-acylation reaction. To gain insight in the extent to which the two factors influence the S_{MD}, the effect of process conditions on the chemo- and regioselectivity were evaluated separately.

The highest chemoselectivity with respect to saturated monoketones was obtained at 90 °C (Table 4.2, entry 2: 83 % saturated monoketones). The major by-products are enones (2-37 mol%), diketones (2-32 mol%) and olefin dimers (0-80 mol%) and trimers (0-17 mol%). Aldehydes and/or alcohols formation by hydroformylation was observed for only two experiments (maximum 2 mol%). The 1-pentene dimers and trimers (Scheme 4.4) are mono-unsaturated (GC-MS) though the position of the double bond and the extent of branching could not be established.

Scheme 4.4 Olefin dimerisation (only one of the possible isomers shown).

The effect of process conditions on the desired saturated monoketone fraction in the product mixture is best described by the following relation ($R^2 = 0.880$):

$$F_{sat.MK} = -13 + 1.08 * T - 0.65 * P_{CO} \qquad (4.6)$$

The effect of hydrogen pressure is statistically not relevant. The relation is visualised in Figure 4.8, a parity plot is provided in Figure 4.9. Higher reaction temperatures have clearly a positive effect on the amount of saturated monoketone formed. The effect of the P_{CO} is less pronounced,

though higher partial CO pressures have a small but significant negative effect on the saturated monoketone selectivity.

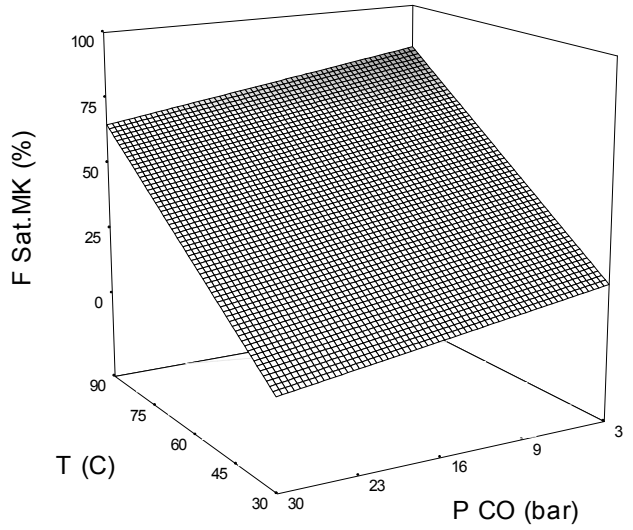

Figure 4.8 Chemoselectivity towards saturated monoketones versus reaction temperature and P_{CO} (P_{H2} = 80 bar).

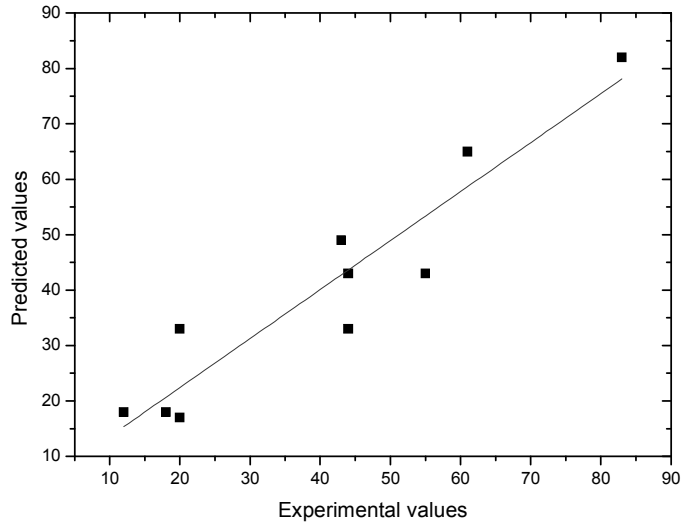

Figure 4.9 Experimental versus predicted values for the chemoselectivity of the saturated monoketone fraction.

For some of the reactions, olefin dimers and trimers were actually the main products (Table 4.2). The amount of olefin dimers in the mixture was modeled as a function of process conditions and is best described by the following relation:

$$F_{Dim} = 85 - 0.96 * T - 0.52 * P_{CO} \qquad (4.7)$$

The relation is visualised in Figure 4.10. Clearly, the temperature has a pronounced effect on the amount of dimerisation products, with lower temperatures leading to high amounts of dimers. The amount of dimers is also a function of the partial CO pressure, with high pressures leading to a reduction in the amount of dimerisation products.

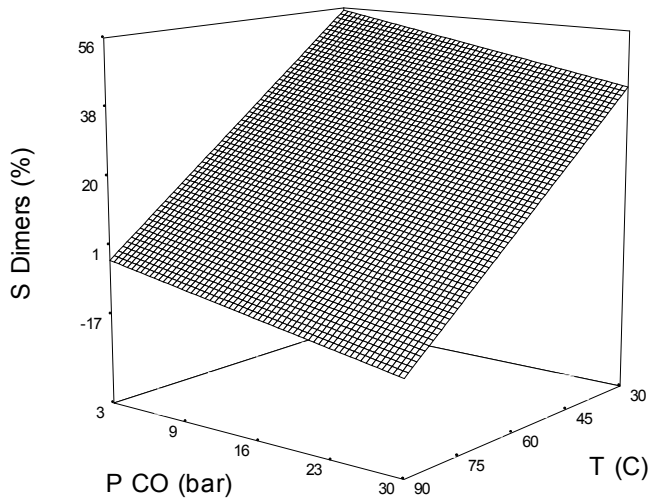

Figure 4.10 Modeled amount of dimerisation products as a function of process conditions.

4.3.5 Regioselectivity

The major regio-isomers present in the saturated monoketone fraction were the head-to-tail and the tail-to-tail isomers, whereas the head-to-head regio-isomers could not be detected (GC). It turned out to be impossible to determine statistically sound relations between the process conditions and the amount of the desired head-to-tail regio-isomers in the reaction mixture.

However, in the majority of the experiments, the desired head-to-tail isomer is formed in the largest amounts.

4.3.6 Olefin conversion

The highest 1-pentene conversion after 5 h was 90%, obtained at 60 °C, a partial CO pressure of 30 bar and a partial H_2 pressure of 120 bar (Table 4.2). This corresponds to an average turn-over frequency (TOF) of 160 mol/(mol Pd.h). The TOF at the initial stage of the reaction is expected to be considerably higher as the TOF reported here is an average over the batch time. Typical literature values for achiral hydro-acylations using alkyldiphosphines in batch reactors at 115 °C are about 1000 mol/(mol Pd.h) for 1-propene and about 100 mol/(mol Pd.h) for higher olefins like 1-octene.[6,7] Thus, particularly considering the relatively low temperature, the TOF for the Josiphos-based catalyst is at the high end of the range given in the literature.

A sound statistical relation for the effects of process conditions on the 1-pentene conversion could not be obtained. One of the possible reasons is the simultaneous occurrence of 1-pentene isomerisation to mixtures of internal olefins (GC analyses of the reaction mixture). It is well known that the activity of L_2PdX_2 catalysts for internal olefins is much lower than for α-olefins.[6,7] The extent of olefin isomerisation will also be affected by process conditions, though to a different extent than hydro-acylation, leading to a complex relation between olefin conversion and process conditions. Furthermore, isomerisation is a reversible process and the internal olefins may isomerise back to 1-pentene and converted to hydro-acylation products.

4.4 Discussion

The hydrocarbonylation of olefins using $(L_2)PdX_2$ catalysts leads to the formation of the desired monoketones (hydro-acylation) as well as to alcohols and aldehydes by hydroformylation and higher ketones by copolymerization reactions.[6,7] A proposed catalytic cycle including the formation of the various product classes is given in Scheme 4.5. The active species is commonly accepted to be a square-planar cationic Pd-hydride complex. [6, 7]

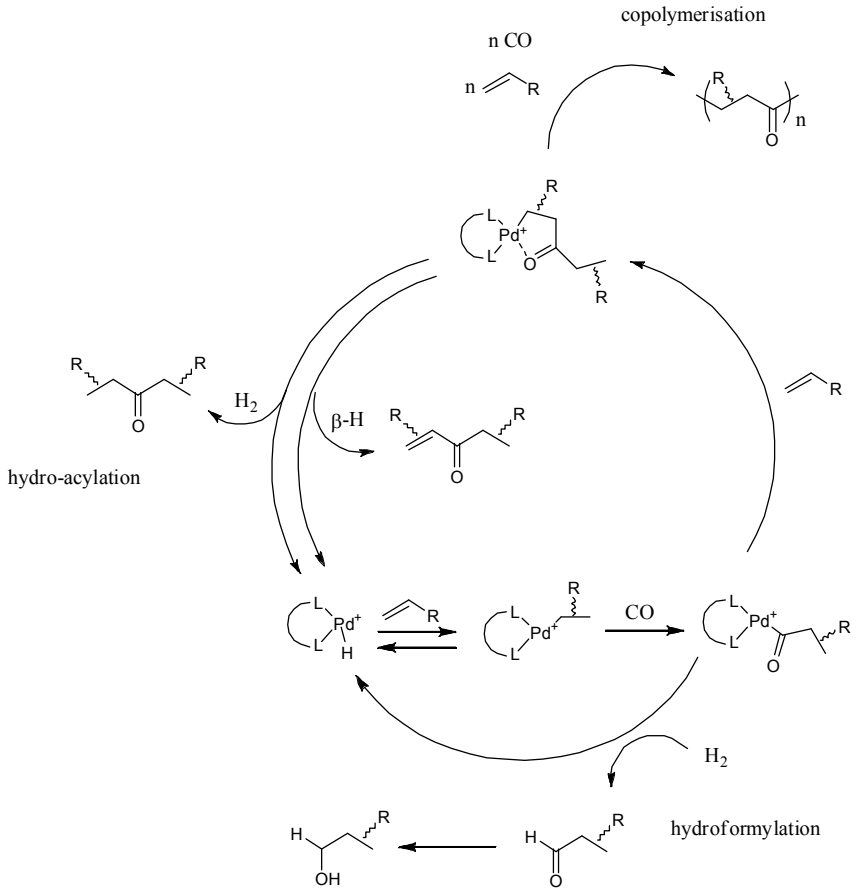

Scheme 4.5 Proposed catalytic cycle for the Pd(II) catalysed reactions of 1-alkenes and syngas.

4.4.1 Chemoselectivity

The major product classes formed using Josiphos ligand L**1** in dichloromethane are saturated monoketones, enones, diketones and non-carbonylation products like olefin dimers and trimers (Table 4.2). Aldehydes/alcohols were not formed in significant amounts under these conditions (< 2 mol%). This suggests that the key intermediate in the catalytic cycle is the Pd-alkyl species with a chelating carbonyl group (top compound in catalytic cycle, Scheme 4.5). This compound may either react with hydrogen to form the desired saturated monoketones, undergo β-hydrogen elimination to produce enones or react with CO and subsequently an olefin to give a diketone. Apparently, all three pathways occur when using L**1**.

The selectivity towards the desired saturated monoketones is shown to be a function of the temperature and to a lesser extent the CO pressure (Equation 4.6), whereas the effect of the hydrogen pressure was statistically not relevant. Higher temperatures and lower CO pressures were shown to favour the formation of saturated monoketones. Higher CO pressures are expected to speed up the rate of CO insertion in the Pd-alkyl bond. This reaction is known to be reversible and only a subsequent olefin insertion will produce a stable Pd-alkyl compound. The latter is subsequently hydrogenated to form a ketone. The observation that the hydrogen pressure does not affect the chemoselectivity is rather surprising. On the basis of Scheme 4.5, it is anticipated that higher hydrogen pressures would lead to higher amounts of the saturated monoketones at the expense of enone formation. However, this is not the case. This is an indication that hydrogen is not directly involved in the formation of saturated monoketones from the Pd-chelate. A possible alternative termination mechanism without direct hydrogen involvement is the reaction of the Pd-chelate with HOTf, present in excess in the reaction mixture, to give a $L_2Pd(OTf)_2$ species and the saturated monoketone (protonolysis). Subsequent reaction of the $L_2Pd(OTf)_2$ with hydrogen then leads to the regeneration of the Pd-H and HOTf (Scheme 4.6).[18] Termination reactions by protonolysis are well known in CO-olefin copolymerisations. For instance, Vavasori and co-workers reported the active involvement of acetic acid in the termination reaction in the ethylene/CO copolymerisations catalysed by $PdCl_2$(dppf) complexes.[17]

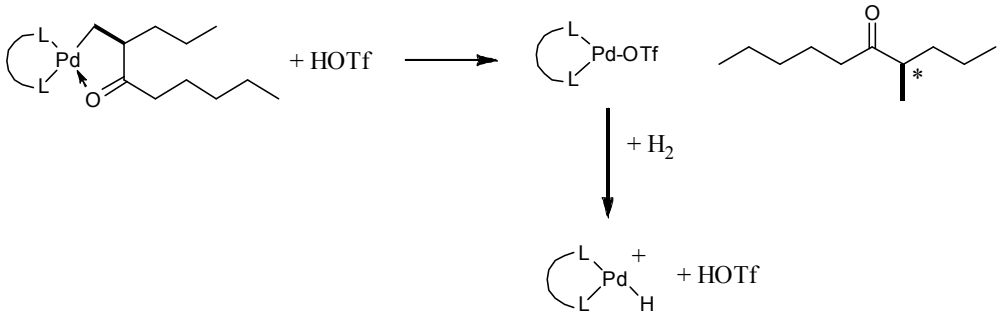

Scheme 4.6 Alternative termination mechanism: Pd-alkyl protonolysis with HOTf.

Remarkable is the formation of 1-pentene oligomers under hydro-acylation conditions. The formation of olefin dimerisation products in the absence of CO with the L_2PdX_2 catalyst used in this study is well known in the literature. Early examples of the dimerisation of linear α-olefins

were reported by Drent (1990)[19] and Jiang *et al* (1993).[20] In 2003, Tsuchimoto *et al*[21] demonstrated that palladium–indium triflate catalysts were highly active for the dimerisation of vinylarenes. More recently, Bedord *et al*[22] developed an (asymmetric) version by using $Pd(OAc)_2$, and a chiral diphosphine ligand in the presence of $In(OTf)_3$ (Scheme 4.7). Josiphos ligands were also shown to be active for the reaction.

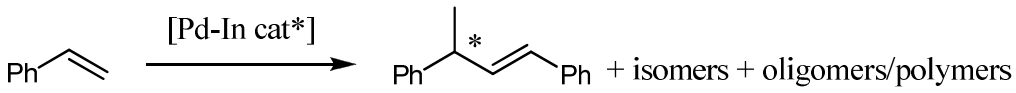

Scheme 4.7. Styrene oligomerisation catalysed by $Pd(AcO)_2$/diphosphine ligand/$In(OTf)_3$ catalyst systems.

A possible explanation for olefin oligomerisation is the (strong) acid catalysed (here HOTf) oligomerisation of 1-pentene. If this would be valid, however, olefin oligomerisation is expected to occur for all reactions and this is certainly not the case (Table 4.2). An alternative explanation is the involvement of cationic Pd catalysts, even though CO is present. In this case, olefin insertion has to compete with CO insertion in a Pd-alkyl bond (Scheme 4.5). When this explanation is valid, higher amounts of olefin dimers are expected at low CO pressures. This was indeed observed experimentally and supported by statistical modelling (Figure 4.10). Thus, on the basis of these findings, a mechanism involving Pd-compounds for 1-pentene oligomerisation is likely.

4.4.2 Regioselectivity

The major regio-isomers present in the saturated monoketone fraction were the head-to-tail and the tail-to-tail isomers, whereas the head-to-head regio-isomers could not be detected (GC). It turned out to be not possible to determine statistically sound relations between the process conditions and the amount of the desired head-to-tail regio-isomers in the reaction mixture. However, in the majority of the experiments, the desired head-to-tail isomer is formed in the largest amounts.

4.4.3 Enantioselectivity

The enantioselectivity was shown to be a strong function of the temperature (Equation. 4.4) whereas the P_{CO} and P_{H2} have no significant effect on the product ee within the experimental ranges. This gives valuable information on the origin of enantioselectivity of the hydro-acylation reaction. The enantioselectivity of the reaction is most likely determined by the second insertion of the olefin in the Pd-alkyl bond of the chelate (Scheme 4.5).[23] To obtain enantiopure 4-methyl-5-decanone, the insertion step should be highly stereoselective. Lower ee values may be explained by either an intrinsically limited chiral induction of the Josiphos ligand or by partial epimerisation of the stereogenic centre after the second olefin insertion step (Scheme 4.8).

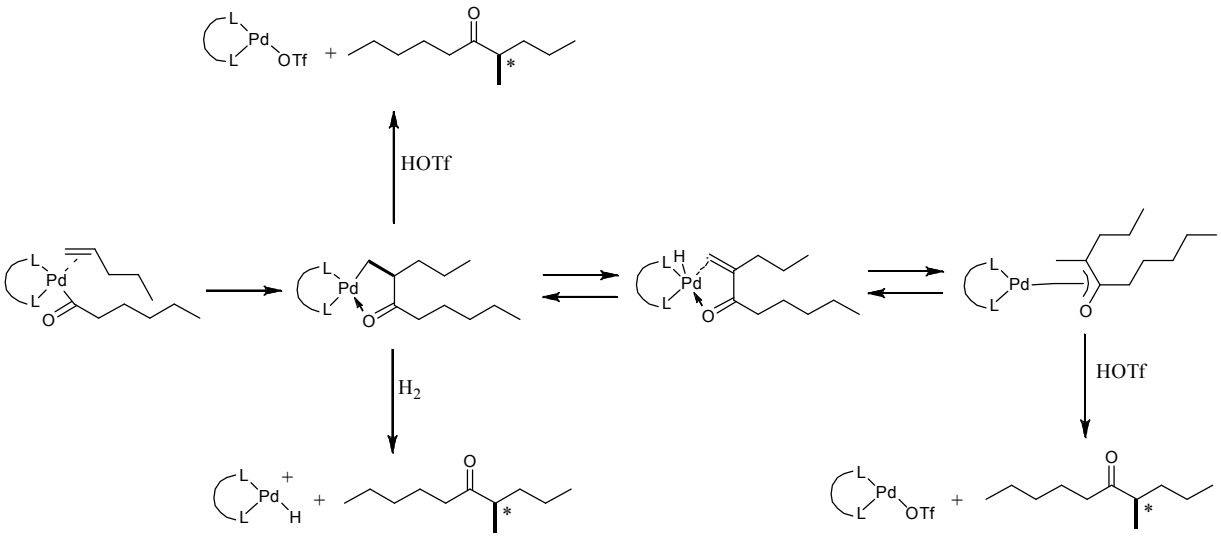

Scheme 4.8 Epimerisation of the stereogenic centre leading to ee reductions.

In the case the ee is only affected by the intrinsic properties of the Josiphos ligand, the partial pressures of CO and hydrogen are not expected to affect the product ee, as was observed experimentally. However, this does not exclude the occurrence of epimerisation. Epimerisation can occur by (reversible) β-hydrogen elimination followed by conjugate hydride addition and formation of the palladium enolate.[24] In this case, the product ee is not only determined by the intrinsic chiral induction during the olefin insertion step but is also a function of the rate of β-hydrogen elimination/enolisation versus the rate of the termination reaction of the Pd-chelate with either HOTf or hydrogen (Scheme 4.8). The termination reaction with hydrogen is less

likely as the amount of saturated monoketones in the mixture was found to be independent of the hydrogen pressure (*vide supra*). Thus, the rate of termination by protonation versus the rate of β-hydrogen elimination likely affects the rate of epimerisation. When this mechanism is valid, the product ee is expected to be independent of the hydrogen pressure and this was indeed the case. Further research including molecular modeling is required to gain further insight into the occurrence of epimerisation and its role in the enantioselectivity of the reaction.

4.5 Conclusions

The effect of process conditions (temperature, partial CO and hydrogen pressure) on the synthesis of enantio-enriched 4-methyl-5-decanone by the Pd-Josiphos L**1** catalysed reaction of 1-pentene with syngas was established. The selectivity of the reaction (S_{MD}) was shown to be a function of the temperature and the highest amounts of 4-methyl-5-decanone were found at the highest temperature in the range (90 °C). The product ee is also strongly temperature depending, with lower temperatures leading to higher ee values. The highest ee of 73% was found at 30 °C. As the requirements for high chemoselectivity and enantioselectivity are clearly conflicting, a high yielding synthesis of enantiopure 4-methyl-5-decanone remains elusive. The effects of process conditions were quantified using statistical modelling. The results provide interesting mechanistic insights in the effects of process conditions on the chemo-, regio- and enantioselectivity of (asymmetric) hydro-acylation reactions.

4.6 References

1 W. A. Loughlin, *Bioresource Technology*, 2000, **74**, 49-62.

2 K. Mori and S. Harashima, *Tetrahedron Letters*, 1991, **32**, 5995-5998.

3 G. J. A. Conceicao, P. J. S. Moran, and J. A. R. Rodrigues, *Arkivoc*, 2003, 500-506.

4 F Gini, *PhD thesis University of Groningen*, 2007.

5 E. P. Siqueira, J. A. R. Rodrigues, and P. J. S. Moran, *Tetrahedron-Asymmetry*, 2001, **12**, 847-852.

6 E. Drent and P. H. M. Budzelaar, *J. Organomet. Chem.*, 2000, **594**, 211-225.

7 E. Drent, W. P. Mul, and P. H. M. Budzelaar, *Comments Inorg. Chem.*, 2002, **23**, 127-147.

8 D. D. Perrin, and W. L. F. Armarego, *Purification of laboratory chemicals*, Pergamon Press, Oxford, 3rd ed, 1988.

9 P. W. N. M. van Leeuwen, *Appl. Catal. ,A*, 2001, **212**, 61-81.

10 O. H. Oldenziel, D. van Leusen, and A. M. van Leusen, *J. Org. Chem.*, 1977, **42**, 3114-3118.

11 P. Wipf, Y. Kim, and P. C. Fritch, *J. Org. Chem.*, 1993, **58**, 7195-7203.

12 E. J. Corey and D. Enders, *Tetrahedron Lett.*, 1976, **17**, 3-6.

13 W. G. M. Braam, *Chromatografie*, Educatieve Partners Nederland BV, Culemborg, The Netherlands, 5, 1994.

14 V. Svojanovský, M. Krejí, K. Tesaík, and J. Janák, *Chromatogr. Rev.*, 1966, **8**, 90-171.

15 A. D. Jorgensen, K. C. Picel, and V. C. Stamoudis, *Anal. Chem.*, 1990, **62**, 683-689.

16 A. F. M. Barton, *Chemical Reviews*, 1975, **75**, 731-753.

17 A. Vavasori, A Bellieni, L. Ronchin, F. Dall'Acqua, L. Toniolo, and G. Cavinato, *J. Mol. Catal. A:Chem.*, 2007, **263**, 9-14.

18 R. A. M. Robertson and D. J. Cole-Hamilton, *Coord. Chem. Rev.*, 2002, **225**, 67-90.

19 E. Drent, *Pure Appl. Chem.*, 1990, **62**, 661-669.

20 Z. Jiang and A. Sen, *Organometallics*, 1993, **12**, 1406-1415.

21 T. Tsuchimoto, S. Kamiyama, R. Negoro, E. Shirakawa, and Y. Kawakami, *Chem. Commun.*, 2003, 852-853.

22 R. B. Bedford, M. Betham, M. E. Blake, A. Garce's, S. L. Millara, and S. Prashar, *Tetrahedron*, 2005, **61**, 9799-9807.

23 H. Heeres, A. J. Minnaard, B. Hessen, and H. J. Heeres, *To be published*, 2009.

24 M. A. Zuideveld, P. C. J. Kamer, P. W. N. M. van Leeuwen, P. A. A. Klusener, H. A. Stil, and C. F. Roobeek, *J. Am. Chem. Soc.*, 1998, **120**, 7977-7978.

Chapter 5. Kinetic studies on asymmetric hydrogenations of methyl-2-acetamido acrylate using a homogenous Monophos™ based Rhodium catalyst

5.1 Introduction

Asymmetric catalysis is a powerful methodology for the preparation of enantiopure organic molecules for the fine chemical and pharmaceutical industry.[1-3] The demand for drugs based on peptides is expected to grow dramatically in the coming years, and consequently, an increasing demand for unnatural enantiopure amino-acids is expected. Such amino-acids may be obtained by the asymmetric hydrogenation of an amino-acid precursor.[4,5] The catalysts applied mainly comprise of the metals rhodium, ruthenium or iridium combined with diphosphine ligands.[6-8] A landmark example is the use of a rhodium catalysts containing the chiral diphosphine DIPAMP ligand (**1,** Figure 5.1) for the synthesis of the anti-Parkinson drug L-DOPA.[7,9] The last decade, new types of chiral monodentate phosphorus ligands, such as the phosphoramidite ligands **2** were introduced in asymmetric hydrogenation reactions.[10-13] The monodentate ligands performed as good, or even better than bidentate ligands in e.g. the hydrogenation of dehydroamino acids and itaconic acid.[7,13,14] For instance, the hydrogenation methyl 2-acetamido cinnamate with Rh-complexes containing the monodentate ligand **3** in dichloromethane at 20 °C led to full conversion after 40 minutes and a product ee (enantiomeric excess) of 95%.[13,14] Under similar conditions, the related bidentate ligand **4** gave a product ee of only 72% at a much lower reaction rate (22% conversion after 20 h).[13,14]

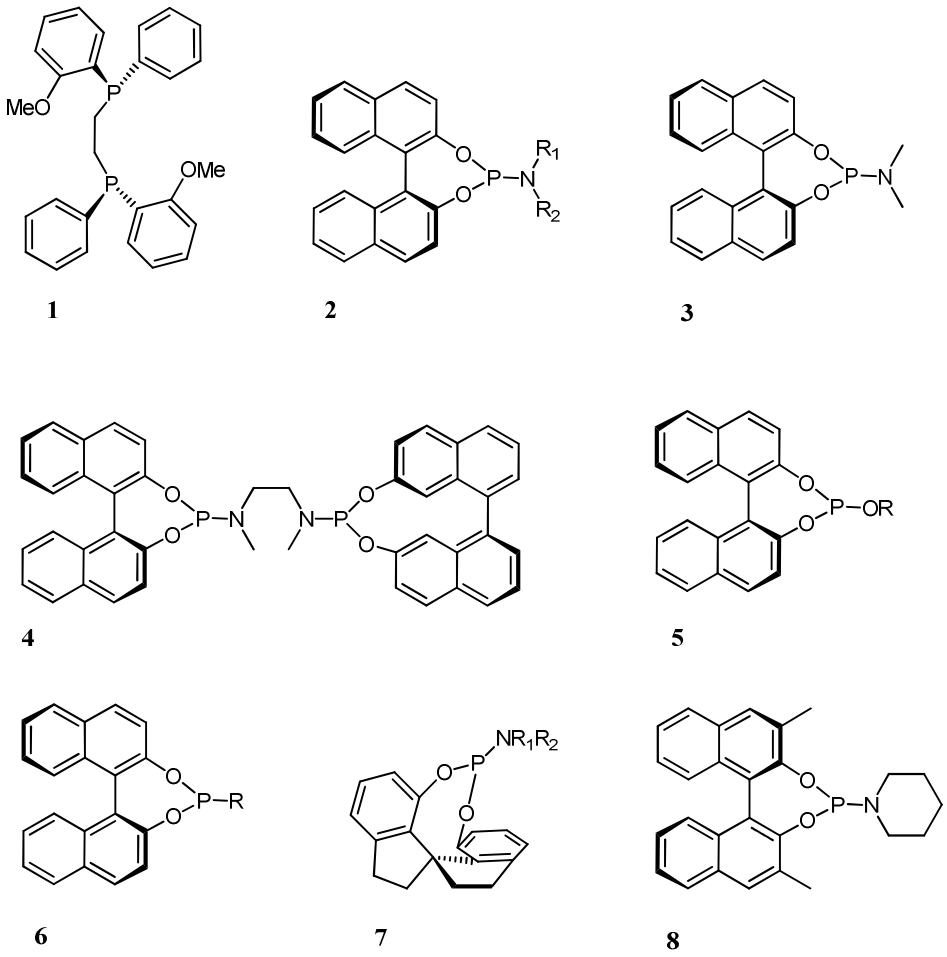

Figure 5.1 Examples of some chiral monodentate and bidentate phosphine ligands.

Other important contributions in this field were reported by e.g. Reetz *et al* using monodentate phosphites **5**, by Pringle *et al* using monodentate phosphonites **6** and by Zhou *et al* using monodentate spiro-phosphoramidites **7**.[15-18]

Monodentate phosphorus ligands and particularly the phosphoramidites are in general easier to synthesize and modify than bidentate phosphorus ligands, allowing the preparation of ligand-libraries for high-throughput, combinatorial chemistry.[6,8,13,19,20]

The use of Rh-monophoshoramidites catalysts has been commercialised recently by DSM for the asymmetric hydrogenation of the substituted acyclic acid **9** (Scheme 5.1). When using the a mixture of the phosphoramidite ligand **8** with PPh_3 at 55 ºC and 80 bar, the product **10** ee was 90% at a TOF of 500 h^{-1} (TON > 5000).[21, 22]

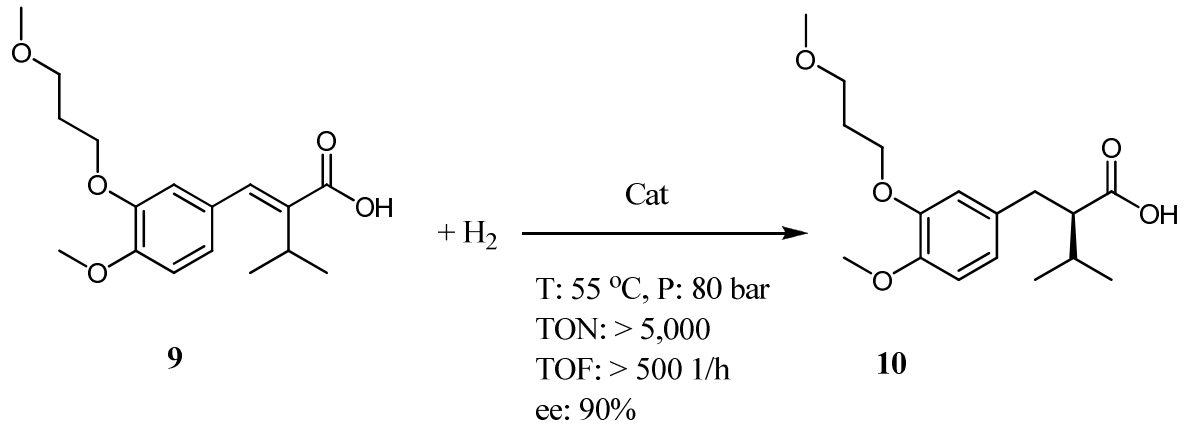

Scheme 5.1 Asymmetric hydrogenation of the substituted acyclic acid **9**, by a rhodium-**8**-PPh_3 catalyst, in the DSM process.

In this contribution, a kinetic study on the asymmetric hydrogenation of the amino-acid precursors methyl 2-acetamido acrylate **11** to (R)-2-acetylamino-propionic acid methyl ester **12** using a homogeneous transition metal complex based on rhodium and the phosphoramidite ligand **3** in IPA will be discussed (Scheme 5.2).

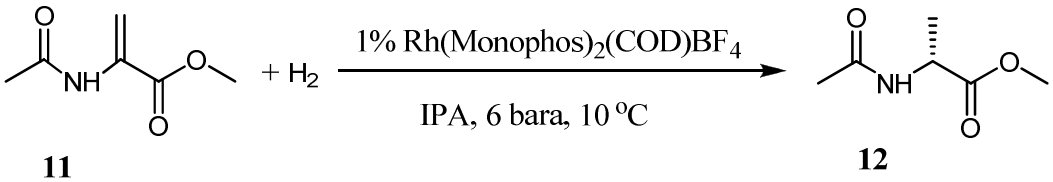

Scheme 5.2 Hydrogenation of methyl 2-acetamido acrylate using a rhodium/Monophos complex.

Exploratory research by van den Berg *et al*[13] showed that this catalyst was very active for the hydrogenation reaction while maintaining high product ee values. Kinetic and mechanistic studies on the hydrogenation of unsaturated substrates with transition metal catalysts containing bidentate phosphorous ligands have been reported in the literature[23-26] However, to our knowledge, kinetic studies on asymmetric hydrogenations using phosphoramidite ligands have

not been reported to date. In this contribution the effects of various process conditions (e.g. hydrogen pressure and catalyst-substrate ratios) on catalyst activity are quantified in an overall kinetic model for the reaction. The model may be applied for reactor engineering (scale-up) purposes but also prove valuable input for mechanistic studies.[27, 28]

5.2 Experimental

5.2.1 Chemicals

Methyl-2-acetamido acrylate (98%) was purchased from Sigma Aldrich and was further purified by sublimation (35 ºC, 0.2 mmHg). Bis(1,5-cyclooctadiene)rhodium(I) tetrafluoroborate was purchased from Acros. (S)-Monophos (97%) was purchased from STREM Chemicals. IPA (99.7%) was purchased from LAB SCAN and purified by distillation on CaH_2 under nitrogen before use. Nitrogen (purity ≥ 99.999 vol%) and hydrogen (purity ≥ 99.9999 vol%) were purchased from Hoek Loos.

5.2.2 Synthesis of $Rh(Monophos)_2(COD)BF_4$

Using standard Schlenk techniques, $[Rh(COD)_2]BF_4$ (377.0 mg, 0.928 mmol) and (*S*)-MonoPhos (667.3 mg, 1.857 mmol) were dissolved in dichloromethane (15-20 ml) and stirred for 1 h at ambient temperature. The mixture was reduced in volume under vacuum (600 mbar) to about 5 ml. To this concentrate, pentane (20 ml) was added and stirring was continued for 1 h to induce crystallisation. A fine yellow precipitate was formed. This precipitate was filtered under nitrogen and dried under vacuum (200 mbar). A yellow powder was obtained in 92% yield (871.2 mg, 0.857 mmol). This material was stored in a glove-box and used for all hydrogenation experiments without further purification. ^{1}H-NMR ($CDCl_3$) δ 2.11-2.53 (m), 2.76-2.88 (m), 5.04-5.23(s), 7.73-8.12 (m); ^{31}P-NMR ($CDCl_3$) δ 138-141 (br, s).

5.2.3 Experimental set-up for hydrogenation experiments

The kinetic experiments were performed in a batch autoclave (Figure 5.2). The reactor was equipped with a cooling mantle connected to a cooling bath to maintain isothermal conditions (10

°C). The reactor was stirred with an overhead stirrer, equipped with a gas inducing impeller. A glass insert was placed in the reactor to minimize contact of the liquid with the reactor wall. The catalyst solution was introduced into the reactor from a catalyst feed vessel using a slight overpressure in the vessel and reduced pressure in the reactor (200 mbar).

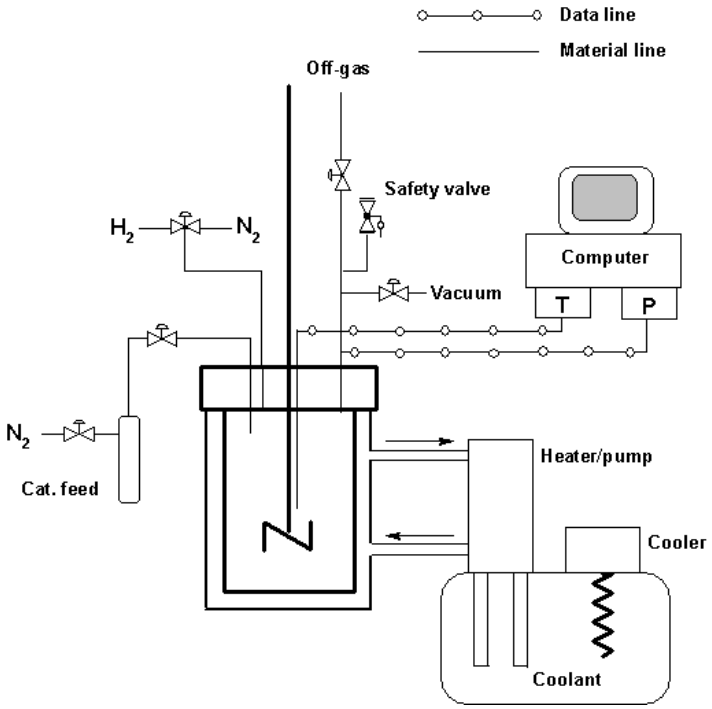

Figure 5.2 Schematic representation of the reactor setup.

Hydrogen was introduced at the start of the reaction by opening the valve in the hydrogen line. After introduction, the valve was closed and the pressure in the reactor decreased in time by hydrogen uptake. The initial hydrogen pressure was varied between 6-10 bara. Accurate on-line measurement and registration (0.9 s intervals) of the hydrogen pressure in the autoclave as a function of time allowed calculation of the reaction rates.

5.2.4 Determination of the volumetric G-L mass transfer coefficient ($k_L.a$)

The G-L volumetric mass transfer coefficient $k_L.a$ (1/s) of hydrogen was determined by performing a physical absorption experiment. The reactor was loaded with 75 ml of IPA and

cooled to 10 ºC, under stirring. After reaching the desired temperature, the stirrer was stopped and hydrogen was fed to the reactor till a pressure of 5.4 bara. Subsequently, the stirrer was started (1400 rpm) and the hydrogen pressure was measured in time. The volumetric mass transfer coefficient may then be obtained from the pressure vs. time curve using Equation 5.1.

$$k_l.a \cdot t = \left(\frac{\alpha}{\alpha + 1} \right) \ln \left(\frac{P^0{}_{H_2}}{(\alpha + 1) \cdot P_{H_2} - \alpha \cdot P^0{}_{H_2}} \right) \qquad (5.1)$$

In which

$$\alpha = \frac{V_g \cdot He}{V_l \cdot R \cdot T} \qquad (5.2)$$

Here, P^0H_2 (Pa) is the hydrogen pressure at t = 0 and PH_2 the pressure at a certain time t. V_g (m^3) is the gas hold-up in the reactor, V_l (m^3) the liquid hold-up. *He* is the Henry constant ($Pa.m^3.mol^{-1}$), *R* is the gas constant (8.314 $J.mol^{-1}.K^{-1}$) and *T* the reactor temperature (K).[29]

5.2.5 General procedure for a hydrogenation experiment

Methyl 2-acetamido acrylate together with IPA (2 ml) were placed in the autoclave and cooled to 10 ºC. The reactor was closed and purged several times with nitrogen gas. Subsequently the catalyst precursor [Rh((*S*)-MonoPhos)$_2$(COD)]BF_4, dissolved in 3 ml IPA (under N_2) was introduced via the catalyst feed by reducing the pressure in the autoclave to 200 mbar. Next, the solvent (70 ml IPA) was introduced in the reactor via the catalyst feed vessel. While stirring, the autoclave was again extensively purged with nitrogen for a period of five minutes. The system was evacuated to 200 mbar and the stirrer was switched off. Subsequently, the system was pressurized with hydrogen and the hydrogen inlet valve was closed. Data collection was started and the stirrer was switched on at 1400 rpm. After the pre-determined reaction time, the pressure in the autoclave was reduced to atmospheric pressure. A sample was taken from the liquid phase, filtered over silica gel to remove catalyst residues and analysed by GC.

5.2.6 Determination of substrate concentration

During the reaction, the hydrogen pressure in the autoclave was measured continuously. In combination with the known gas phase volume and temperature the uptake of hydrogen as a function of time may be determined using the ideal gas-law. This information combined with the initial substrate intake and the known reaction stoichiometry (hydrogen and the substrate react in a 1:1 ratio) allows calculation of the concentration of the substrate as a function of time.

5.2.7 Analysis

^{1}H NMR and ^{31}P{^{1}H} NMR spectra were recorded on a Varian VXR-200 spectrometer at 200 MHz and 81 MHz respectively. ee determinations of the products were performed by means of a GC (HP 6890) FID equipped, with a CP Chirasil-L-Val column (25 m × 250 μm × 0.25 μm). A N_2-flow of 1.3 ml/min was applied and the oven temperature was set at 110°C. To ensure accurate determination of the ee, a racemic mixture of the product was prepared and injected in the GC. The racemate was obtained by hydrogenation of the substrate using Pd/C (10%).[20]

5.2.8 Kinetic modeling

Parameter estimation was performed using the Matlab software package. Here the Lsqnonlin method for solving non-linear least squares problems was used to minimize the error between measured and modelled values. Output of the kinetic model are the kinetic parameters with their confidence boundary limits (95%), the Akaike's Information Criterion (AIC) and the mean relative error (MRE).

The AIC correlates the degree of correlation between data and modelled points with the number of fitting parameters (Equation 5.3).

$$AIC = \log(V) + 2d / n \qquad (5.3)$$

Here, V is the loss function, d is the number of estimated parameters, and n is the number of estimation data values. Evaluation of the AIC number is a useful tool to discriminate between the various models. As a rule, the best model has the lowest AIC-number.[30]

The MRE number calculates the mean relative error between the modelled and the experimental data (Equation 5.4).

$$MRE = \frac{1}{n} * \sum_{i=1}^{n} \frac{Ym_i - Ye_i}{Ye_i} \cdot 100 \qquad (5.4)$$

Here, Y_m represents the modelled date and Y_e the experimental data. Several runs with different initial parameter values were performed to determine the absolute and not a local minimum of the optimisation function.

5.3 Results and discussion

5.3.1 Catalyst precursor synthesis

A pre-formed catalyst precursor, $[Rh(Monophos)_2(COD)]BF_4$ **14** was applied for all experiments. The catalyst precursor was synthesised by reacting $[Rh(COD)_2]BF_4$ **13** with Monophos **3** in a 1 to 2 molar ratio in dichloromethane at room temperature (Scheme 5.3). The catalyst precursor was isolated as a yellow powder in 92% yield by precipitation using pentane.

Scheme 5.3 Synthesis of the $Rh(Monophos)_2(COD)]BF_4$ precursor.

Compound **14** was characterised by NMR. In ^{31}P-NMR, a broad peak was observed at 138-141 ppm, indicative for the occurrence of dynamic processes. Van den Berg studied the dynamics by variable temperature NMR.[20] When reacting **13** with 2.1 equivalents of **3** in CD_2Cl_2, three complexes were identified in solution; a complex with only one Monophos bound to Rh and two complexes with two Monophos ligands bound to Rh (unsymmetrical and symmetrical complexes).

5.3.2 Kinetic experiments

The hydrogenation reactions of **11** with catalyst precursor **14** were performed in a batch set-up using IPA as the solvent. For all experiments a reaction temperature of 10 ºC was applied. Initial hydrogen pressures were varied between 6-10 bara and substrate/catalyst ratios between 85 and 610 were used. A total of 12 experiments were performed. An overview of the reaction conditions and experimental results are given in Table 5.1. For all experiments, except 3 (entries 10-12), substrate conversion was quantitative within 1400 s. Typical substrate versus time profiles for a number of selected experiments are given in Figure 5.3.

Table 5.1 Overview of experiments[a].

Entry	P (bara)	[Cat] (mmol/l)	[S] (mmol/l)	S/C	ee (%)
1	8	0.2	77	385	98.2
2	6	0.2	74	370	97.6
3	10	0.2	60	300	98.7
4	8	0.2	60	300	98.6
5	6	0.4	60	150	98.4
6	8	0.2	32	160	97.8
7	6	0.2	31	155	97.8
8	8	0.2	19	95	97.8
9	6	0.2	17	85	98.2
10	10	0.1	60	600	96.3
11	8	0.1	60	600	95.2
12	6	0.1	61	610	94.9

a. Reactions were performed in 75 ml of IPA at 10 ºC.

To ensure measurement of the intrinsic reaction kinetics without possible mass transfer effects of hydrogen from the gas to liquid phase, the volumetric G-L mass transfer coefficient ($k_L.a$) of the system was determined. At the selected stirring speed of 1400 rpm, the value of $k_L.a$ was 0.361 s^{-1}. This implies that the characteristic time for mass transfer of hydrogen form the gas to liquid phase ($1/k_L.a$) is in the order of a few seconds. For the fastest reaction, the characteristic

time for reaction (defined as the time required for 66% conversion) is about 200 s (*vide infra*). On the basis of this estimation, it can be concluded that the characteristic time for reaction is two orders of magnitude lower than the characteristic time for mass transfer, implying that true, intrinsic kinetics were determined in this study.

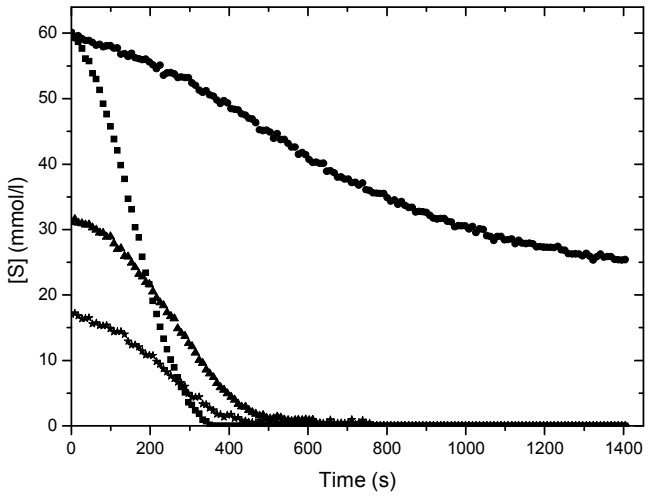

Figure 5.3 Experimental substrate concentration profiles for entry 3 (■), 7 (▲) 9 (★) and 11 (●).

5.3.3 Effect of process conditions on catalyst activity and product ee

Careful inspection of the slope of the rate profiles between 0-100 s (Figure 5.3) and between 100 and 300 s indicates that the slope increases when the reaction progresses. Apparently, catalyst activity is higher between 100-300 s than at the start of the hydrogenation reaction. This induction period indicates that the conversion of the catalyst precursor **14** to the actual catalytic species **16** (S = solvent molecule, here IPA) (see Scheme 5.4) is relatively slow compared to the time scale of the catalytic hydrogenation.

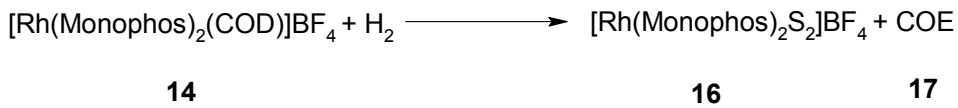

Scheme 5.4 Conversion of catalyst precursor to active catalyst.

The conversion of **14** to **16** has been studied separately and is assumed to involve hydrogenation of one of the C-C double bonds in COD **15** to cyclo-octene **17**.[20] The experimental profiles also indicate that catalyst deactivation during a run occurs to a significant extent and needs to be included in the kinetic model. This is particularly evident from the runs performed at low catalyst concentrations (e.g. run 11 in Figure 5.3). The reaction rate levels off considerably after 800 s and 100% substrate conversion was not observed after 1400 s reaction time. Catalyst degradation during the reaction may be caused by reactions with impurities leading to for instance ligand decomposition and the formation of inactive catalyst and reduced metal clusters.[8,31] Some of these degraded catalyst species may be active as non-stereoselective catalysts for the hydrogenation of the substrate.[32-34] The occurrence of catalyst deactivation, particularly for those experiments at low catalyst concentrations, was confirmed by the ee data (Table 5.1). The ee for all experiments ranged between 94.9 and 98.7%. The lowest ee values were indeed found for the experiments suffering from catalyst deactivation, i.e. those carried out with a high S/C ratio at low catalyst loadings (0.1 mmol).

5.3.4 Model generation

The experimental data described in this paper were modelled using mechanistic models available for the hydrogenation of C-C double bonds using transition metal complexes. Among these, the mechanism proposed by Halpern and the dihydride mechanism by Imamoto are widely applied.[22-26] The Halpern mechanism was developed to describe the asymmetric hydrogenation of methyl-(Z)-α-acetamidocinnamate (MAC) catalyzed by a (1,2-bis((phenyl-o-anisoyl)phosphino)ethane}rhodium(I) catalyst.[22,25,26] The dihydride mechanism has been used to model hydrogenations using aliphatic bidentate diphosphines.[23,24] For this reason, we have applied the Halpern mechanism for kinetic modeling.

The Halpern catalytic cycle starts with exchange of the solvent molecules (S) of the L_2RhS_2 cation **16** with the substrate and the formation of compound **18** (Scheme 5.5). The substrate can bind in two ways to the chiral rhodium catalyst, leading to two diastereomeric complexes. Substrate coordination is assumed to be reversible. The next step involves the oxidative addition of molecular hydrogen to the Rh(I) centre and the formation of a Rh(III) dihydride **19**. This step is irreversible and in most cases the rate determining step in the Halpern mechanism. Subsequently, irreversible migratory insertion occurs with the formation of a Rh-C bond **20**. Finally, reductive elimination occurs and the product is formed together with the original L_2RhS_2 cation. This reaction is also assumed to be irreversible.

The mechanism originally incorporates two catalytic cycles for both the L and D enantiomer. Because of the high enantiomeric excesses obtained in our experiments, the catalytic cycle of only one of the enantiomers was taken into consideration (Scheme 5.5).

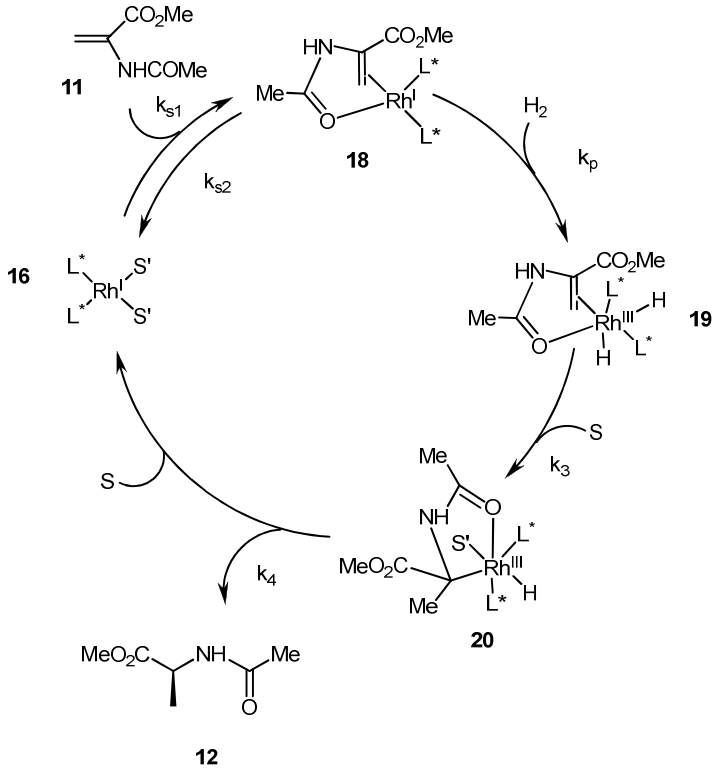

Scheme 5.5 Halpern mechanism for the hydrogenation of methyl-2-acetamido acrylate **11** with the rhodium Monophos catalyst **16**.

To derive the overall kinetic expression for the rate of product formation, only the rate determining step (oxidative addition of hydrogen) and reversible substrate binding need to be considered. Application of the pseudo steady state hypothesis for the intermediates and first order reactions in substrates results in the following rate equation for the formation of the product P (Equation 5.5).

$$R_p = \frac{k_P \cdot k_{S1} \cdot [H_2] \cdot [S] \cdot [C_{Active}]}{k_{S2} + k_P \cdot [H_2] + k_{S1} \cdot [S]} \qquad (5.5)$$

Here, [P], [S], [H_2] and [C_{active}] are the concentrations of the product, substrate, hydrogen and active catalyst concentration in the liquid phase. When performing the reaction in a batch reactor, the following equation for the formation of product P holds:

$$\frac{d[P]}{dt} = \frac{k_P \cdot k_{S1} \cdot [H_2] \cdot [S] \cdot [C_{Active}]}{k_{S2} + k_P \cdot [H_2] + k_{S1} \cdot [S]} \qquad (5.6)$$

The concentration of hydrogen in the gas phase and not that in the liquid phase is measured experimentally. The hydrogen concentration in both phases may be related using the distribution coefficient *m* (Equation 5.7). The value of *m* in IPA at 10 °C was determined experimentally and found to be 0.081, which is close to the value reported in the literature.[35]

$$m = \frac{[H_2]_L}{[H_2]_G} \qquad (5.7)$$

With the introduction of *m*, batch Equation 5.6 may be rewritten as:

$$\frac{d[P]}{dt} = \frac{k_P \cdot k_{S1} \cdot m \cdot [H_2]_g \cdot [S] \cdot [C_{Active}]}{k_{S2} + k_P \cdot m \cdot [H_2]_g + k_{S1} \cdot [S]} \qquad (5.8)$$

The concentration of the active catalyst $[Rh(Monophos)_2S_2]^+$ ([C_{active}]) is a function of time. The active catalyst is formed *in situ* by COD hydrogenation of $[Rh(Monophos)_2(COD)]^+$

(Scheme 5.4). We have assumed that the reaction of the catalyst precursor [Rh(Monophos)$_2$(COD)]$^+$ with hydrogen is first order in hydrogen and catalyst precursor (C_i). This results in Equation 5.9, where k_a is the activation constant (L.mmol^{-1}.s^{-1}).

$$\frac{d[C_i]}{dt} = k_a \cdot m \cdot [H_2]_g \cdot [C_i] \qquad (5.9)$$

As observed experimentally (*vide supra*), catalyst deactivation appears to play a role and should be included in the model. Catalyst deactivation is assumed to be first order in active catalyst (C_a), leading to Equation 5.10. Here, k_d represents the catalyst degradation constant (s^{-1}) and C_d the concentration of degraded catalyst.

$$\frac{d[C_d]}{dt} = k_d \cdot [C_a] \qquad (5.10)$$

The rhodium mass balance (Equation 5.11) holds for any batch time t:

$$[C_{i0}] = [C_i] + [C_a] + [C_d] \qquad (5.11)$$

Here, C_i is the pre-catalyst concentration ([Rh(Monophos)$_2$(COD)]BF$_4$) at any time t and $C_{i,0}$ the initial pre-catalyst concentration. Combination of Equation's 5.9, 5.10 and 5.11 leads to the following mass balance for the active species:

$$\frac{d[C_a]}{dt} = k_a \cdot m \cdot [H_2]_g \cdot [C_i] - k_d \cdot [C_a] \qquad (5.12)$$

Integration using the initial condition (t = 0) [C_i] = [C_{i0}], [C_a] = 0 and [C_d] = 0 leads to equation 5.13.

$$[C_{Active}] = \frac{[C_{i0}] \cdot k_a \cdot m \cdot [H_2]_g}{k_d - k_a \cdot m \cdot [H_2]_g} \left[e^{-k_a \cdot m \cdot t \cdot [H_2]_g} - e^{-k_d \cdot t} \right] \qquad (5.13)$$

However, slow catalyst deactivation during a run is likely not the only source leading to a decrease of the catalyst concentration during a run. Instantaneous deactivation of the catalyst when mixing the catalysts with the solvents and reactants due to the presence of small amounts of impurities cannot be excluded. This was supported by performing experiments with undistilled, although properly degassed, IPA. The TOF of a run was reduced considerably compared to a run with freshly distilled IPA from CaH_2. Although the latter was used for all experiments, the presence of residual impurities cannot be included and this may result in instantaneous deactivation of part of the catalyst precursor. To compensate for this effect a parameter *IL* (instantaneous loss) is introduced (Equation 5.14).

$$\left[C_{i,eff,0}\right] = \left[C_{i,0}\right] - IL \qquad (5.14)$$

Combination with equation 5.13 gives equation 5.15.

$$\left[C_{Active}\right] = \frac{\left[C_{i0} - IL\right] \cdot k_a \cdot m \cdot \left[H_2\right]_g}{k_d - k_a \cdot m \cdot \left[H_2\right]_g} \left[e^{-k_a \cdot m \cdot t \cdot \left[H_2\right]_g} - e^{-k_d \cdot t}\right] \qquad (5.15)$$

Experimental studies for Monophos-Rh catalyst systems revealed that not all catalyst precursors $[Rh(Monophos)_2(L)_2]BF_4$ (L= COD, NBD) is quantitatively converted to catalytically active species during the hydrogenation reaction. Van den Berg used electron spray mass spectrometry to investigate the rhodium species present during the hydrogenation reaction of (Z)-methyl 2-acetamido-3-phenylacrylate (3) in CH_2Cl_2 using $[Rh(NBD)_2]BF_4$/Monophos (1: 2 ratio) as the catalyst precursor at 1 bar of hydrogen.[20] Surprisingly, rhodium compounds with three and four Monophos ligands attached (L_3Rh and L_4Rh) were also present in the mixture. The latter was isolated and characterised by X-ray analysis. These compounds are expected to be less active than the L_2Rh compounds and may even be totally inactive. This statement was supported by experimental studies[20] and theoretical calculations of van Speybroek *et al*.[36] Thus, part of the Rh is not active in the hydrogenation reaction.

This effect is taken into account in the kinetic modelling studies by the term *IL*. Thus, the term *IL* not only describes the loss of active catalyst due to impurities in the system but also quantifies

the fact that not all catalyst precursor $[Rh(Monophos)_2(COD)_2]BF_4$] is converted to the active catalyst $[Rh(Monophos)_2(S)_2]BF_4$].

5.3.5 Modeling results

The experimental data of 12 experiments (1884 data points) were modelled simultaneously using Equation 5.8 in combination with Equation 5.15. This allows calculation of the kinetic constants and their confidence intervals. The results are given in Table 5.2.

Table 5.2 Kinetic parameters for the Halpern model.

	Halpern model		Halpern model excluding k_{s2}	
Parameter	Value	CI [a]	Value	CI [a]
k_{s1} (L/mmol.s)	3.78E-01	5.27E-02	3.80E-01	4.82E-02
k_{s2} (1/s)	7.85E-11	7.34E-01	-	-
k_p (1/s)	9.02E-01	2.42E-01	9.14E-01	1.72E-01
k_a (L/mmol.s)	9.96E-04	2.78E-04	9.82E-04	1.81E-04
k_d (1/s)	1.99E-03	5.40E-04	2.01E-03	3.03E-04
IL (mmol/L)	7.09E-02	1.35E-03	7.10E-02	1.34E-03
AIC	-11.79		-11.82	
MRE(%)	11.3		11.3	

a. Confidence boundary limits (95%).

Inspection of the kinetic parameters reveals that the value of k_{s2} is very small and that the error in the value is high. Therefore, it was decided to exclude k_{s2} from Equation 5.8. The values of the kinetic parameters are close to the values found for the kinetic model including k_{2s}, see Table 5.2.

As can be seen Figure 5.4. and the values of AIC and MRE, the experimental data are adequately modelled using the kinetic expression derived from the Halpern model.

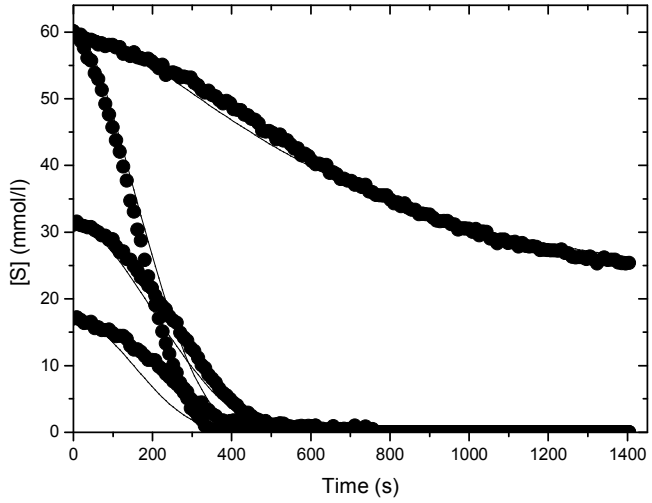

Figure 5.4 Experimental and modeled substrate concentration versus time for entry 3, 7, 9 and 11, with the Halpern model excluding k_{s2}. Experimental data (●), modeled data (-).

5.3.5.1 Model implications

The values of the kinetic parameters give valuable information on the rates of substrate coordination and dissociation to the metal centre (k_{s1} and k_{s2}) as well as the rate of oxidative addition of hydrogen (k_p, see Scheme 5.5.). The value of k_{s2} was found to be very small and this parameter was discarded from the model. This indicates that the rate of substrate dissociation is very low and that the substrate binds much better to the Rh-cation than the solvent molecules. This observation is in agreement with the theoretical calculations of van Speybroek *et al*[36] and also in agreement with work of Halpern for bidentate ligands.[25,26]

Thus, both step 1 and step 2 in the catalytic cycle may be treated as irreversible. It is of interest to compare the relative rates of both steps. In the case of irreversible complexation k_{s2} in Equation 5.8 is zero and Equation 5.8 may be rewritten as:

$$\frac{d[P]}{dt} = \frac{k_P \cdot k_{S1} \cdot m \cdot [H_2]_g \cdot [S] \cdot [C_{Active}]}{k_P \cdot m \cdot [H_2]_g + k_{S1} \cdot [S]} \qquad (5.16)$$

Two limiting situations may be distinguished. In the first extreme, $k_{p.}m.[H_2]_g << k_{s1}[S]$ and Equation 5.16 simplifies to Equation. 5.17. Here, the rate is fully determined by the rate of oxidative addition of hydrogen.

$$\frac{d[P]}{dt} = k_P \cdot m \cdot [H_2]_g \cdot [C_{Active}] \qquad (5.17)$$

In the other extreme $k_{p.}m.[H_2]_g >> k_{s1}[S]$ and Equation 5.16 simplifies to Equation 5.18

$$\frac{d[P]}{dt} = k_{S1}.[S] \cdot [C_{Active}] \qquad (5.18)$$

Here, the rate of complexation of the substrate determines the rate and the rate becomes independent of the hydrogen pressure. With the ranges of substrate and hydrogen concentration known and the values of the kinetic parameters available (Table 5.2), it can be shown that $k_{p.}m.[H_2]_g \approx k_{s1}[S]$ and that none of the limiting situations is valid. Thus, the rate of the substrate complexation and the oxidative addition are in the same range and determine the overall kinetics.

The active catalyst concentration during a run is a delicate balance between activation of the catalyst by hydrogenation of COD (Scheme 5.4.), irreversible deactivation, loss of activity due to the formation of low or even inactive rhodium species (L_4Rh and L_3Rh) and deactivation due to impurities in the solvent and reagents (IL). With the kinetic parameters available for these processes, the actual catalyst concentration during a run may be simulated using Equation 5.15. The results are given in Figure 5.5 (given for entry 3,4 and 11).

Clearly, catalyst activation by COD hydrogenation is a relatively slow process and the maximum concentration of active catalyst is reached after 200-400 s. After 400 s, the concentration of active catalyst drops by irreversible deactivation.

The value for *IL*, being the loss of active catalyst by impurities in the reagents and the formation of inactive/slightly active rhodium complexes, was found to be 0.07 mmol/L. Thus, with a catalyst intake of 0.1 mmol/l (e.g. entries 10-12 in Table 5.1.) the majority of the rhodium will not end up in the catalytic cycle. This is clearly illustrated in Figure 5.5. for entry 11. The maximum amount of active catalyst is calculated to be only 0.01 mmol/l and reduces to 0.00302

mmol/l at 1400 s. This is also supported by the experimental data, quantitative conversion is not observed for entry 11 and catalyst activity after 1404 s is very low (Figure 5.3).

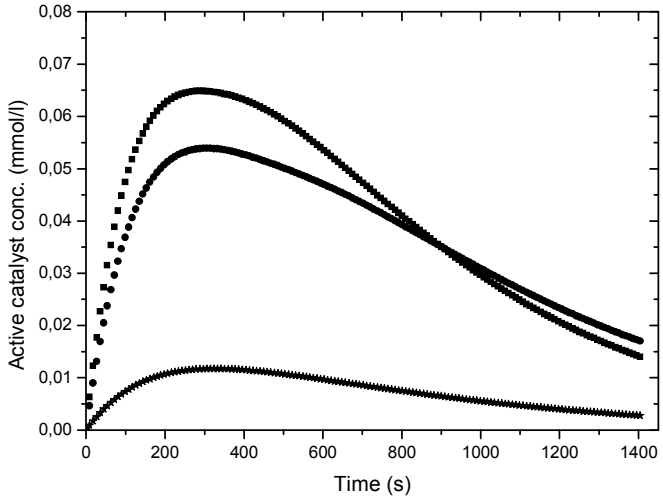

Figure 5.5 Modelled active catalyst concentration for entry 3 (■), 4 (●) and 11 (★).

5.4 Conclusions

A kinetic investigation on the enantioselective hydrogenation of methyl-2-acetamido acrylate to 2-acetylamino-propionic acid methyl ester with hydrogen using a chiral Rhodium/MonoPhos™-complex in IPA was performed. The product ee was > 97.6% for all experiments with a S/C ratio < 400. It was found that the overall kinetics can be modelled adequately using the Halpern mechanism for the hydrogenation of C-C double bonds in combination with a catalyst activation and deactivation process.

5.5 References

1 D. Cutler, A. Barbier, and K. Pestell, *Trends Pharmacol. Sci.*, 2002, **23**, 258-259.

2 N. B. Johnson, I. C. Lennon, P. H. Moran, and J. A. Ramsden, *Acc.Chem. Res.*, 2007, **40**, 1291-1299.

3 R. Noyori, *Adv. Synth. Catal.*, 2003, **345**, 15-32.

4 H. Shimizu, I. Nagasaki, K. Matsumura, N. Sayo, and T. Saito, *Acc. Chem. Res.*, 2007, **40**, 1385-1393.

5 W. C. Zhang, Y. X. Chi, and X. M. Zhang, *Acc. Chem. Res.*, 2007, **40**, 1278-1290.

6 G. Erre, S. Enthaler, K. Junge, E. Gladiali, and M. Beller, *Coord. Chem. Rev.*, 2008, **252**, 471-491.

7 T. Jerphagnon, J. L. Renaud, and C. Bruneau, *Tetrahedron-Asymmetry*, 2004, **15**, 2101-2111.

8 P. W. N. M. van Leeuwen, *Homogeneous catalysis understanding the art*, Kluwer Academic Publishers, Dordrecht, 2004.

9 W. S. Knowles, *Adv. Synth. Catal.*, 2003, **345**, 3-13.

10 B. L. Feringa, M. Pineschi, L. A. Arnold, R. Imbos, and A. H. M. de Vries, *Angew. Chem. Int. Ed.*, 1997, **36**, 2620-2623.

11 B. L. Feringa, *Acc. Chem. Res.*, 2000, **33**, 346-353.

12 R. Naasz, L. A. Arnold, M. Pineschi, E. Keller, and B. L. Feringa, *J. Am. Chem. Soc.*, 1999, **121**, 1104-1105.

13 M. Van den Berg, A. J. Minnaard, E. P. Schudde, J. van Esch, A. H. M. de Vries, J. G. de Vries, and B. L. Feringa, *J. Am. Chem. Soc.*, 2000, **122**, 11539-11540.

14 M. Van den Berg, A. J. Minnaard, R. M. Haak, M. Leeman, E. P. Schudde, A. Meetsma, B. L. Feringa, A. H. M. de Vries, C. E. P. Maljaars, C. E. Willans, D. Hyett, J. A. F. Boogers, H. J. W. Henderickx, and J. G. de Vries, *Adv. Synth. Catal.*, 2003, **345**, 308-323.

15 C. Claver, E. Fernandez, A. Gillon, K. Heslop, D. J. Hyett, A. Martorell, A. G. Orpen, and P. G. Pringle, *Chem. Commun.*, 2000, 961-962.

16 Y. Fu, J. H. Xie, A. G. Hu, H. Zhou, L. X. Wang, and Q. L. Zhou, *Chem. Commun.*, 2002, 480-481.

17 M. T. Reetz and G. Mehler, *Angew. Chem. Int. Ed.*, 2000, **39**, 3889-+.

18 M. T. Reetz and T. Sell, *Tetrahedron Lett.*, 2000, **41**, 6333-6336.

19 K. Junge, G. Oehme, A. Monsees, T. Riermeier, U. Dingerdissen, and M. Beller, *Tetrahedron Lett.*, 2002, **43**, 4977-4980.

20 M. Van den Berg, *Rhodium-Catalyzed Asymmetric Hydrogenation using Phosphoramidite Ligands, PhD Thesis.*, 2006.

21 T. Sturm, W. Weissensteiner, and F. Spindler, *Adv. Synth. Catal.*, 2003, **345**, 160-164.

22 J. G. de Vries, and C. J. Elsevier, *The handbook of homogeneous hydrogenation*, Wiley-VCH, Weinheim, 2007.

23 I. D. Gridnev, N. Higashi, K. Asakura, and T. Imamoto, *J. Am. Chem. Soc.,*, 2000, **122**, 7183-7194.

24 I. D. Gridnev, Y. Yamanoi, N. Higashi, H. Tsuruta, M. Yasutake, and T. Imamoto, *Adv. Synth. Catal.,* 2001, **343**, 118-136.

25 J. Halpern, *Science*, 1982, **217**, 401-407.

26 C. R. Landis and J. Halpern, *J. Am. Chem. Soc.*, 1987, **109**, 1746-1754.

27 S. Caravieilhes, C. de Bellefon, and N. Tanchoux, *Catal. Today*, 2001, **66**, 145-155.

28 R. A. Sanchez-Delgado and M. Rosales, *Coord. Chem. Rev.*, 2000, **196**, 249-280.

29 K. R. Westerterp, W. P. M. Swaaij, A. A. C. M. Beenackers, and H. Kramers, *Chemical reactor design and operation*, Wiley, Chichester, Student ed, 1987.

30 H. Motulsky, and A. Christopoulos, *Fitting models to biological data using linear and nonlinear regression a practical guide to curve fitting*, Oxford University Press, Oxford, 2004.

31 X. L. Xi, Y. L. Liu, J. Shi, and S. K. Cao, *J. Mol. Catal. A: Chem.*, 2003, **192**, 1-7.

32 A. Behr, D. Obst, C. Schulte, and T. Schosser, *J. Mol. Catal. A: Chem.*, 2003, **206**, 179-184.

33 H. U. Blaser, H. P. Jalett, and F. Spindler, *J. Mol. Catal. A: Chem.*, 1996, **107**, 85-94.

34 I. Gergely, C. Hegedus, H. Gulyas, A. Szollosy, A. Monsees, T. Riermeier, and J. Bakos, *Tetrahedron-Asymmetry*, 2003, **14**, 1087-1090.

35 E. F. Stefoglo, V. I. Drobyshevich, V. A. Semikolenov, I. V. Kuchin, and O. P. Zhukova, *Chem. Eng. J.*, 2003, **91**, 199-204.

36 V. van Speybroeck, and J. G. de Vries, *N3C abstract*, 2007.

Chapter 6. Combined Dehydration/(transfer)-Hydrogenation of C6-sugars (D-glucose and D-fructose) to γ-valerolactone using ruthenium catalysts

6.1 Introduction

Concerns about the environment and a decline in easily recoverable crude oil reserves have stimulated the search for renewable energy carriers and green chemicals. Biomass is considered a very promising feedstock for biofuels and bio-based (performance) chemicals.[1-4] A number of studies have been performed to identify interesting biomass derivatives to be used as future platform chemicals for the chemical industry.[2,5,6] The majority of the selected platform chemicals are derived from the cellulose and hemi-cellulose fraction of (ligno-) cellulosic biomass. Our research activities involve the production of γ-valerolactone (GVL) from the C6-sugars (D-glucose, D-mannose and D-galactose) present in the cellulose and hemi-cellulose fraction of biomass and derivatives derived thereof (D-fructose). GVL is considered a very attractive biomass derived compound. It may be used as a solvent for example in lacquers and as a food additive.[7,8] Furthermore, it is considered a potential biofuel and was shown to be a suitable replacement for ethanol in gasoline-ethanol blends.[8] GVL may also be converted to a number of interesting derivatives. Three examples are provided in Scheme 6.1. Hydrogenation of GVL provides access to methyltetrahydrofuran (MTHF), which is as potential fuel additive.[9] The reaction with GVL and formaldehyde leads to the formation of α-methylene-γ-valerolactone (MGVL), a new acrylic monomer which may be converted to novel acrylic polymers with improved product properties (e.g. thermal stability).[10] Another interesting option is ring-opening of GVL with methanol followed by dehydration to produce methylpentenoate (MP). This compound may be converted by hydroformylation, hydrocyanation or hydroxycarbonylation to caprolactone, caprolactam and adipic acid, respectively.[11]

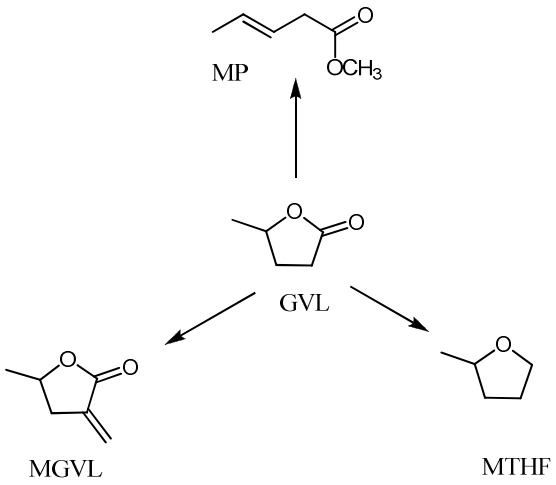

Scheme 6.1 Examples of interesting derivatives from GVL.

GVL is typically obtained from levulinic acid (LA) by a catalytic hydrogenation using molecular hydrogen (Scheme 6.2). The intermediate 4-hydroxypentanoic acid is rather unstable and cyclisation to GVL occurs easily.[9]

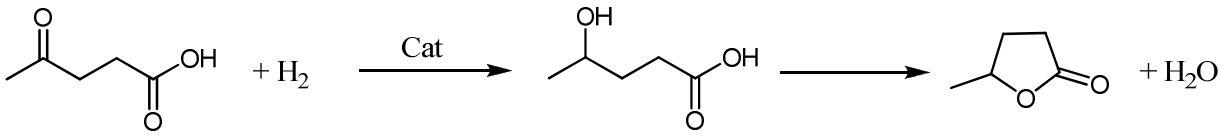

Scheme 6.2 Catalytic hydrogenation of LA to GVL.

The hydrogenation of LA to GVL using heterogeneous catalysts in combination with molecular hydrogen has been studied extensively.[10-16] Typically the reactions are either carried out solvent free or in organic solvents like dioxane, ethylether and supercritical CO_2 (sCO_2). In most cases temperatures between 106 and 273 °C and pressures between 34 and 150 bar were applied. The highest GVL yield was 97% for a Ru/C catalyst at 150 °C and 34.5 bar hydrogen pressure in dioxane.[10] Recently, Bourne *et al.*[12] showed that water in combination with sCO_2 may also be used as the reaction medium. After reaction, the sCO_2 layer is enriched with GVL and may easily be recovered from the reaction mixture.

A number of homogeneous catalysts have also been reported for the hydrogenation of LA to GVL.[17-19] Joo *et al.*[17,18] demonstrated the use of water soluble homogeneous ruthenium catalysts with sulphonated triphenylphosphine ligands (e.g. $HRuCl(Dpm)_3$, Dpm = diphenylphosphinobenzene-m-sulfonic acid) for the hydrogenation of oxo- and unsaturated acids. However, catalyst activity for the hydrogenation of keto-acids like LA was low.[17-19] Recently, Horvath and co-workers reported the use of $Ru(Acac)_3$ in combination with TPPTS (tris(3-sulfonatophenyl)phosphine) for the hydrogenation of LA in water at 140 °C and 69 bar hydrogen.[20,21] After 12 h, LA conversion was complete and GVL was obtained in essentially quantitative yield (> 95%).

Although most hydrogenations have been performed with molecular hydrogen, transfer hydrogenations using formic acid or a derivative have also been reported for both homogeneous and heterogeneous catalyst systems. For instance, Haan *et al.*[22] demonstrated the hydrogenation of LA or ethyllevulinate to GVL using formic acid as the hydrogen donor with a variety of heterogeneous catalysts (e.g. Ni/Pt on silica, Re/Pt on silica, Ni). The reactions are typically carried out in the gas phase at 200-350 °C and pressures between 1-10 bar. The highest GVL yield (81 mol%) were obtained using ethyllevulinate as the substrate, a commercial Ni catalyst at 250 °C and a WHSV (weight hourly space velocity) of 1.1 g substrate/(g cat.h). Horvath *et al.*[21] applied a homogeneous Ru compound $[(\eta^6\text{-}C_6Me_6)Ru(bpy)(H_2O)][SO_4]$ in water for the transfer hydrogenation of LA using formic acid as the hydrogen donor. Both GVL and 1,4-pentanediol were obtained in 25% yield.

We here report our studies on the direct synthesis of GVL from C6-sugar sources (D-glucose, D-fructose, sucrose and cellulose) without isolation of the intermediate LA. Compared to the use of LA as a starting material, this approach reduces the number of processing steps and may lead to a reduction in the manufacturing costs of GVL. An overview of the reaction sequence is given in Scheme 6.3. The reaction of C6-sugars to LA is an acid catalysed hydrolysis reaction and is typically performed in water using strong mineral acids like HCl and H_2SO_4.[2,23-25] The use of heterogeneous catalysts has also been reported.[2,24,26-28] By-products of the reaction are 5-hydroxymethylfurfural (HMF), formic acid (FA) and insoluble solid materials known as humins.[24,29,30] HMF is an intermediate product which under appropriate conditions may be converted essentially quantitatively to LA. The insoluble humins are formed in a parallel mode from both the C6-sugar precursor as well as from the intermediate HMF.[24,29,30] Typical yields for

LA from D-glucose are about 62 mol%,[23,24] whereas the yields for D-fructose are considerably higher (78 mol%).[25,26]

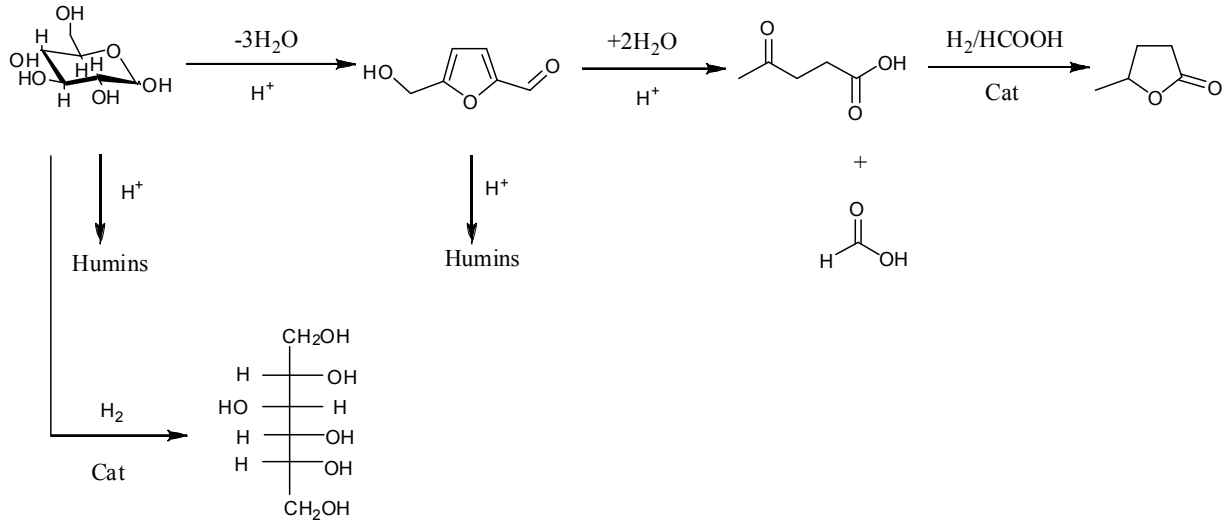

Scheme 6.3 Hydrogenation of D-glucose to D-sorbitol and the acid catalyzed hydrolysis of D-glucose to LA and subsequently hydrogenation of LA to GVL.

To obtain GVL from a C6-sugar in a one pot approach without isolation of the intermediate LA, the combined action of an acid catalyst and a hydrogenation catalyst is required. Examples of this approach, either with homogeneous or heterogeneous catalysts and/or molecular hydrogen or formic acid as the hydrogen source, are scarce.

Braca *et al.*[31] reported the use of Ru-carbonyls ($Ru(CO)_4I_2$) in combination with HI for the conversion of D-glucose and D-fructose to GVL. When using syngas (CO/H_2) in combination with D-glucose, GVL yields up to 40 mol% were obtained. Recently, Horvath *et al.*[20,21] reported the use of water soluble homogeneous Ru-catalysts prepared *in situ* from $RuCl_3$ and TPPTS in combination with H_2SO_4 (0.5 mol/l) as the acid catalyst and molecular hydrogen as the hydrogen donor. With sucrose, the main products were D-sorbitol and D-mannitol, indicating that the acid catalysed conversion of sucrose to LA was much slower than the direct hydrogenation of the D-glucose and D-fructose, the monomeric building blocks of sucrose. By applying higher acid concentrations (1.8 mol/l), the rate of the acid catalysed dehydration reaction of sucrose to LA was considerably higher than the direct hydrogenation to D-sorbitol and D-mannitol leading to GVL yields of up to 40%.[8,20]

To the best of our knowledge, the direct synthesis of GVL from C6-sugars by the combined action of a heterogeneous hydrogenation and a homogeneous acid dehydration catalyst either using molecular hydrogen or with a hydrogen donor such as formic acid has not been reported to date. Particularly the use of formic acid as the hydrogen donor is attractive as this is the co-product of the conversion of C6-sugars to LA (Scheme 6.3). We here report our research on the catalytic hydrogenation/acid hydrolysis of monomeric C6 sugars (D-glucose and D-fructose) as well as sucrose and cellulose in water using Ru/C as the hydrogenation catalyst, trifluoroacetic acid (TFA) as the acid catalyst and either molecular hydrogen or formic acid as the hydrogen donor.

6.2 Materials and methods

6.2.1 Chemicals

D-glucose, sulphuric acid (96%), formic acid (98-100%) and trifluoroacetic acid (98%) were purchased from Merck. Levulinic acid (98%), D-fructose (98%) and 5-hydroxymethylfurfural (98%) were purchased from Acros Organics. Ru/C (5% w/w), γ-valerolactone (99%), 2-methyl-tetrahydrofuran (≥ 99%) and cellulose (microcrystalline powder, 20 μm) were obtained from Sigma Aldrich. $RuCl_3.3H_2O$ (technical grade) was purchased from Riedel de Haën, Na_3TPPTS (TPPTS, tris(3-sulfonatophenyl)phosphine) was obtained from Strem Chemicals. Sucrose was purchased from Fisher Scientific. De-ionized water was used to prepare the various solutions.

6.2.2 Experimental procedures

Reactions were carried out in a Parr 100 ml autoclave (max. 350 bar pressure, max. temperature 350 ºC). A schematic representation of the reactor setup is given in Figure 6.1 The reactor is electrically heated and when appropriate, may be cooled using water. The reactor temperature is controlled by a Eurotherm 2208e controller. The reactor content is stirred by a Heidolph RZR 2050 overhead stirrer, equipped with a standard impeller. The pressure and temperature as a function of reaction time are measured continuously and transferred to a PC using the VirtualBench-logger (version 2.5) software package from National Instruments®.

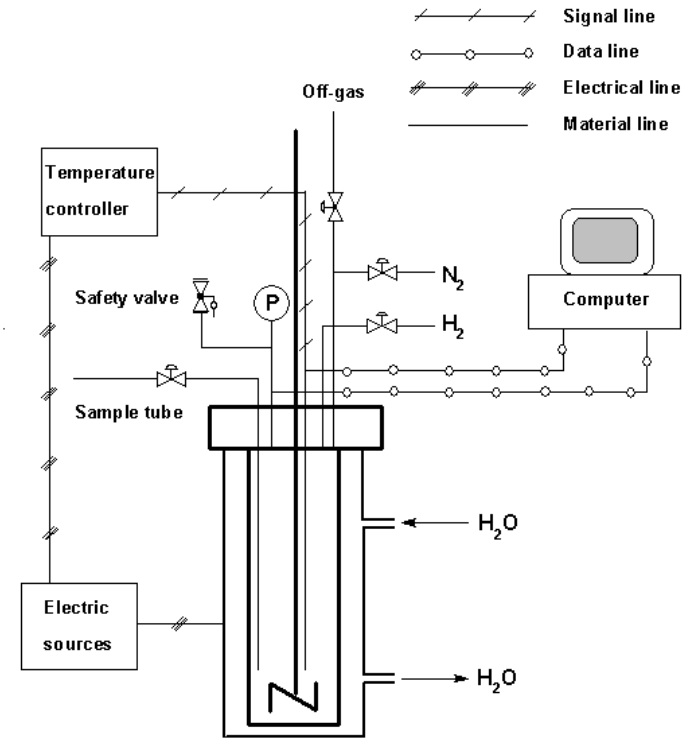

Figure 6.1 Schematic representation of the reactor setup.

6.2.2.1 Typical experimental procedure for the combined dehydration/transfer hydrogenation of D-fructose to GVL with Ru/C, TFA and formic acid

The reactor was filled with D-fructose (4.9 g, 0.03 mol), Ru/C (0.5 g), FA (3.7 g, 0.08 mol) and a solution of TFA in water (0.5 mol/l in water, 50 ml). Subsequently, the reactor was flushed several times with nitrogen to remove air. The reactor was pressurized (50 bar) with nitrogen and heated to the desired reaction temperature (180 ºC). A stirrer speed of 1800 rpm was applied throughout an experiment. After the pre-determined reaction time (typically 16 h), the reactor was cooled, depressurized and flushed several times with N_2. The reaction mixture was filtered over silica gel to remove humins and catalyst. The solution was diluted with de-ionized water and analyzed by High Performance Liquid Chromatography (HPLC) to determine the D-fructose conversion and product composition.

6.2.2.2 Typical experimental procedure for the combined dehydration/hydrogenation of D-glucose to GVL with Ru/C and TFA

The reactor was filled with D-glucose (9.9 g, 0.06 mol), Ru/C (0.5 g) and a solution of TFA in water (1 mol/l in water, 50 ml). After closing, the reactor was flushed several times with nitrogen to remove air. The reactor was pressurized (60 bar) with hydrogen and heated to the desired reaction temperature (180 ºC) while maintaining a stirrer speed of 50 rpm. After 10 minutes at 180 ºC, the hydrogen pressure was set at 94 bar and the stirrer speed was set at 1800 rpm. The hydrogen pressure was maintained at 94 bar throughout the experiment by periodic addition of hydrogen gas. After the pre-determined reaction time (typically 8 h), the reactor was cooled, depressurized and flushed several times with nitrogen. The reaction mixture was filtered over silica gel to remove humins and catalyst. The solution was diluted with de-ionized water and analyzed by HPLC to determine the D-glucose conversion and product composition.

6.2.2.3 Typical experimental procedure for the dehydration/hydrogenation of D-glucose to GVL with a homogeneous Ru/TPPTS catalyst and TFA

The homogeneous Ru/TPPTS catalyst complex was pre-formed before an actual dehydration/hydrogenation experiment. $RuCl_2.3H_20$ (0.1 mmol, 26 mg) was dissolved in de-ionised water (10 mL). Subsequently Na_3TPPTs (0.3 mmol, 172 mg) and NaI (0.13 mmol, 20 mg) were added and the solution was stirred for 10 minutes. The resulting solution was added to the pressure reactor containing D-glucose (4.9 g, 0.03 mol) and TFA (0.63 mol/l, 40 mL). The actual hydrogenation experiment was carried out as described above, with the exception that a stirrer speed of 1800 rpm was applied throughout the experiment.

6.2.2.4 Experimental procedure for the conversion of D-glucose and D-fructose to LA using TFA as the catalyst

The reactions were carried out in glass ampoules (inside diameter of 3 mm, wall thickness of 1.5 mm, and length of 15 cm). The ampoules were filled with ± 0.5 cm^3 of reaction mixture (D-glucose or D-fructose, TFA and water) and sealed using a torch. The sealed ampoules were placed in a special rack, which can hold up to 20 ampoules, and placed in a constant temperature oven (± 1 °C). At different reaction times, ampoules were taken from the oven and quenched into

an ice-water bath (4 °C) to stop the reaction. The reaction mixture was taken out of the ampoule and insoluble humins were separated using a micro centrifuge (Omnilabo International BV) for 15 minutes at 1200 rpm. The particle-free solution was diluted with de-ionized water and subsequently analyzed using HPLC.

6.2.3 Analytical methods

The liquid phase after reaction was analysed using HPLC. A HPLC apparatus equipped with a Hewlett Packard 1050 pump, a Bio-Rad organic acid column (Aminex HPX-87H) and a differential refractometer was used. The mobile phase consisted of an aqueous solution of sulphuric acid (5 mmol/l) operated at a flow rate of 0.55 cm^3 min^{-1}. The column was operated at 60 ^oC. The amounts of the products were calculated using calibration curves obtained from standard solutions of known concentrations.

6.3 Results and discussion

6.3.1 Brønsted acid selection

A wide variety of inorganic Brønsted acid like H_2SO_4, HNO_3 and HCl, have been tested for the conversion of D-glucose and D-fructose to levulinic acid.[2,23-25] High yields at short reaction times are possible using strong acids (pK_a < 2) and H_2SO_4 was shown to be particularly attractive.[24] However, sulphuric acid is likely poorly compatible with Ru catalysts due to the presence of sulphur.[32,33] For instance, Osada *et al.*[33] compared the activity of fresh Ru/TiO_2 with that of Ru/TiO_2 soaked in aqueous sulphuric acid before catalytic testing. It was found that the activity of the latter catalyst was considerably lower due to adsorption of sulphur to the ruthenium metal catalyst. Catalytic experiments (*vide infra*) within the framework of this research also confirm this observation.

An attractive alternative organic acid could be trifluoroacetic acid (TFA). The pK_a is 0.5 and recently Marzialetti *et al.*[34] successfully used TFA for the hydrolysis of loblolly pine to mono-saccharides. To gain insights in the potential of TFA for the conversion of C6-sugars to levulinic acid, a number of experiments were conducted with D-glucose and D-fructose in water according to a procedure published recently by our group.[24,29] The experiments with D-glucose were carried

out at different TFA concentrations (0.1-1 mol/l) at 180 °C with a fixed D-glucose intake (0.1 mol/l). The concentration of HMF and LA were determined as a function of time and the results are given in Figure 6.2.

The highest yield of LA was 57 mol% which is only 2% less than the best experiments with sulphuric acid.[24] The major by-products were FA and insoluble materials known as humins. Thus, TFA appears an attractive alternative for H_2SO_4 for exploration in combined acid hydrolysis/hydrogenation experiments.

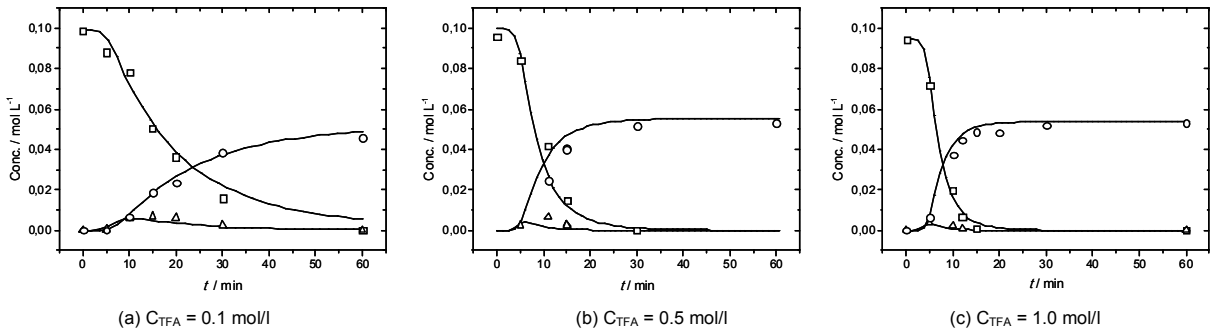

Figure 6.2 Experimental and modelled data for D-glucose conversion to LA at various TFA concentrations ($C_{GLC,0}$ = 0.1 mol/l, T = 180 ºC, t = 60 min.). Experimental data: □: C_{GLC}, ○: C_{LA}, Δ: C_{HMF}. Lines are model predictions.

The experimental data were modelled using a power law model previously developed for sulphuric acid, taking into account the different H^+ concentrations due to differences in pK_a values between sulphuric acid and TFA.[24,29] The results are depicted in Figure 6.2 and good agreement between experiments and model was observed. Thus, it appears that the kinetic models developed for sulphuric acid are broadly applicable, provided that the H^+ concentration is corrected for the pK_a of the acid under study. The temperature effects and the D-glucose intake on activity and LA selectivity were modelled for TFA and the results are given in Figure 6.3. Thus, to reach the highest LA yield (57 mol%) at reasonably short batch times, a temperature of 180 °C seems preferred. The LA yield is a function of the D-glucose with higher concentrations leading to lower yields, see Figure 6.3 for details.[24]

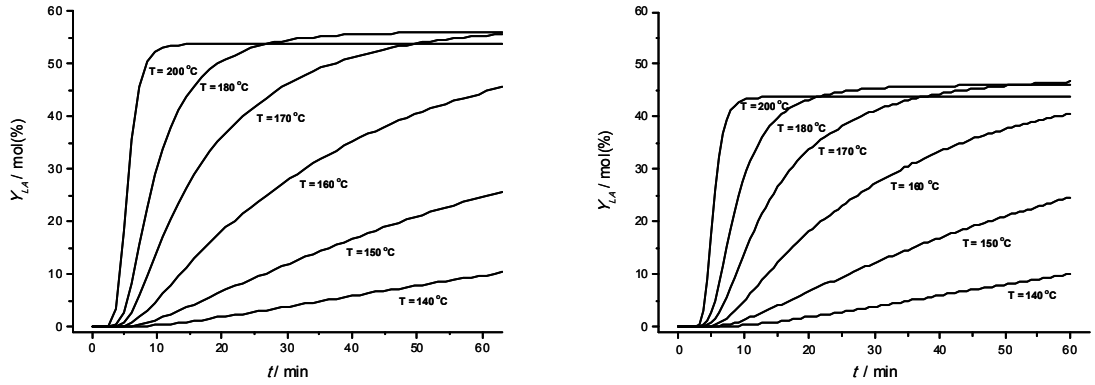

Figure 6.3 Modelled LA yield for the reaction of D-glucose with TFA at two D-glucose intakes (0.1 and 0.5 mol/l) at various temperatures (C_{TFA} = 0.5 mol/l).

A number of experiments were also carried out with D-fructose instead of D-glucose using the optimum conditions for D-glucose (180 °C, 60 min reaction time, $C_{C6\text{-}sugar,0}$ = 0.1 mol/l) with varying TFA concentration (0.1-1 mol/l). The results are illustrated in Figure 6.4. The highest LA yield was 70 mol%, which is considerably higher than found for D-glucose. These results are in line with literature data, which indicate that the conversion of D-fructose rich feeds to LA is more efficient than for D-glucose rich feeds.[30,35]

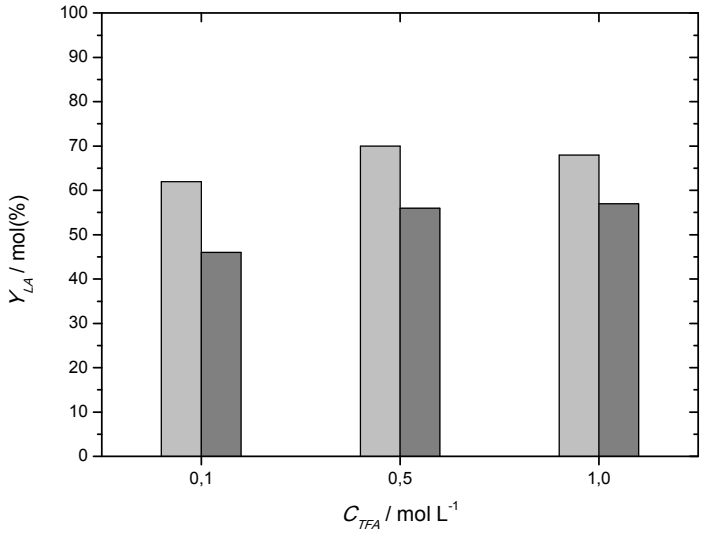

Figure 6.4 LA yield for the reaction of D-fructose (■) and D-glucose (■) ($C_{FRT,0}$ = $C_{GLC,0}$ = 0.1 mol/l) to LA at different TFA concentrations (T = 180 ºC, t = 60 min).

6.3.2 Combined transfer hydrogenations-dehydration of C6-sugars to GVL with formic acid as the hydrogen source

A number of experiments with Ru/C in combination with TFA and with formic acid (FA) as the hydrogen donor were carried out to gain insights in the potential of combined C6-sugar dehydration to LA followed by a transfer hydrogenation of LA to GVL (Scheme 6.3). The reactions were carried out at 180 °C in an aqueous medium using D-fructose as the C6-sugar. The latter was selected for its higher selectivity towards LA in the first step of the sequence in Scheme 6.3 (*vide supra*). External FA was supplied to speed up the reaction rate, typically a FA to D-fructose intake of 3.2 mol/mol was applied. The first experiment (entry 1 in Table 6.1) resulted in the formation of 16 mol% GVL. The major liquid phase component was the intermediate LA (53 mol%). Thus, although transfer hydrogenation occurred to a certain extent, the reaction is much slower than the conversion of D-fructose to LA. Of interest is the sum of the yields of LA and GVL (69 mol%), which is close to the maximum amounts of LA from the acid catalysed dehydration of D-fructose under the experimental conditions applied (Figure 6.4). Thus, excessive losses in selectivity by humin formation due to the presence of Ru/C and TFA are not a major issue. Subsequent hydrogenation products of GVL like MTHF and 1,4-

pentanediol were not detected in the liquid phase (HPLC). In addition, hydrogenation products of D-fructose (D-sorbitol and D-mannitol)[36] were also not detected and indicate that the dehydration of D-fructose to LA is much faster than the (transfer) hydrogenation of D-fructose to D-sorbitol/mannitol.

Table 6.1 Dehydration/transfer hydrogenation of D-fructose using Ru/C and TFA in combination with formic acid[a].

Entry	Reaction time (h)	P N_2 (bar)	FA/D-fructose mol ratio (mol/mol)	Yield LA (mol %)	Yield GVL (mol %)
1	8	0	3.2	53	16
2	8	50	3.2	39	32
3	16	50	3.2	17	43
4	16	50	6.6	11	52

a. A 10 wt% intake of Ru/C on D-fructose was applied. The TFA concentration was 0.5 mol/l in water, the reaction temperature was 180 °C. Complete D-fructose conversion was observed for all experiments.

To increase the effective FA concentration in solution and thus to speed up the rate of the transfer-hydrogenation reaction of LA to GVL, the amount of FA in the liquid phase was increased by performing subsequent experiments at higher pressures (50 bar N_2). At otherwise similar conditions, the yield of GVL increased to 32 mol% (entry 2, Table 6.1). Further improvements were possible by extending the reaction time and using higher FA intakes. With these measures, a maximum yield of GVL of 52 mol% (entry 4, Table 6.1) could be obtained. Still some unreacted LA was present (11 mol%) whereas the major by-products were insoluble humins, formed in the first step in the reaction sequence (Scheme 6.3). It may be concluded that the selectivity of the overall conversion of D-fructose to GVL is determined by the (fast) reaction of D-fructose to LA (max. 70 mol%) and that the activity is solely determined by the subsequent (selective) transfer hydrogenation of LA to GVL.

The exact mechanism of the hydrogenation reaction is not clear yet. Transfer hydrogenations of LA with FA or derivatives have been reported in the literature, see introduction section for details. It is generally accepted that transfer hydrogenation with FA involve the formation of a metal-formate species which decomposes to a metal-hydride and CO_2. Subsequent reaction of the metal-hydride with LA results in reduction of the ketone moiety and the formation of GVL after cyclisation of the intermediate 4-hydroxypentanoic acid (Scheme 6.2). In this mechanism, free

molecular hydrogen is not formed. An alternative mechanism, though closely related, involves the formation of molecular hydrogen by decomposition of FA under reaction conditions. The hydrogen is again activated at the metal and used to hydrogenate LA to GVL. Decomposition of formic acid to molecular hydrogen is known for certain homogeneous Ru catalysts.[37] To gain insights in the role of decomposition of formic acid to hydrogen with the heterogeneous Ru/C catalyst used in this study, the reaction of FA in water (0.6 mol/l) in the presence of TFA (0.5 mol/l) and Ru/C was performed (180°C, 8h). After reaction, both the liquid phase and the gas phase was collected and analysed. The gas phase consisted mainly of hydrogen and CO_2 (> 95 mol%) in a 1 to 1 molar ratio. The FA conversion is 77 %. Thus, it may be concluded that FA is slowly catalytically decomposed under the reaction conditions to hydrogen and CO_2. Whether free hydrogen plays a role in the hydrogenation reaction of LA to GVL is speculative at this state and needs further research.

6.3.3 Dehydration/ hydrogenations of C6-sugars to GVL with molecular hydrogen as the hydrogen source

Initial experiments with molecular hydrogen were performed with D-glucose and H_2SO_4 as the acid catalyst for the conversion of D-glucose to LA and Ru/C as the heterogeneous hydrogenation for the subsequent hydrogenation to GVL (Scheme 6.3). The reactions were carried out in a batch reactor at a reaction temperature of 160 - 180 ºC and reaction times between 2.5-3 h. Complete D-glucose conversions were observed in all cases. The major product in the liquid phase was LA (15-26 mol%). Large amounts of brown insoluble products were formed (humins). The desired GVL was not detected in the reaction mixture. Apparently, the hydrogenation reaction of LA to GVL does not take place at these conditions, likely by Ru/C deactivation due to the presence of sulphuric acid (*vide supra*).

Subsequent reactions with molecular hydrogen and Ru/C (5 or 10 wt% on C6-sugar) as the hydrogenation catalyst were carried out with TFA as the acid catalyst (0.5 mol/l) at 180 ºC, a hydrogen pressure of 94 bar (semi-batch mode) and with D-glucose and D-fructose intakes between 0.1-1.1 mol/l. An overview of the experiments is given in Table 6.2. In all experiments, complete conversion of the C6-sugar was observed.

Table 6.2 Dehydration/hydrogenation of various C6-sugar sources using TFA and Ru/C in combination with molecular hydrogen[a].

Entry	Catalyst intake (wt% on substrate)	t (h)	D-glucose (mol/l)	D-fructose (mol/l)	Sucrose (mol/l)	Cellulose (mol/l)[b]	Yield LA (mol %)	Yield FA (mol %)	Yield GVL (mol %)
1[c]	10	8	0.5				0	0	0
2[d]	10	8	0.5				8	29	27
3[e]	10	8	0.5				4	16	38
4[e]	5	8	1.1				4	10	29
5[e]	10	4		0.1			56	16	16
6[e]	10	8		0.5			4	7	62
7[e]	5	8		1.1			3	7	54
8[e]	10	8			0.3		9	10	52
9[e]	10	8				0.5	6	16	29

a. All experiments were conducted at 180 ºC and 0.5 mol/l TFA. b. Calculated as the number of glucose units. c. Hydrogen (initial 60 bar at room temperature) present during heating to 180 ºC, 1800 rpm stirring speed applied throughout the experiment. d. Heating under a nitrogen atmosphere to 180 °C at 1800 rpm stirring speed. After 10 minutes, the reactor was pressurised with hydrogen (94 bar, semi-batch mode). e. Hydrogen (initial 60 bar at room temperature) present during heating to 180 ºC at 50 rpm stirring speed. After 10 minutes at 180 °C, the reactor was set at hydrogen pressure of 94 bar (semi-batch mode) and the stirrer speed was set at 1800 rpm.

For the first experiment (entry 1, Table 6.2) with D-glucose, a constant stirrer speed of 1800 rpm was applied throughout the experiment. Hydrogen was present during heating of the reaction mixture to 180 °C Analysis of the reaction mixture after reaction (HPLC) did not reveal the presence of GVL. Instead, large amounts of D-sorbitol, the hydrogenation product of D-glucose were present together with unidentified components. Apparently, the hydrogenation of D-glucose under these conditions is much faster than the dehydration of D-glucose to HMF and LA (Scheme 6.3). The occurrence of excessive hydrogenation of D-glucose is likely related to the rate of heating the batch reactor from room temperature to reaction temperature (180 °C). Typically this takes about 10-15 min. This heating period is expected to have a large effect on the product distribution and may be rationalised by considering the kinetics of the acid catalysed dehydration of D-glucose to HMF and LA[24] and the hydrogenation of D-glucose to sorbitol with a Ru/C catalyst.[38,39] The activation energy for the conversion of D-glucose to HMF in water is 152 kJ/mol[24] whereas values for the D-glucose hydrogenation with Ru/C in water are between 34

and 73 kJ/mol.[38,39] Thus, the conversion of D-glucose to HMF/LA is more sensitive to the temperature and is favoured at higher temperatures whereas the hydrogenation of D-glucose to D-sorbitol is favoured at low temperatures. Thus, the high selectivity to hydrogenation products of D-glucose as observed in our experiments is in line with kinetic data for both reactions and is due to the relatively long heating time of the batch set-up. The preferred way to reduce D-glucose hydrogenation would be the application of an infinitely low heating time in the batch set-up. However, this is practically not possible and the highest possible heating rates were applied already in this study.

An alternative procedure to reduce the rate of the hydrogenation reaction and thus to enhance the formation of HMF/LA during the heating period is to perform the heating stage in the absence of hydrogen (Table 6.2, entry 2). Indeed, this has a positive effect on the product selectivity and D-sorbitol could not be detected in the reaction mixture. The main products were GVL (27 mol%), residual LA (8 mol%) due to incomplete hydrogenation to GVL and insoluble brown solids (humins) formed by the acid catalysed conversion of D-glucose to HMF/LA. This experiment confirms that the undesired hydrogenation reaction of D-glucose to D-sorbitol mainly takes place during the heating period of the batch reactor.

Further improvements in the GVL yield were possible by performing an experiment with heating in the presence of hydrogen and a low rotation speed of the impeller during the heating period (50 rpm). The yield of GVL when using D-glucose as the C6-sugar source was 38 mol%, D-sorbitol formation was not observed (Table 6.2, entry 3). In this case, the rate of hydrogenation of D-glucose to D-sorbitol is likely much lower than the dehydration rate of D-glucose to LA by a reduction of the hydrogen mass transfer rate of the gas phase to the liquid phase due to a reduction of the volumetric mass transfer coefficient (k_L.a) of hydrogen.

The highest GVL yield when using D-glucose was 38 mol%, with 4 mol% unconverted LA. The highest LA yield for the acid catalysed dehydration of D-glucose in separate experiments in absence of hydrogen and Ru/C (*vide supra*) with a D-glucose concentration of 0.5 mol/l at 180 °C and 0.5 mol/l TFA was 46 mol%. Thus, the sum of the GVL and LA yield in the hydrogenation reaction (42 mol%) is close to the maximum achievable yield for the dehydration step (46 mol%). This implies that the selectivity of the Ru-catalysed hydrogenation reaction of LA to GVL is high under these conditions, in line with literature data.[10]

The use of TFA is essential to obtain GVL. This was confirmed by an experiment with D-glucose using Ru/C as catalyst and molecular hydrogen in the absence of TFA (94 bar hydrogen, 180°C, 8 h reaction time). After reaction, GVL was not detected in the reaction mixture (HPLC) and the main products were D-sorbitol, D-mannitol and glycerol. The sum of the yields of these components is 67 mol%. The latter is known to be formed by the subsequent hydrogenation of D-sorbitol/mannitol in the reaction mixture when using Ru/C catalysts.[40]

Further GVL yield improvements were possible when using D-fructose instead of D-glucose. The highest GVL yield was 62 mol% at complete D-fructose conversion (Table 6.2, entry 6). The residual amount of LA was 4 mol%, the main by-products were insoluble humins. D-Sorbitol/manitol and GVL hydrogenation products (1,4-pentanediol and MTHF) could not be detected by HPLC. The higher yields for D-fructose compared to D-glucose are in line with the separate experiments for the acid catalysed conversion of D-glucose and D-fructose to LA, where the highest yields were observed for D-fructose (*vide supra*). At similar conditions as the hydrogenation experiments (180 °C, 0.5 mol/l TFA, 0.5 mol/l D-fructose), the yield of LA from D-fructose was 63 mol%. For the combined dehydration/hydrogenation to GVL, the GVL yield was 62 mol%, which is close to the maximum value on the basis of the acid catalysed hydration reaction of D-fructose to LA. This implies that the hydrogenation reaction of LA to GVL is very selective and that the yield loss is due to humin formation in the first dehydration step of the sequence (Scheme 6.3).

Of interest is the ratio of LA and FA in the reaction mixture after the hydrogenation reaction. When considering only the acid catalysed dehydration of D-glucose to LA, the reaction stoichiometry predicts the formation of LA and FA in a one to one mol ratio (Scheme 6.3). In case FA is inert, the amount should be close to the amount of GVL formed (assuming 100% selectivity for the hydrogenation reaction of LA to GVL, which appears a valid assumption, *vide supra*). This is not the case and FA is present in considerably lower amounts. These findings may be rationalised by assuming that FA acts as a transfer hydrogenation agent and is active for the hydrogenation of LA, in line with the transfer hydrogenation experiments described in section 6.2. However, decomposition of FA to hydrogen and CO_2 and subsequent reaction of the hydrogen formed (*vide supra*), cannot be excluded.

Besides the monomeric C6-sugars (D-fructose and D-glucose), a dimeric sugar (sucrose) and a polymer (cellulose) were also tested at optimised conditions for D-fructose. In both cases,

significant amounts of GVL were formed besides humins and unconverted LA. For sucrose, the GVL yield was 52 mol%, which is higher than the 40 mol% reported in the literature for water soluble homogeneous Ru-catalysts prepared *in situ* from $RuCl_3$ and TPPTS in combination with H_2SO_4 (0.5 mol/l) as the acid catalyst and molecular hydrogen as the hydrogen donor.[20,21]

The non-optimised GVL yield for cellulose was 29 mol%. This yield is lower than for D-glucose (38 mol%), though promising. These yield trends are in line with available literature data for the acid catalysed conversion of cellulose to LA.[30] The LA yields from cellulose are lower than when using D-glucose as the feed.

6.3.4 Conversion of D-glucose to GVL by TFA in combination with a homogeneous water soluble ruthenium hydrogenation catalyst

The dehydration/hydrogenation of D-glucose to GVL with molecular hydrogen was also performed using a homogeneous Ru catalyst in combination with TFA. For this purpose, a water-soluble Ru-catalysts prepared in situ from $RuCl_3$ and TPPTS was applied. NaI was added to increase the reaction rate.[41] The reaction was performed at a reaction temperature of 180 ºC using 0.5 mol/l TFA and 94 bar of hydrogen. A catalyst to D-glucose ratio of 1 to 270 mol/mol was applied, the initial concentration of D-glucose was 0.5 mol/l.

After 8 h reaction time, the reaction was terminated and the composition of the liquid phase was determined using HPLC. Complete D-glucose conversion was observed. The major products in the liquid phase were LA (19 mol%) and GVL (23 mol%), furthermore substantial amounts of insoluble humins were formed. The presence of significant amounts of LA indicates that the hydrogenation reaction of LA to GVL is far from quantitative at these conditions. The sum of the GVL and LA yields is 42 mol%. This value is close to the maximum LA yield for the acid catalysed conversion of D-glucose under these conditions (46 mol%). The observed GVL yield is lower than reported by Horvath[20,21] for a similar catalyst using sulphuric acid in combination with sucrose (40 mol%). Sucrose is a dimer of D-fructose and D-glucose and higher yields of the intermediate LA are expected compared to D-glucose only. Further studies, e.g. by applying longer reaction times and/or higher catalyst intakes and D-fructose instead of D-glucose will be required to attain complete LA conversion to GVL. When assuming that the hydrogenation of LA to GVL is highly selective at these conditions, a maximum yield of 42 mol% is to be expected under the experimental conditions/intakes applied.

6.4 Conclusions

The catalytic synthesis of GVL from C6-sugars (D-glucose and D-fructose) in water using an acid catalyst (TFA) in combination with a heterogeneous hydrogenation catalyst (Ru/C) and either molecular hydrogen or formic acid as the hydrogen donor has been explored. Unprecedented transfer-hydrogenations with formic acid gave an optimised yield of GVL (52 mol%) at 180 °C, 16 h reaction time and D-fructose as the C6-sugar source. The major by-products were insoluble solids, known as humins, formed during the acid catalysed conversion of D-fructose to LA. The highest yield of GVL (62 mol%) was obtained with D-fructose using molecular hydrogen as the hydrogen source, TFA as the acid and Ru/C as the hydrogenation catalyst. Complete conversion of D-fructose was observed at these conditions. The major by-products were formic acid and insoluble solid materials (humins).

The yield and the rate of GVL formation is a delicate balance between the two individual reactions (acid catalysed dehydration of the C6-sugar to LA followed by a catalytic hydrogenation) in the sequence. The first step is a fast reaction (10-30 min) under the conditions employed, however, the selectivity is always below 70%. The subsequent hydrogenation with either formic acid or hydrogen is slow (order of hours), although apparently very selective.

The dehydration/hydrogenation of D-glucose to GVL with molecular hydrogen was also explored using TFA in combination with a water soluble homogeneous Ru catalyst prepared in situ from $RuCl_3$ and TPPTS. The yields of GVL (23 mol%) were lower than for the reactions with Ru/C and substantial amounts of LA were present in the mixture (19 mol%). This suggests that at the reaction conditions and intakes applied in this study, the hydrogenation activity of the homogeneous catalyst is lower than for Ru/C.

The study also identified TFA as an attractive alternative for mineral acids for the conversion of C6-sugars to LA. With this finding, aqueous/fluoro-biphasic system for the conversion of C6-sugars to LA may be envisaged with a fluoro-phase (e.g. perfluorohexane)[42] soluble TFA derivative like heptadecafluorononanoic acid (pKa: 0.36). This would facilitate acid catalyst recycle considerably, which is one of the main drawbacks of the current mineral acid based concepts for LA synthesis.

6.5 References

1 http://www1.eere.gov/biomass/biomass

2 A. Corma, S. Iborra, and A. Velty, *Chem. Rev.*, 2007, **107**, 2411-2502.

3 G. W. Huber, S. Iborra, and A. Corma, *Chem. Rev.*, 2006, **106**, 4044-4098.

4 L. Petrus and M. A. Noordermeer, *Green Chem.*, 2006, **8**, 861-867.

5 A. Effendi, H. Gerhauser, and A. V. Bridgwater, *Renew. Sustain. Energy Rev.*, 2007, doi:10.1016/j.rser.2007.04.008.

6 B. N. Kuznetsov, V. E. Tarabanko, and S. A. Kuznetsova, *Kinet. Catal.*, 2008, **49**, 517-526.

7 A.P. Dunlop, and J.W. Madden, *US Patent* 2786852, 1957.

8 I. T. Horváth, H. Mehdi, V. Fábos, L. Boda, and L. T. Mika, *Green Chem.*, 2008, **10**, 238-242.

9 J. J. Bozell, L. Moens, D. C. Elliott, Y. Wang, G. G. Neuenschwander, S. W. Fitzpatrick, R. J. Bilski, and J. L. Jarnefeld, *Resour. Conserv. Recycl.*, 2000, **28**, 227-239.

10 L. E. Manzer, *Appl. Catal. A*, 2004, **272**, 249-256.

11 J. P. Lange, J. Z. Vestering, and R. J. Haan, *Chem. Commun.*, 2007, 3488-3490.

12 R. A. Bourne, J. G. Stevens, J. Ke, and M. Poliakoff, *Chem. Commun.*, 2007, 4632-4634.

13 H. S. Broadbent, G. C. Campbell, W. J. Bartley, and J. H. Johnson, *J. Org. Chem.*, 1959, **24**, 1847-1854.

14 R. V. Christian, H. D. Brown, and R. M. Hixon, *J. Am. Chem. Soc.*, 1947, **69**, 1961-1963.

15 L.P. Kyrides and J.K. Craver, *US Patent*, 2368366, 1945.

16 H. A. Schuette and R. W. Thomas, *J. Am. Chem. Soc.*, 1930, **52**, 3010-3012.

17 F. Joo and M. T. Beck, *React. Kinet. Catal. Lett.*, 1975, **2**, 257-263.

18 F. Joo, Z. Toth, and M. T. Beck, *Inorg. Chim. Acta*, 1977, **25**, L61-L62.

19 K. Osakada, S. Yoshikawa, and T. Ikariya, *J. Organomet. Chem.*, 1982, **231**, 79-90.

20 H. Mehdi, A. Bodor, R. Tuba, and I. T. Horváth, *Abstracts of Papers of the American Chemical Society*, 2003, 226, U721.

21 H. Mehdi, V. Fábos, R. Tuba, A. Bodor, L. T. Mika, and I. T. Horváth, *Top. Catal.*, 2008, **48**, 49-54.

22 J.P. Lange, and L. Petrus, *WO Patent*, 2007099111, 2007.

23 L.J. Carlson, *US Patent*, 3065263, 1962.

24 B. Girisuta, L. P. B. M. Janssen, and H. J. Heeres, *Chem. Eng. Res. Des.*, 2006, **84**, 339-349.

25 B. F. M. Kuster, and H. S. Vanderbaan, *Carbohydr. Res.*, 1977, **54**, 165-176.

26 J. Jow, G. L. Rorrer, M. C. Hawley, and D. T. A. Lamport, *Biomass*, 1987, **14**, 185-194.

27 K. Lourvanij, and G. L. Rorrer, *Appl. Catal. ,A*, 1994, **109**, 147-165.

28 K. Lourvanij, and G. L. Rorrer, *J. Chem. Technol. Biotechnol.*, 1997, **69**, 35-44.

29 B. Girisuta, L. P. B. M. Janssen, and H. J. Heeres, *Green Chem.*, 2006, **8**, 701-709.

30 B. Girisuta, L. P. B. M. Janssen, and H. J. Heeres, *Ind. Eng. Chem. Res.*, 2007, **46**, 1696-1708.

31 G. Braca, A. M. R. Galletti, and G. Sbrana, *J. Organomet. Chem.*, 1991, **417**, 41-49.

32 T. Miyazawa, S. Koso, K. Kunimori, and K. Tomishige, *Appl. Catal. ,A*, 2007, **329**, 30-35.

33 M. Osada, N. Hiyoshi, O. Sato, K. Arai, and M. Shirai, *Energy Fuels*, 2008, **22**, 845-849.

34 T. Marzialetti, M. B. V. Olarte, C. Sievers, T. J. C. Hoskins, P. K. Agrawal, and C. W. Jones, *Ind. Eng. Chem. Res.*, 2008, **47**, 7131-7140.

35 V. E. Tarabanko, M. Y. Chernyak, S. V. Aralova, and B. N. Kuznetsov, *React. Kinet. Catal. Lett.*, 2002, **75**, 117-126.

36 B. Kusserow, S. Schimpf, and P. Claus, *Adv. Synth. Catal.*, 2003, **345**, 289-299.

37 C. Fellay, P. J. Dyson and G. Laurenczy, *Angew. Chem. Int. Ed.,* 2008, **47**, 3966-3968.

38 R. R. Broekhuis, B. M. Budhlall, and A. F. Nordquist, *Ind. Eng. Chem. Res.*, 2004, **43**, 5146-5155.

39 E. Crezee, B. W. Hoffer, R. J. Berger, M. Makkee, F. Kapteijn, and J. A. Moulijn, *Appl. Catal. ,A*, 2003, **251**, 1-17.

40 D. K. Sohounloue, C. Montassier and J. Barbier, *React. Kinet. Catal. Lett.*, 1983, **22**, 391-397.

41 E. Fache, C. Santini, F. Senocq, and J. M. Basset, *J. Mol. Catal.*, 1992, **72**, 337-350.

42 J. A. Gladysz and D. P. Curran, *Tetrahedron*, 2002, **58**, 3823-3825.

Dankwoord

Eindelijk is het af!! Het heeft wat langer geduurd dan normaal en inderdaad de laatste loodjes wegen het zwaarst.

Als eerste wil ik mijn promotor Prof. Erik Heeres bedanken. Erik bedankt voor de mogelijkheid om onder jou te mogen promoveren en bedankt voor de vele hulp, je ideeën, je steun, ik heb heel veel van je geleerd.

Vervolgens wil ik de leden van de leescommissie bedanken. Bedankt Prof. Broekhuis, Prof. Minnaard en Prof. de Vries voor het snelle nakijken en voor het commentaar, de correcties en suggesties.

The studies on olefin hydro-acylation described in Chapters 2-4 were performed in close collaboration with the organic chemistry department of the RUG. I would particularly like to thank Dr. Francesca Gini for her help with the chemistry and analyses. Also I would like to thank Prof. Adri Minnaard, Prof. Bart Hessen and Prof. Drent for their contribution and advice in this project.

Niels van Veghten, Prof. Roffel, Prof. de Vries, Dr. Michel van den Berg, wil ik ook hartelijk bedanken voor hun bijdrage in het onderzoek dat wordt beschreven in het 5de hoofdstuk. Niels jij bent begonnen met dit onderzoek en hebt me met alles enorm geholpen. Michel bedankt voor de hulp bij katalytische problemen en voor het leveren en helpen vervaardigen van gezuiverd substraat en de rhodium katalysator. Prof. Roffel wil ik bedanken voor de bijdrage bij het modeleren van het systeem in Matlab. Prof de Vries, ook u hartelijk bedankt voor de vele discussies over het mechanisme van de katalyse.

In the 6th chapter on the synthesis of γ-valerolactone from sugars I got a lot of help from the following colleagues; Ratna Handana, Dr. Dai Chunai, Dr. Buana Girisuta, and C.B. Rasrendra. Buana, I would like to thank you for your help with the experiments and the HPLC-analysis and for your skilful advice. Ratna and Dai, also thank you for your aid with the experiments and the analysis. And C.B., also many, many thanks for helping me with the experiments, analysis, data modeling and by giving me valuable input and advice.

Bij het uitvoeren van onderzoek is de analyse van reactiemengsels zeer belangrijk geweest. Ik wil graag Theodora Tiemersma-Wegman, Albert Kievit, Jan Henk Marsman, Arnold Dalmolen, Peter

Evers, Leon Rohrbach, Ollie Haminga, Fitna Adham, Wim Kruizinga en Hans van de Velde hartelijk bedanken voor alle analytische ondersteuning.
Verder wil ik de jongens (the TD-boys) van de technische dienst zeer bedanken, jullie zijn de smeerolie in het lab (dit is goed bedoeld!). Bedankt Erwin, Anne en Marcel voor jullie technische ondersteuning en ook voor jullie gezelligheid en de leuke uitstapjes. O ja, ook nog bedankt voor het repareren van die laatste monsterbuis.
Marya van der Duin-de Jonge, bedankt voor al je hulp bij de tocht door de papierenjungle en natuurlijk bedankt voor de gezelligheid bij de pauzes en uitstapjes.
Nidal bedankt dat je een van mijn paranimfen wilt zijn en bedankt voor de vele discussies (gelukkig ook vaak niet over werk), de gezelligheid, het advies, het nakijken van mijn proefschrift en de vriendschap en de vele excuses om toch nog maar even naar de kroeg te gaan.
Arthur, beste vriend, bedankt dat je mijn paranimf wilt zijn en ook bedankt voor het nakijken van mijn proefschrift.
Jelle, jij ook bedankt voor de gezelligheid in het lab, de goede workouts en het mogen misbruiken van je reactor, nog sorry van die laatste monsterbuis trouwens.
A.I.O. Biernouilli: Ik denk dat geen van de afdelingen in het FWN gebouw zo'n leuke club aio's heeft als dat van ons. Vele borrels, bbq's en feestjes …: Marcel Wiegman (de drijvende kracht), Nidal Hammoud Hassan, Jelle Wildschut, Gerard Kraai, Boelo Schuur, Arjan Kloekhorst, bedankt!.
Verder wil ik nog alle mensen van de afdeling bedanken. Agnes Ardiyanti, Anant Samdani, Asaf Sugih, Asal Pasop-Hamarneh, Bernard Huisman, Bilal Niazi, Claudio Toncelli, Cornelis de Jonge, Diego Wever, Francesca Fallani, Francesca Gambardella, Francesco Picchioni Farchad Mahfud, Gerald Jonker, Henk van de Bovenkamp, Henky Muljana, Ignacio Melian-Cabrera, Iker Aguirrezabal Telleria, Jaap Bosma, Jan Willem Miel, Jasper Huisman, Jos Winkelman, Kevin van Hulssen, Laura Junistia, Laurens Bosgra, Leon Janssen, Lidia Lopez Perez, Louis Daniel, Mochamed Chalid, Muhammad Iqbal, Poppy Sutanto, Robert Wilting, Sameer Nalawade, Sebastian Noel, Sjoerd van de Knoop, Teddy Teddy, Youchun Zhang.
Tenslotte wil ik nog Jakob Heeres, Cobie Heeres, Jan-Ludolf Heeres (mijn vader, moeder en broer) en Marika Mustonen (mijn vriendin) bedanken voor hun onvoorwaardelijke steun en geduld.

List of Publications

1. **Heeres, H.**; van Vegten, C. H.; de Vries, J. G.; Roffel, B.; Heeres, H. J., Kinetic studies on asymmetric hydrogenations using a homogeneous MonoPhos based rhodium catalyst. World Congress of Chemical Engineering, Glasgow (Scotland), 10-14 July **2005** (poster presentation).

2. **Heeres, H.**; Melián-Cabrera, I.; Minnaard, A.; Gini, F.; Hessen, B.; Heeres, H.J., Insights in (asymmetric) hydroacylation pathways Olefins-to-Chiral ketones through Pd-phosphine catalysts. 7th International Symposium on Cataysis Applied to Fine Chemicals (7th CAFC), Bingen (Germany), 23-27 October **2005**. (poster presentation by Melián-Cabrera, I).

3. Mahfud, F.H.; **Heeres, H.**; Heeres, H.J., Upgrading of fast pyrolysis oil using mild oxidation using ozone. Pyrolysis Network (Pyne) Newsletter, **2006**, 20, 5 (Published).

4. **Heeres, H.**; Heeres, H.J., Conversion of olefins and syn-gas to ketones using homogeneous palladium-phosphine catalysts. 8th Nederlands Catalysis and Chemistry Conference, Noordwijkerhout, 5-7 March **2007** (oral presentation).

5. **Heeres, H.**; Handana, R.; Chunai, D.; Rasrendra, C.B.; Girisuta, B.; Heeres, H.J., Combined dehydration/(transfer)-hydrogenation of C6-sugars (D-glucose and D-fructose) to γ-valerolactone using ruthenium catalysts. Green Chem., **2009**, 11, 1247-1255

6. **Heeres, H.**; Heeres, H.J., Enantioselective hydro-acylations of 1-alkenes to α-methylketones using palladium/diphosphine catalysts. Manuscript ready for submission.

7. **Heeres, H.**; Heeres, H.J., Enantioselective syngas conversions: Hydro-acylation of 1-alkenes to α-methylketones using a palladium/Josiphos catalyst. Manuscript ready for submission.